

**BIOCHEMICAL AND FUNCTIONAL ANALYSIS OF DAYWAKE, A NOVEL
WAKE-SLEEP REGULATOR IN *DROSOPHILA MELANOGASTER***

By

GABRIEL VILLEGAS

A dissertation submitted to the

School of Graduate Studies

Rutgers, The State University of New Jersey

In Partial fulfillment of the requirements

For the degree of

Doctor of Philosophy

Graduate Program in Biochemistry

Written under the direction of

Isaac Edery

And approved by

New Brunswick, New Jersey

October, 2020

Abstract of The Dissertation

BIOCHEMICAL AND FUNCTIONAL ANALYSIS OF DAYWAKE, A NOVEL WAKE-SLEEP REGULATOR IN *DROSOPHILA MELANOGASTER*

By GABRIEL VILLEGAS

Dissertation Director:

Isaac Edery

D. melanogaster is an extremely powerful genetic animal model to study why and how we sleep. Like humans, the majority of sleep in *D. melanogaster* occurs during the night. However, similar to many other day-active animals, *D. melanogaster* exhibits a midday sleep or “siesta”, most frequently associated with limiting exposure to the hot midday sun. Recent evidence indicates a strong genetic component influencing siesta behavior in humans. While nighttime and daytime sleep serve different functions, the role and mechanisms for siesta are little understood.

Initial studies from our laboratory showed that midday siesta in *D. melanogaster* is down-regulated by the cold-enhanced splicing of the 3' terminal intron (termed *dmpi8*) in the *period* (*per*) gene, a key component of the circadian (~24 h) clock. More recent results revealed that *dmpi8* splicing influences midday siesta *in-trans* via up-regulating the expression of a slightly overlapping gene termed *daywake* (*dyw*) that functions in an anti-siesta capacity. Overall, the main

idea from prior work is that *dyw* mainly functions in thermal-adaptation whereby its increased levels on cool days reduces siesta levels by promoting midday wakefulness on days where the threat from heat exposure is diminished.

The *dyw* gene encodes a juvenile hormone binding protein (JHBP), which are known to be secreted into the hemolymph as part of signaling cascades. In this thesis I raised anti-DYW antibodies and used them to characterize the DYW protein at the biochemical and cellular levels in both flies and cultured *Drosophila* cells. DYW is found in key circadian cells in the brain, the pigment-dispersing factor (PDF)-expressing neurons, consistent with earlier work showing that manipulating *dyw* levels in these cells modulates midday siesta. DYW levels in the head are responsive to temperature and differ in male and female adult flies. There are two major isoforms of DYW in adult flies that appear to reflect post-translational differences. Indeed, studies in cultured *Drosophila* cells indicate that DYW stability and/or maturation is heavily dependent on a glycosylation event at a single residue position. Further, this work shows that DYW is secreted and that this secretion is reliant on the presence of an N-terminal signal peptide comprised of the first 25 residues in DYW. My studies suggest a model whereby DYW functions as a JHBP that is produced in the brain followed by cleavage and entry into the circulatory system where it interacts with target tissues to regulate sleep-wake behavior.

In related work, CRISPR technology was used to generate *dyw* knock-out (*dyw*-KO) flies. Remarkably, although *dyw*-KO flies exhibit increased midday sleep compared to wildtype controls as expected, when challenged with malnourishment

we observe major differences in the regulation of nighttime sleep between *dyw*-KO flies and controls. This finding suggests that with prolonged hunger, *dyw* mainly stimulates wake during the night. Presumably, this helps in foraging for food but shifts this activity towards the night when the threat from sun exposure is eliminated.

Together the studies presented in this thesis substantially increase our understanding of how *dyw* functions. It is proposed that *dyw* has a more broad adaptive role in integrating multiple survival threats (e.g., heat, hunger) to optimize day-night levels of wake-sleep behavior to best meet current environmental challenges. Because *dyw* is part of a larger family of lipid-binding carriers found in animals, the work might reveal further insights into the interplay between sleep and metabolism, key to human well-being and linked to many diseases. In addition to my work on *dyw*, this thesis also includes some key results from my earlier studies aimed at biochemically characterizing the PER circadian clock protein.

Acknowledgments

I would like to thank the following for their support and guidance through my doctoral studies.

To Isaac Edery for his guidance and support both as a mentor and friend.

To Drs. Bill Belden, Beatrice Haimovich and Jerry Langer for their advice and continuous and unconditional encouragement.

To my current and previous lab mates: Rudra Dubey, Chaya Dharia, Weihuan Cao, Zhichao Zhang, Nick Pontillo, Alessa Vindas-Cruz and Chloe Azadegan. And a special and heartfelt thanks to Yong Yang for his advice and guidance as a lab mate and friend

To my family; my wife Danielle and son Evan. My father Frank and mother Mireya. My sister Sarah, her husband Mario, uncles Rick, David and Sergio and Aunts Elia and Estrella for their inescapable and never-ending optimism and reassurance.

And finally, to my in-laws who have shown so much support; my brother-in-law Chris, his wife Kim. My Father- and Mother-in-law Jay and Jackie, as well as Jo Anne, Anthony, Joseph, Jennifer.

Table of Contents

Abstract of The Dissertation	ii
Acknowledgments	v
Table of Contents	vi
List of Illustrations.....	xi
List of Tables	xiv
Chapter 1: Introduction	1
Overview of circadian rhythms and sleep	1
<i>Drosophila melanogaster</i> as a model system to study wake-sleep behavior	5
Thermosensitive splicing of an intron in the <i>per</i> 3' UTR affects daily activity patterns.....	8
Weak 5' and 3' splice sites underlie the temperature sensitivity of <i>dmpi8</i> splicing.....	11
<i>dmpi8</i> splicing regulates midday sleep in a clock independent manner...	12
Variation in midday siesta and <i>dmpi8</i> splicing in natural populations of <i>Drosophila melanogaster</i>	14
(1) A prominent SNP in the <i>per</i> 3' UTR from lies in the United States is causally linked to midday sleep and <i>dmpi8</i> splicing efficiency...	16

(2) Midday siesta levels and dmip8 splicing efficiency co-vary with altitude in <i>D. melanogaster</i> from tropical Africa.....	16
(3) <i>per</i> 3' UTR SNPs, siesta levels and dmip8 splicing efficiency exhibit a latitudinal cline in <i>D. melanogaster</i> from Australia	17
Identification of a novel anti-siesta gene called <i>daywake</i> that is regulated <i>in-trans</i> by dmip8 splicing	17
Brief summary of juvenile hormone binding proteins	21
Overview of Thesis	23
Chapter 2: The Anti-Siesta protein DAYWAKE is secreted, regulated by glycosylation and accumulates in key brain clock neurons.....	24
Abstract.....	24
Introduction.....	25
Materials & Methods	27
<i>Drosophila</i> Maintenance	27
DAYWAKE Antigen and Antibody Generation	27
Protein Extract Preparation from Adult Flies	29
Western Blotting of Fly Protein Samples.....	30
Affinity Purification of DYW-3xFLAG from Adult Flies	31
Whole Brain Imaging.....	32
Generation of <i>daywake</i> constructs for expression in S2 cells	33

Culture and Transfection of <i>daywake</i> Constructs in <i>Drosophila</i> S2 Cells	34
Protein Extract Preparation from Cultured <i>Drosophila</i> S2 Cells and Culture Media.....	34
Endoglycosidase H Treatment of Protein Extracts from Cultured <i>Drosophila</i> S2 Cells.....	35
Results.....	37
DAYWAKE is found in adult <i>Drosophila</i> heads and is responsive to temperature and <i>dmpi8</i> splicing efficiency	37
DAYWAKE is expressed in circadian clock neurons in the fly brain	41
DAYWAKE is stabilized by glycosylation and undergoes cleavage mediated secretion in cultured <i>Drosophila</i> cells	46
Discussion	50
Conclusion.....	56
STAR★Methods	57
Chapter 3: <i>Daywake</i> regulates sleep behavior in a temperature, sex and nutrition dependent manner	61
Abstract.....	61
Introduction	62

Materials & Methods	64
Generation of CRISPR <i>dyw</i> -KO flies.....	64
Generation of transgenic flies in a <i>dyw</i> -KO genetic background ...	64
Analysis of daily activity and sleep	65
Western Blotting.....	66
Results.....	67
Generation of <i>dyw</i> -KO flies	67
The anti-siesta activity of <i>dyw</i> is readily observed at cooler temperatures in both males and females	67
Transgenic rescue of <i>dyw</i> -KO flies shows a role for <i>dmpi8</i> splicing efficiency in mediating the effects of <i>dyw</i> on daily sleep regulation	73
Malnutrition reveals an unexpected effect on nighttime sleep in <i>dyw</i> - KO flies	77
Discussion	83
Star★Methods	88
CHAPTER 4: Summary	90
Addendum 1: Optimization of anti-DYW antibody.....	100
Brief Overview	100
Optimization steps	102

(1) High Background and Speckling.....	102
(2) Extraction buffer stringency.	102
(3) Streaking indicative of keratin cross-reactivity.	102
Addendum 2: Proteomic approach to characterize relationship between PER phosphorylation and structure	104
Brief Overview	104
Rationale for experimental approach	106
Addendum 3: Transgenic <i>Drosophila</i> models generated that were not used in this thesis	111
References	113

List of Illustrations

Figure 1.1. Schematic representation of the main circadian transcriptional-translational feedback loop in <i>Drosophila</i>	3
Figure 1.2. Measuring and evaluating activity and sleep in adult flies.	7
Figure 1.3. Thermal adaptation of midday siesta in <i>D. melanogaster</i> is regulated by thermosensitive splicing of <i>per</i> intron dmpi8.	9
Figure 1.4. Initial model linking thermosensitive dmpi8 splicing and daily activity distributions.	10
Figure 1.5. Midday siesta levels in natural populations of <i>Drosophila melanogaster</i> exhibit latitudinal and altitudinal clines.	15
Figure 1.6. The splicing efficiency of dmpi8 regulates midday siesta levels in an indirect manner via the slightly overlapping gene called <i>dyw</i>	18
Figure 1.7. Proposed model for how dmpi8 splicing/ <i>dyw</i> regulate midday siesta in a temperature sensitive manner.	19
Figure 1.8. Overview of Juvenile Hormone Binding Protein function in <i>Drosophila</i>	22
Figure 2.1. Anti-DYW antibody identifies a closely migrating DYW doublet in flies.	38
Figure 2.2. Decreasing daily temperature leads to an increase in DYW protein levels.	40
Figure 2.3. DYW protein levels are elevated in natural populations of <i>Drosophila</i> which differ in their dmpi8 splicing efficiencies.	42

Figure 2.4. A major amount of DAYWAKE detected in the head is produced in circadian clock cells.....	43
Figure 2.5. DYW is expressed in the key circadian small- and large-ventrolateral neurons (s-LNv and l-LNv) in the fly brain.	45
Figure 2.6. DYW produced in S2 cells is secreted in a signal-peptide dependent manner and stabilized by glycosylation at amino acid N182.	48
Figure 3.1. Strategy for generating <i>dyw</i> -KO flies using CRISPR.....	68
Figure 3.2. <i>dyw</i> -KO flies exhibit increased midday siesta at 18°C.....	70
Figure 3.3. <i>dyw</i> -KO flies exhibit increased midday siesta at 25°C.....	72
Figure 3.4. <i>dyw</i> -containing transgenes reverse the increased daytime sleep observed in <i>dyw</i> -KO mutant flies in a manner consistent with <i>dmpi8</i> splicing efficiency.	75
Figure 3.5. A more expansive <i>dyw</i> -containing transgene also reverses the increased daytime sleep observed in <i>dyw</i> -KO flies.	76
Figure 3.6. Malnutrition reveals a large effect on nighttime sleep in <i>dyw</i> -KO flies.	78
Figure 3.7. Malnutrition generally leads to reduced daytime and nighttime sleep in both <i>dyw</i> -KO and wildtype flies.....	80
Figure 3.8. A <i>dyw</i> -containing transgene reverses the increased daytime but not nighttime sleep in <i>dyw</i> -KO flies under conditions of malnutrition.	82

Figure A1. Initial results testing the anti-DYW antibodies using our standard Western Blotting conditions.	101
Figure A1.2. Optimization of anti-DYW antibodies for immunoblotting.	101
Figure A2.1. Use of Hydrogen-Deuterium Exchange Mass Spectroscopy to investigate if hyper-phosphorylated PER has a more open conformation compared to its non-phosphorylated state.....	105
Figure A2.2. HDX-MS suggests that hyperphosphorylation of PER leads to a more open conformation of the SLIMB binding region but no effect on the PAS region.	108

List of Tables

Table 2.1 List of primers	36
Table 2.2 Key Resources Table	57
Table 3.1: Key Resources Table	88
Table A3.1. List of lines generated in <i>dyw</i> -KO backgrounds.	111

Chapter 1: Introduction

Overview of circadian rhythms and sleep

In order to synchronize biological needs and behaviors with the 24 h spinning of our planet and the environmental changes associated, living organisms evolved an endogenous circadian ($\cong 24$ h) timing system that allows them to anticipate and adapt to daily changes in the environment. Circadian timing systems are observed in organisms from bacteria to mammals and the daily rhythms they drive are defined by three hallmark features: 1) Persist with a period of $\cong 24$ h in the absence of external stimuli; 2) can be reset by environmental cues, typically daily light-dark cycles and; 3) they exhibit little change in periodicity over a wide range of physiologically relevant temperatures—termed, temperature compensation [1].

By synchronizing circadian rhythms to local time, life forms perform biological activities at advantageous times, such as foraging for food when resources are more available and sleeping during times when predators are on the prowl. Circadian rhythms are observed at numerous levels of biological organization, from daily fluctuations in enzymatic activities to physiological and behavioral fluctuations. Despite the diversity in rhythmic behaviors observed within and between life-forms, the underlying “clock” mechanisms exhibit similar logic based on transcriptional-translational feedback loops (TTFL) that lead to daily fluctuations in gene expression.

In animals, circadian clocks are based on several interlinked TTFLs, each loop acting either in a positive or negative regulatory role. These feedback loops

rely on a pair of transcription factors, termed central clock transcription factors. To generate a self-sustaining molecular oscillator, clock transcription factors drive expression of other central clock genes whose protein products function in a negative manner to block the activity of the clock transcription factors. As a result of post-transcriptional regulatory mechanisms, mainly time-of-day specific phosphorylation, the negatively acting factors only function during a certain time of day, leading to daily fluctuations in the activity of central clock transcription factors. In addition to participating in autoregulatory circuits, the cyclical transcriptional activity from these central clock transcription factors also drive expression of species/tissue/cell-specific sets of downstream clock-controlled genes (*ccgs*), which are ultimately responsible for the daily rhythms in cellular, physiological and behavioral phenomena that are observed.

The work presented in this thesis used *Drosophila melanogaster* as a model animal system and I will focus on the clock mechanism in this species. Studies using *Drosophila melanogaster* over the last 35 years led to groundbreaking insights into the molecular underpinnings governing circadian clocks. Indeed, the field of circadian molecular genetics was initiated in *Drosophila* with the first clock gene characterized and isolated, the *period* (*per*) gene. Numerous findings have led to a complex clock mechanism that includes many interacting players that assemble into a “clockosome” that undergoes dynamic changes in interactions and activities to build a timing motor that drives cyclical gene expression.

The primary TTFL in the *Drosophila* system includes four central clock factors, *per*, *timeless* (*tim*), *clock* (*dClk*) and *cycle* (*cyc*) (see Figure 1.1, below).

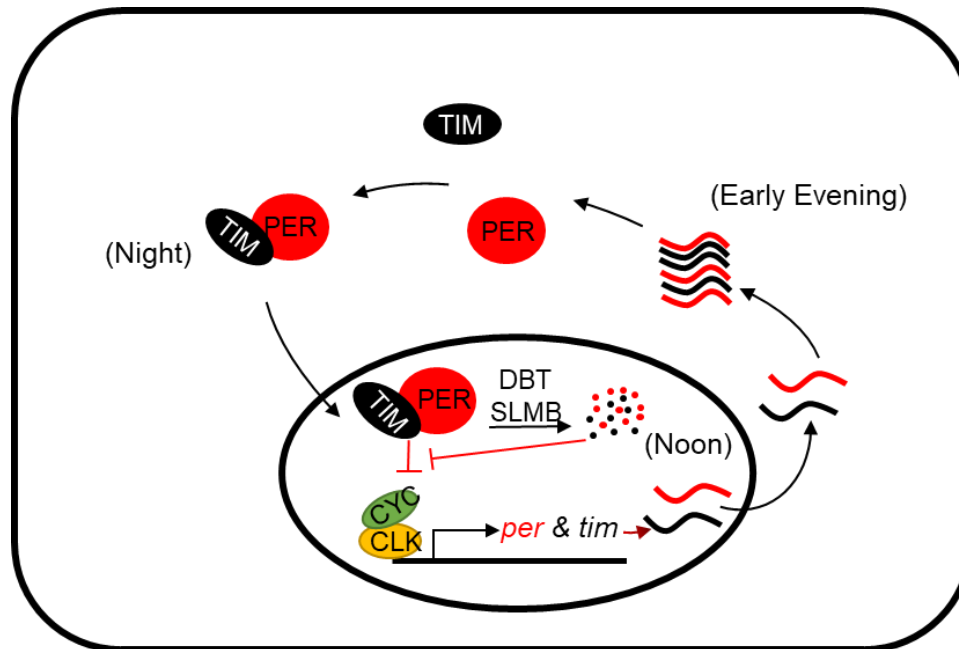


Figure 1.1. Schematic representation of the main circadian transcriptional-translational feedback loop in *Drosophila*. A highly simplified model of the main feedback loop found in the *D. melanogaster* clock circuitry. The outer oval represents the cell membrane, while the inner black oval represents the nuclear membrane. Briefly, CLK and CYC form a dimer that binds upstream of the *per* and *tim* promoters, stimulating their transcription. After a post-translational time-delay, an increase in PER and TIM stability leads to formation of a PER-TIM complex that enters the nucleus and represses the transcriptional activity of CLK-CYC. After several hours in the nucleus, PER and TIM are targeted for degradation, allowing another round of CLK-CYC-dependent transcription. Key players in the degradation of the PER-TIM complex are the kinase DBT and the F-box protein SLMB. Red bar-ended lines indicate inhibitory relationships. Squiggly lines, mRNA; small ovals, proteins. Approximate times throughout the cycle are included. See text for more details.

CLK and CYC form a dimer that drive transcription of *per* and *tim*, beginning in the mid-day and ending in the early night. The buildup of the PER and TIM proteins lag by several hours until they form a stable PER-TIM complex that enters the nucleus around mid-night where it binds CLK-CYC, inhibiting its activity. PER and TIM undergo rapid degradation in the early morning, re-activating CLK-CYC to begin another round of *per/tim* expression. A complex series of progressive phosphorylation events drive the daily cycle in PER levels and cytoplasmic-nuclear localization. Importantly, the kinase DOUBLETIME (DBT; homolog of the human CK1 ϵ) drives progressive increases in PER phosphorylation until it reaches a hyper-phosphorylated state that is recognized by the F-Box protein SLMB (homolog of β -TrCP), targeting it for rapid proteasome-mediated degradation in the nucleus. This molecular self-sustaining ~24 h clock machine is synchronized to local time as light evokes the rapid degradation of TIM, timing the rapid formation of PER-TIM complexes to the early night when light levels decrease.

Although not all the features of the *Drosophila* clock are conserved in mammals, much is. The key clock transcription factors are CLOCK and BMAL1 (homologs of dCLK and CYC), and they are inhibited by PER proteins (there are 3 *Per* genes in mammals; *Per1*, *Per2*, *Per3*). Moreover, the mammalian PER proteins undergo daily cycles in phosphorylation and stability whereby CK1 ϵ and β -TrCP play analogous roles to their fly counterparts. Interestingly, several inherited human sleep disorders are caused by mutations affecting PER phosphorylation. Our lab played a significant role in understanding the dynamics of PER phosphorylation leading to a novel model that proposed the time-of-day

specific phosphorylation of PER leads to conformational changes in its structure that eventually facilitate recognition by SLMB. Indeed, the first part of my thesis work involved trying to test this model, and some of that work is shown in Appendix 1 (discussed below; see Addendum 2). However, I shifted focus and studied another aspect of *per* regulation, which is linked to sleep research and the main subject matter of my thesis.

***Drosophila melanogaster* as a model system to study wake-sleep behavior**

Drosophila offers several advantages when studying daily wake-sleep behavior. The experimental procedure for measuring their activity and sleep is relatively straight forward, genetic manipulation is accomplished quite easily and the biochemical basis of their biological clocks are well understood [1, 2].

While there are several different platforms to measure daily wake-sleep behavior in *Drosophila*, a widely used method is based on recording locomotor activity. The majority of researchers measuring daily activity cycles rely on the commercially available “*Drosophila* Activity Monitor System”. Briefly, glass tubes containing a single fly and a small amount of carbohydrate-based food at one end are placed in specially designed monitors that house an infrared light source on one side of the tube and a photomultiplier recorder on the other side (Fig. 1.2A and B). As the flies move back and forth inside the tube, they break the infrared light beam and these beam-breaks per unit time are recorded. In a typical experiment, the fly-containing monitors are placed in incubators at 25°C and the flies entrained

(synchronized) by exposure to 12 h light/12 h dark cycles [12:12LD; where Zeitgeber time 0 (ZT0) = lights-on, and ZT12 = lights-off] over the course of many days. Under these standard conditions, wildtype *D. melanogaster* exhibit a bimodal distribution of activity, with morning and evening peaks of activity separated by a midday dip or siesta and nighttime inactivity (Fig. 1.2C). Aside from entrainment, additional lighting schemes commonly used include constant darkness (DD) or constant light (LL) and are used to measure various circadian parameters such as periodicity.

This same experimental approach has also been used to measure sleep in *Drosophila* (Fig. 1.2D). Twenty years ago, two independent research groups showed that *D. melanogaster* exhibits physiological, pharmacological and behavioral aspects similar to mammalian sleep [3, 4]. Thus, in a similar fashion to how *D. melanogaster* was used to advance our knowledge of circadian rhythms, the genetic and neurobiological advantages of this organism have established this species as a great model to study sleep. Extended periods of quiescence in *D. melanogaster* exhibit the hallmarks of sleep by several criteria: 1) A sleep state can be physiologically reversed as opposed to states such as coma; 2) the threshold for sensory mediated arousal is increased during sleep; 3) sleep distribution throughout the day is regulated by the circadian clock; 4) sleep is homeostatically regulated, meaning that after depriving flies of sleep they show a subsequent sleep-rebound to compensate for that lost; and 5) distinct changes in neuronal activity occur during this period [2-4].

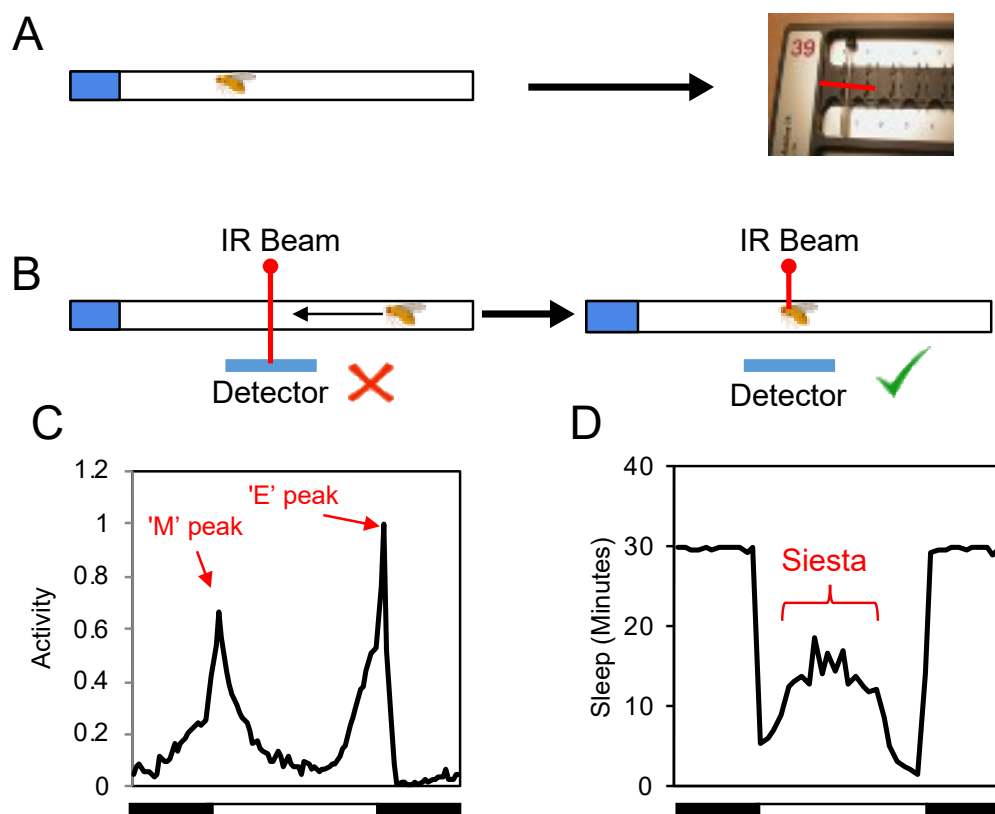


Figure 1.2. Measuring and evaluating activity and sleep in adult flies. (A) Schematic representation of an experimental setup using the Drosophila Activity Monitor (DAM) System. Glass tubes containing individual flies and food source (blue) are loaded into activity monitors (right), which are placed in environmental incubators to control daily light-dark cycles and temperature. **(B)** Locomotor activity is measured by counting beam-breaks using an IR beam and a photomultiplier tube recorder ("Detector"). These beam breaks are continuously recorded for many days, and typically grouped in 5 min windows. **(C)** Typical daily locomotor profile showing the clock-controlled morning and evening peaks. **(D)** Typical daily sleep profile; flies mainly sleep during the night but show a midday siesta. Data plotted in 30 min intervals. (C, D) The horizontal bars beneath these plots denote light status, black for 12 h of dark; white for 12 h of light.

D. melanogaster usually sleep for several hours in the night that is characterized by numerous sleep bouts (20-50 min) that are interspaced by brief awakenings (> 1 min). After careful observation, the accepted standard in the field is that 5 or more contiguous min of no recorded locomotor indicates that the flies were sleeping during that time-window [5, 6]. This verified behavioral definition provides a simple and straightforward method to characterize sleep in *Drosophila* with methods and equipment already well established in the field based on circadian studies. In addition to measuring total sleep, other parameters such as sleep bout length and number of sleep bouts can be used for more in-depth analysis of sleep behavior.

Thermosensitive splicing of an intron in the *per* 3' UTR affects daily activity patterns

Temperature is a well-known regulator of sleep as anyone trying to sleep at night when its warm can attest. Daytime arousal levels are also influenced by temperature, most famously the midday siesta. Similar to many animals, as temperature increases, flies tend to exhibit reduced activity levels during the midday [7-9] (Fig 1.3A). In addition, the evening and morning peaks of activity are shifted towards the cooler night-time hours. The evolutionary significance of this temperature dependent change in daily activity is almost certainly a protective mechanism driving flies to rest and seek shelter during warmer days when there is prolonged exposure to the deleterious effects of the hot midday sun.

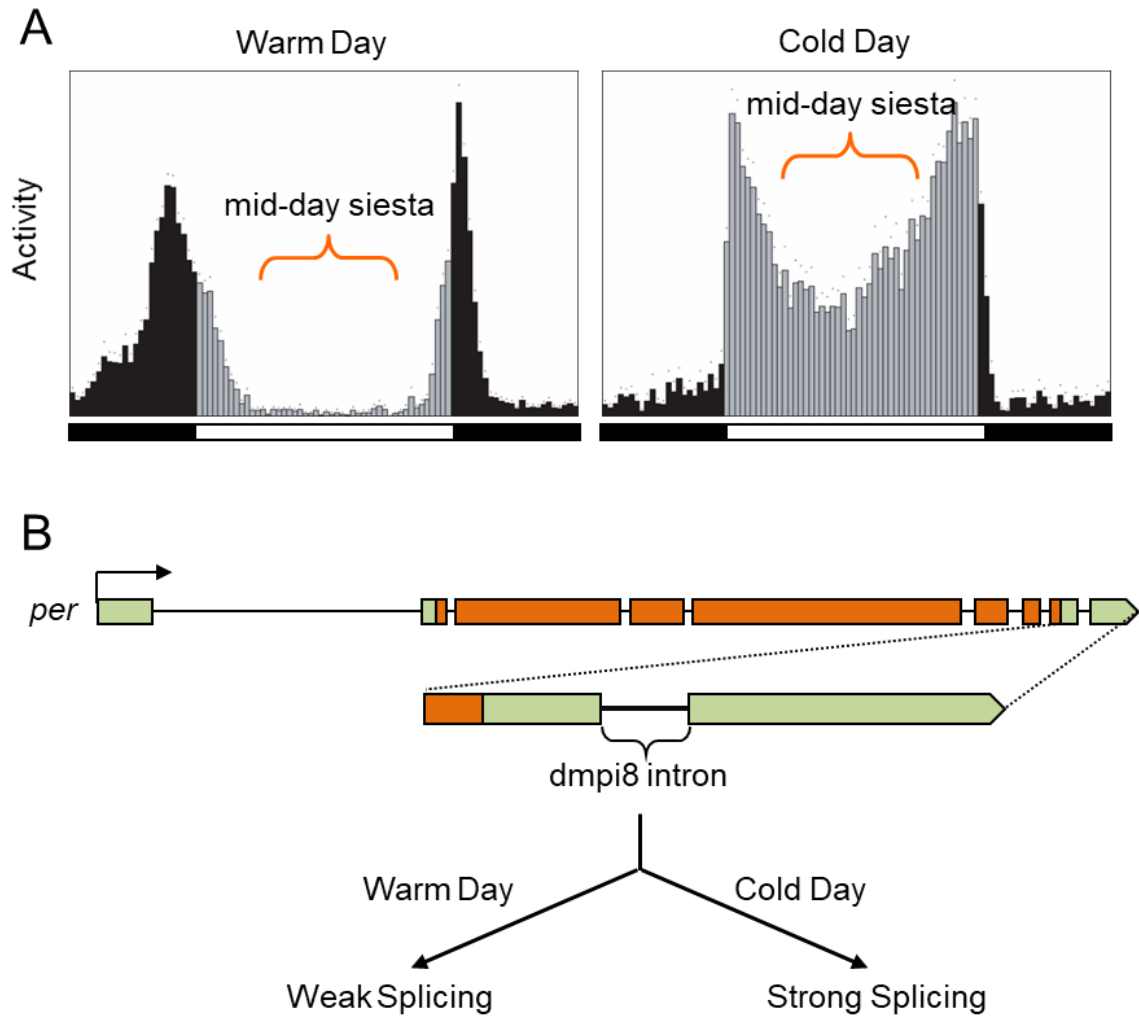


Figure 1.3. Thermal adaptation of midday siesta in *D. melanogaster* is regulated by thermosensitive splicing of *per* intron *dmpi8*. (A) At higher ambient temperatures (left panel), the morning and evening bouts of activity are shifted towards the nighttime hours and there is less activity during the midday compared to the daily activity distribution observed on cooler days (right panel). (B) *per* contains 8 introns, with the eighth (termed *dmpi8*) found in the 3'UTR (shown enlarged). Splicing of the *dmpi8* intron is more efficient at cooler temperatures, somehow contributing to decreased midday siesta levels.

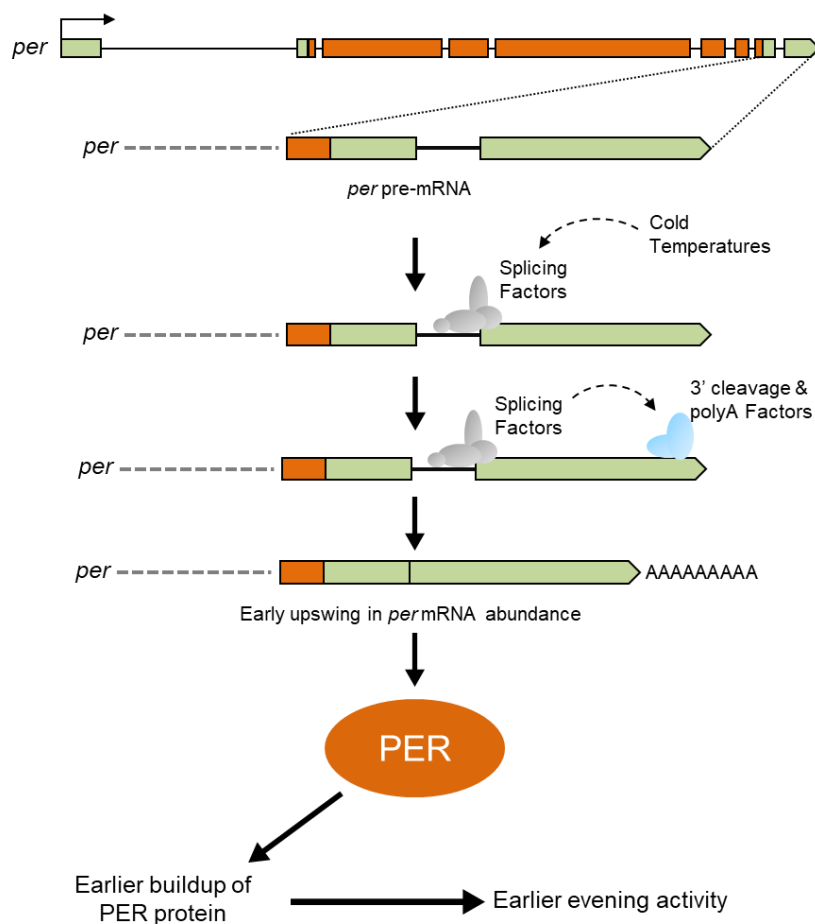


Figure 1.4. Initial model linking thermosensitive *dmpi8* splicing and daily activity distributions. Initially it was proposed that on cold days, splicing factors were more strongly associated with *dmpi8* in the *per* 3' UTR (shown top). Because active splicing as opposed to retention/removal of intron sequences was required for thermal adaptation of daily activity, it was proposed that enhanced binding of spliceosome at cooler temperatures led to an increase in 3'-end formation factors, which in turn resulted in a more rapid upswing in *per* mRNA/protein levels. This more rapid upswing in the daily levels of PER protein was suggested to advance the evening peak of activity and consequently decrease midday siesta. (Adapted from Majercak et al., 1999 [9]).

Studies in the Ederly lab used *D. melanogaster* as model system to investigate how the distribution of daily activity is modulated by temperature. A key outcome from these studies was the discovery that the thermal adaptation of midday siesta levels is regulated by an intron in the 3' untranslated region (UTR) of *per*, termed *dmpi8* (*Drosophila melanogaster period* intron #8) (Fig 1.3B) [10]. Intriguingly, the splicing efficiency of *dmpi8* increases as ambient temperatures drop [9], a phenomenon which has been described in other organisms [11, 12]. It was proposed that at cooler temperatures the splicing machinery associates more strongly to *dmpi8* splice sites and may aid in the recruitment of polyadenylation and 3' cleavage factors to the nascent *per* transcript increasing the rate of accumulation of mature *per* mRNA (Figure 1.4). This rapid accumulation of *per* mRNA at cooler versus warmer temperatures would advance the rate of PER protein buildup in the cytoplasm allowing for earlier entry into the nucleus. As a result of phase-advanced upswing in PER levels, it was assumed that this was causally lined to an earlier evening bout of activity and increased midday day activity (Figure 1.4). As will be explained below, this "clock-centric" view based on *dmpi8* splicing efficiency modulating daily activity profiles via affecting PER dynamics turned out to be wrong.

Weak 5' and 3' splice sites underlie the temperature sensitivity of *dmpi8* splicing

Introns contain 5' and 3' splice sites (ss) which play a critical role in recruitment of the splicing machinery to the intron. The *per* gene was assessed using a splice

site prediction program, which predicts strengths of 5' and 3' ss [8, 13]. Of all 8 introns in *per*, *dmpi8* was predicted to have the weakest splicing recognition signals. Weak splice sites have been shown to contribute to thermosensitive intron splicing in other models presumably by thermal destabilization of the interaction between the 5' splice site and U1 snRNA via base-pairing [14, 15]. Indeed, transgenic *Drosophila* models carrying a modified *dmpi8* intron whereby the 5' and 3' ss were optimized by site-directed mutagenesis (hereafter referred to as *dmpi8UP*), led to constitutively high splicing efficiency under a range of temperatures and exhibited decreased midday siesta compared to wildtype transgenic controls (hereafter referred to as *dmpi8WT*) [8]. These results are also consistent with earlier findings that higher *dmpi8* splicing efficiency is linked to decrease in midday siesta levels.

***dmpi8* splicing regulates midday sleep in a clock independent manner**

As discussed above, *D. melanogaster* mainly sleep during the day but also show a midday dip in activity or siesta [6, 16]. We assumed that splicing of *dmpi8* was affecting the daily distribution of activity via altering the dynamics of *per* mRNA/protein cycling and hence the clock. For example, prior work showed that the morning and evening peaks of activity are regulated by two separate oscillators that are coupled. Thus, we envisaged that changes in *dmpi8* splicing efficiency could delay/advance the morning and evening oscillators or its coupling strength by its direct effects on *per* mRNA/protein cycling. For example, higher *dmpi8*

splicing leads to an earlier upswing in PER protein, which would advance the evening peak and hence *secondarily* decrease midday siesta.

Nonetheless, we considered the possibility that *dmpi8* splicing might have a direct effect on sleep (not simply activity levels or its timing) during the midday. Indeed, *dmpi8UP* flies exhibit significantly less sleep during the midday compared to *dmpi8WT* flies, while nighttime sleep is virtually identical in both genotypes. Moreover, daytime sleep in *dmpi8UP* flies is more fragmented and less consolidated, suggesting less sleep drive. Curiously, the sleep differences between *dmpi8UP* and *dmpi8WT* flies persisted in constant light (LL) conditions. This was highly unexpected because extended exposure of flies to LL results in abrogation of the clock and PER protein levels remain constitutively low. These findings showed that the effect of *dmpi8* splicing efficiency on sleep levels does not rely on a functioning circadian clock [17].

Moreover, administering short light pulses during the night is a commonly used method to measure sensory mediated arousal thresholds in *Drosophila*. *dmpi8UP* flies remained awake longer and exhibited higher locomotor activity after exposure to these brief nocturnal light pulses when compared to *dmpi8WT* flies (similar results were seen when mechanical stimulation was used to test arousal threshold) [17] suggesting that *dmpi8* splicing may be exerting its effects on sleep by lowering sensory mediated arousal thresholds when it is spliced more efficiently. In summary, efficient *dmpi8* splicing has a wake-promoting effect in *D. melanogaster* during the day, and although the mechanism by which this effect was mediated was not yet known, it was clear that a functioning circadian clock

was not required and further suggested that it was independent of PER protein. As will be shown below, this was confirmed with the discovery of *daywake* (*dyw*).

Variation in midday siesta and *dmpi8* splicing in natural populations of *Drosophila melanogaster*

Unlike other species within the *Drosophila* genus, *D. melanogaster* has successfully spread beyond its ancestral range in the grasslands of tropical Africa to colonize every continent except Antarctica (Fig. 1.5A) [18], adapting to wide ranging changes in ambient temperature [19]. As mentioned above, the thermosensitive splicing of *dmpi8* contributes to the thermal adaptation of midday siesta in *D. melanogaster*. Based on these findings, and the wide spatial adaptation of *D. melanogaster*, prior work from our group used natural populations of *D. melanogaster* from different parts of the world to determine if midday siesta and/or *dmpi8* splicing efficiency showed natural variation. The overriding prediction was that flies adapted to cooler environments might exhibit decreased midday siestas and possibly increased *dmpi8* splicing compared to their more warm-adapted counterparts since there was less danger from daytime heat. To date, three different populations were analyzed; 1) from the Eastern coast of the United States; 2) as a function of altitude in tropical Africa; and 3) temperate and tropical regions along the eastern coast of Australia. Key findings from these studies are summarized below:

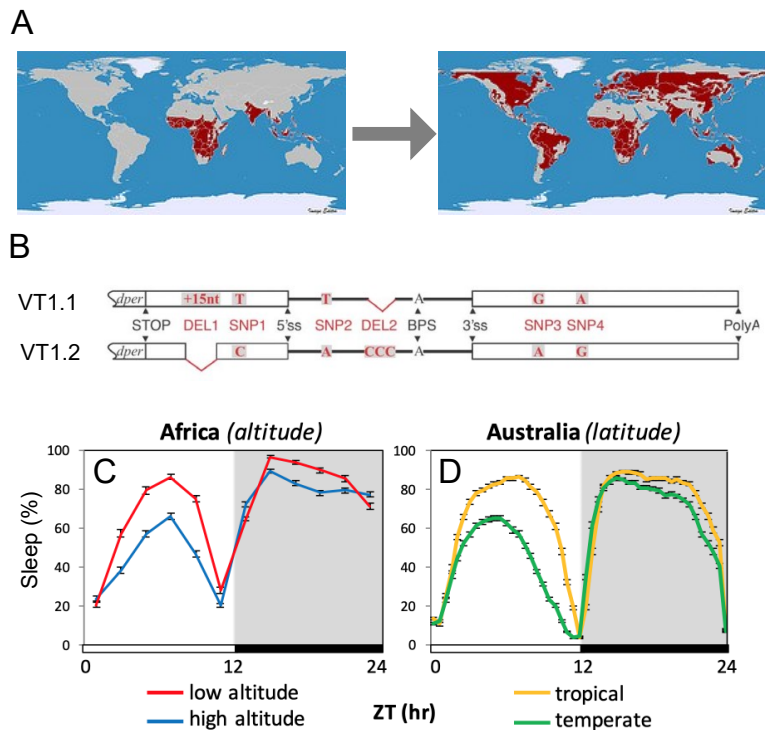


Figure 1.5. Midday siesta levels in natural populations of *Drosophila melanogaster* exhibit latitudinal and altitudinal clines. (A) *D. melanogaster* is thought to have originated in tropical regions of Africa. However, unlike other *Drosophila* species, *D. melanogaster* successfully colonized many regions around the world—spreading as a result of human travel. **(B)** Two main haplotypes of the *per* 3' UTR are observed in flies from the Atlantic coast of the United States. SNP3 is a key regulator of *dmpi8* splicing efficiency, whereby the G variant (VT1.1) leads to more efficient splicing compared to the A variant (VT1.2). **(C, D)** Populations adapted to high altitudes in tropical Africa (C) and temperate regions in Australia (D) exhibit decreased midday siesta levels compared to their low-altitude and tropical counterparts, respectively. Image sources (A), (B) Low et al., PLoS One, 2012. [7]; (C) [20]; (D) [21].

(1) A prominent SNP in the *per* 3' UTR from flies in the United States is causally linked to midday sleep and *dmpi8* splicing efficiency

In *D. melanogaster* populations collected along the Atlantic coast from Florida up to Vermont, no latitudinal cline in siesta was observed. However, sequencing of the *per* 3' UTR identified two major haplotypes, VT1.1 and VT1.2 (Fig 1.5B), consisting of four single nucleotide polymorphisms (SNPs1-4) among these groups [7]. Studies examining the effect of these haplotypes on *dmpi8* splicing using transgenic *Drosophila* models showed a marked difference in splicing efficiency between the two. Further testing revealed SNP3, which exists as either a G or A variant in haplotypes VT1.1 and VT1.2 respectively, to be largely responsible for the difference in *dmpi8* splicing levels between the 2 haplotypes, with SNP3/A variants splicing *dmpi8* less efficiently than SNP3G variants.. Importantly, this correlated with midday sleep levels; i.e., SNP3G flies have less midday siesta compared to SNP3A flies.

(2) Midday siesta levels and *dmpi8* splicing efficiency co-vary with altitude in *D. melanogaster* from tropical Africa

Tropical African fly populations adapted to higher altitudes, where daytime temperatures are generally cooler, exhibited reduced midday sleep and elevated *dmpi8* splicing compared to flies adapted to lower altitudes as predicted (Fig. 1.5C) [20]. In addition, 5 SNPs were identified in the *per* 3' UTR of African populations beyond SNPs1-4 previously reported in the flies from the United States (see above). However, no altitudinal cline in the frequency or distribution of the *per* 3'

UTR polymorphisms was observed. Thus, although *dmpi8* splicing efficiency showed an altitudinal cline that correlated with midday sleep, we could not uncover why *dmpi8* splicing changed as a function of altitude.

(3) *per* 3' UTR SNPs, siesta levels and *dmpi8* splicing efficiency exhibit a latitudinal cline in *D. melanogaster* from Australia

Intriguingly, midday siesta in fly populations collected along the eastern coast of Australia show variability as a function of latitude. Groups from temperate regions, where it is typically cooler, demonstrated more efficient *dmpi8* splicing as well as an attenuated siesta compared to their tropical counterparts (Fig. 1.5D). In contrast to American and African fly populations, however, a latitudinal cline in several *per* 3' UTR SNPs was observed. Thus, it appears that for *D. melanogaster* along the eastern coast of Australia, natural selection operating at the level of spatial segregation of ancestrally derived polymorphisms in the 3' UTR of *per* contributed to the establishment of an adaptive thermal cline in a sleep behavior. Part of the work presented in this thesis includes fly populations from Australia [7, 21].

Identification of a novel anti-siesta gene called *daywake* that is regulated *in-trans* by *dmpi8* splicing

As previously discussed, *D. melanogaster* exhibits more robust midday siesta at warmer temperatures, a phenomenon causally linked to thermosensitive splicing

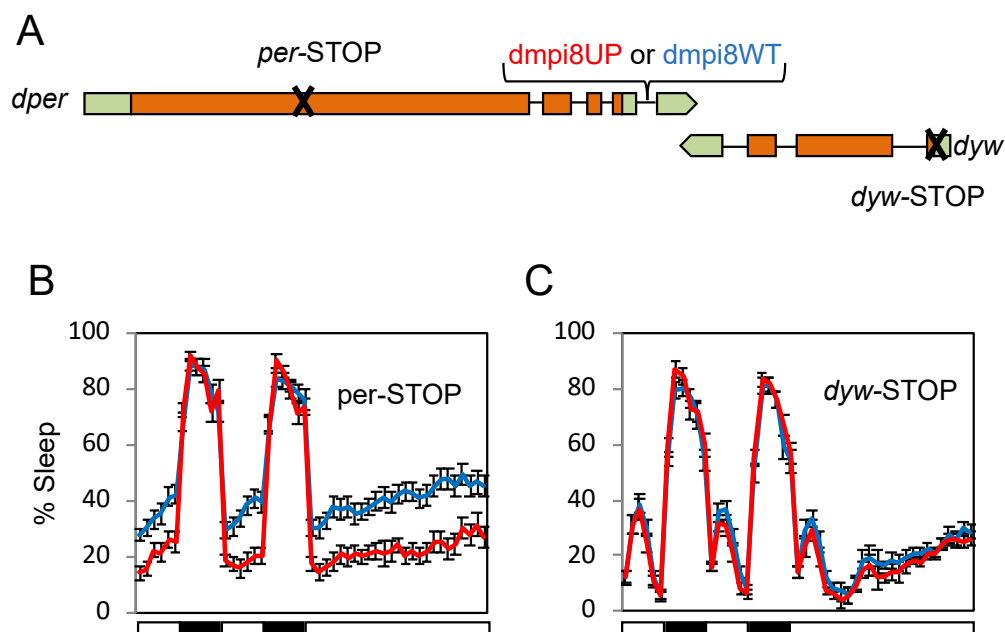


Figure 1.6. The splicing efficiency of *dmpi8* regulates midday siesta levels in an indirect manner via the slightly overlapping gene called *dyw*. (A) To test if *dmpi8* splicing efficiency regulates midday siesta levels via PER protein or DYW protein, several transgenes were evaluated in flies. Two variants of *dmpi8* were compared; *dmpi8UP* has higher *dmpi8* splicing efficiency and reduced midday siesta compared to the wildtype situation, *dmpi8WT*. We modified the *dmpi8UP* and *dmpi8WT* transgenes so that they carried premature stop codons in either *per* or *dyw*. (B) Abrogating PER protein production (*per-STOP*) has no effect on the ability of the *dmpi8UP* intron (red) to decrease daytime sleep compared to the control situation (blue). This difference continues in constant light. (C) However, eliminating *dyw* protein (*dyw-STOP*) abrogated the midday sleep difference between *dmpi8UP* and *dmpi8WT*. Horizontal bars; white, light; black, dark. Shown are the last two days in LD followed by LL. Adapted from Yang & Edery, 2019 [22].

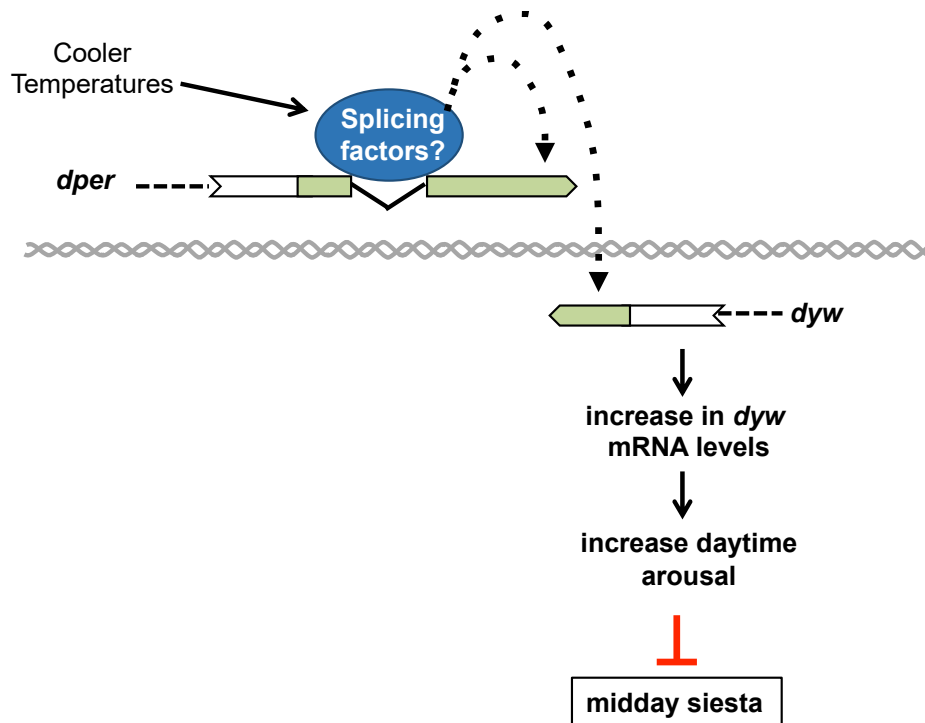


Figure 1.7. Proposed model for how *dmpi8* splicing/*dyw* regulate midday siesta in a temperature sensitive manner. On cold days, the association of the spliceosome with the *dmpi8* intron is enhanced, possibly due to stronger Watson-Crick base pairing between the U1-snRNA and the weak *dmpi8* splicing signals. Splicing of the *dmpi8* intron increases *per* mRNA levels (not shown; see Fig. 1.4). Though the mechanism remains unclear, it has been suggested that spliceosome binding enhances 3'-end formation, increasing *per* mRNA levels (Fig. 1.4). Likewise, since the 3' UTRs of *dyw* and *per* overlap by 49 base pairs, we propose spliceosome binding to *dmpi8* also functions *in-trans* to increase *dyw* transcript levels via a similar mechanism as that occurring for *per* transcripts. To the best of our knowledge, this type of *trans* gene regulation via splicing has not been described previously. Adapted from Yong & Edery, 2019 [22].

of the *dmpi8* intron [7, 8, 23]. Transgenic *dmpi8*WT flies (wildtype for *dmpi8* splicing) show attenuated daytime sleep compared to *dmpi8*UP lines (constitutively high *dmpi8* splicing), differences which persisted in constant light conditions suggesting that the effect of *dmpi8* splicing on daytime sleep is independent of the circadian clock [8, 17].

To more directly test the possibility that *dmpi8* splicing does not function via PER protein in regulating siesta, several transgenic models were generated whereby a stop codon was introduced into the *per* coding region of the *dmpi8*UP and *dmpi8*WT transgenes (Fig. 1.6A). Remarkably, midday siesta was still much lower in *per*-STOP[*dmpi8*UP] compared to *per*-STOP[*dmpi8*WT] transgenic flies (Fig 1.6B) [17, 22]. There is a slightly overlapping gene at the 3' end of *per*, which was originally called 0.9. It encodes a predicted juvenile hormone binding protein (JHBP) [24, 25]. Surprisingly, placing a stop codon in the 0.9 gene abrogated the sleep differences from *dmpi8*UP and *dmpi8*WT. Moreover, the increased splicing efficiency of *dmpi8*UP led to higher levels of 0.9 transcripts compared to *dmpi8*WT. Additional studies using RNAi and overexpression showed that the 0.9 gene functions in an anti-siesta manner, which led to it being renamed *daywake* (*dyw*) (Fig 1.6C).

This relationship between *dmpi8* splicing and *dyw* expression was similarly observed in WT laboratory strains incubated at different temperatures; at low temperatures where *dmpi8* is spliced more efficiently, *dyw* transcript levels were higher and vice versa in warmer conditions. Lastly, the well-established UAS-Gal4 system was used to exogenously up- or down-regulate *dyw* expression in a variety

of tissue types. In these flies, overexpression of *dyw* lead to significantly lower daytime sleep and conversely down-regulation of *dyw* resulted in elevated sleep levels. These results indicated that *dyw* is a negative regulator of midday sleep that mediates the effects of *dmpi8* splicing on midday sleep. It was suggested that splicing factors assembled on *dmpi8* are able to help recruit mRNA maturation factors to the overlapping 3' end of *dyw* increasing the rate at which *dyw* accumulates in the cell (Figure 1.7). Characterizing the DYW protein, its regulation, spatial distribution and function forms the basis for this thesis.

Brief summary of juvenile hormone binding proteins

Juvenile hormone (JH) is an insect hormone secreted by the corpus allatuma (Fig 1.8 Panels A and B) which has been shown to counteract the effects of the metamorphosis promoting hormone 20-hydroxyecdysone (20E), thus maintaining insects in the juvenile state, hence its name [24-26]. During development, JH and 20E play critical yet opposite roles in the timing of metamorphosis until late in the larval stage when JH levels quickly disappear and transition to the pupa occurs. JH is a lipophilic molecule, as such JH signaling via secretion into the aqueous hemolymph (analogous to blood in insects) would prove problematic were it not for Juvenile Hormone Binding Proteins (JHBPs). These proteins bind JH and facilitate its diffusion throughout the hemolymph enabling it to interact with all insect tissues while also preventing undesired JH accumulation in lipophilic structures (Fig 1.8C). Although JH-signaling has been best described during development, more recent

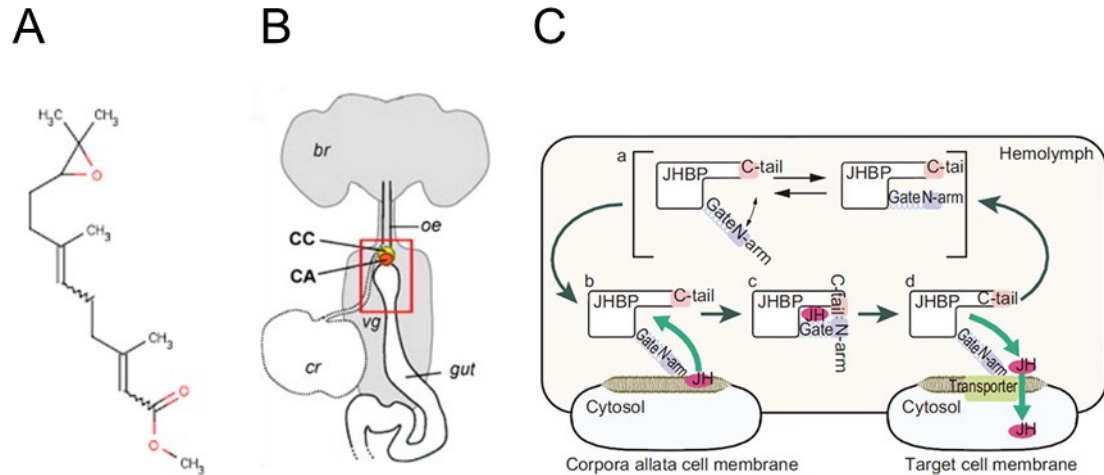


Figure 1.8. Overview of Juvenile Hormone Binding Protein function in *Drosophila*. (A) Structure of juvenile hormone (JH). (B) JH is produced by the corpus allatum, followed by secretion into the hemolymph. Abbreviations: CA, corpus allatum; CC, corpus cardiacum; br, brain; vg, ventral ganglia; oe, oesophagus; cr, crop. (C) Circulating juvenile hormone binding proteins (JHBPs) in the hemolymph binds JH made in the corpora allatum, protecting it from degradation and delivering the hormone to target tissues, initiating a signal transduction cascade. Although this schematic represents the best-established role for JHBPs, it is possible that JHBPs have other functions besides acting as lipid carriers in the hemolymph. Image sources: (B) Gruntenko et al., *J. Insect Physiol.* [27]; (C) Suzuki et al., *Sci. Rep.* [28]

work has shown roles in feeding behavior and sexual dimorphism in sleep distribution in *Drosophila* [29].

Overview of Thesis

The work presented in this thesis involves the biochemical and behavioral characterization of a recently reported, novel wake-promoting gene known as *daywake* (*dyw*). Chapter 2 describes work that investigates the localization of *dyw* in *Drosophila* as well and also presents evidence detailing the mechanism of DYW protein expression and its biochemical properties. In Chapter 3, we significantly revise the previously reported daytime-specific effects of *dyw*, finding that instead of a limited role in thermal adaptation of siesta, *dyw* has a broader role in coordinating daily wake-sleep behavior with survival demands. I also include three addendum sections detailing: 1) The work necessary to optimize the use of our anti-DYW antibodies for use in quantitative analysis; 2) previous work attempting to test the idea that hyper-phosphorylation of PER modifies its conformation, and lastly; 3) transgenic flies that were generated in the course of this study that were ultimately not used but will form the foundation for further study on *dyw*.

Chapter 2: The Anti-Siesta protein DAYWAKE is secreted, regulated by glycosylation and accumulates in key brain clock neurons

Abstract

Similar to many diurnal animals, *D. melanogaster* exhibits a midday siesta that is more pronounced on warm days. Recent work identified *daywake* (*dyw*) as a novel anti-siesta gene that is upregulated at colder temperatures via a mechanism involving a thermosensitive splicing event from the slightly overlapping *period* (*per*) circadian clock gene. Consistent with the prediction that DYW is a member of the juvenile hormone binding protein (JHBP) family, experiments in cultured *Drosophila* S2 cells reveal that DYW is secreted in a signal-peptide-dependent manner. Mutational analysis identified a key glycosylation site that regulates DYW levels, suggesting this residue is critical for DYW maturation or stability. In flies, it is likely that there are two major isoforms of secreted DYW; glycosylated and non-glycosylated. DYW is found in the head and body, including key circadian clock neurons in the brain. The abundance of DYW is increased at cooler temperatures and higher *dmpi8* splicing efficiency. We suggest that in adult flies, DYW produced in the brain is secreted into the hemolymph where it binds juvenile hormone, initiating downstream signaling cascades that regulate the daytime wake-sleep behavior of flies.

Introduction

Sleep is essential to animal survival. Though the molecular underpinnings of sleep are not fully understood, sleep defects have been associated with a multitude of diseases, including certain cancers, cognitive impairment and diabetes in humans [30-32]. Over the last 20 years, *Drosophila* has emerged as a critical model to further our understanding of sleep [3, 4]. In diurnal animals, such as *Drosophila* and humans, sleep occurs mainly during the nighttime hours, however many also exhibit a daytime sleep drive generally referred to as “siesta” [33]. Similar to *Drosophila*, which tend to have more robust midday sleep at higher temperatures, siesta in humans is most widely observed in warmer climates and recent evidence indicates a genetic basis [34]. While this sleep drive is likely a protective mechanism to avoid heat exposure during hot days, excessive daytime sleep, or “sickness behavior”, is linked to worse prognoses in a wide range of diseases, from diabetes to neurological disorders [35, 36]. It is becoming clearer that nighttime and daytime sleep serve different functions and are likely to be regulated by overlapping but distinct pathways.

The mechanism by which ambient temperature modulates siesta in flies remained elusive for some time. A breakthrough came with the discovery midday siesta is regulated by the thermosensitive splicing of the *dmpi8* intron (*Drosophila melanogaster period* intron 8) found in the 3' UTR of the main circadian gene *per*. Most notably, *dmpi8* splicing efficiency is progressively increased as daily temperatures become cooler, which somehow causally leads to decreases in

midday siesta levels [9]. Later studies revealed that *dmpi8* splicing affects midday sleep independently of PER protein expression [17].

Most recently, we identified the first “anti-siesta” gene called *daywake* (*dyw*) [22]. In the *Drosophila* genome, the 3' UTRs of *dyw* and the reverse oriented *per* slightly overlap. Remarkably, expression of *dyw* is regulated *in-trans* by the splicing efficiency of *dmpi8*. As *dmpi8* splicing efficiency increases with cooler ambient temperatures, *dyw* expression also increases, thereby attenuating midday siesta drive. Due to the thermosensitivity of *dmpi8* splicing and its ability to modulate *dyw* levels, this genetic unit enables flies to remain active during cool days when the risks from heat exposure are diminished.

How *dyw* functions in regulating daytime sleep is not clear. The *dyw* gene encodes a putative juvenile hormone binding protein (JHPB) which are typically secreted into the hemolymph (fly equivalent of blood) where they bind the lipophilic juvenile hormone (JH), delivering it to target tissues and initiating downstream signaling cascades. Although JHPBs are mainly associated with developmental roles, some have also been shown to affect behavior, such as feeding and courtship [37, 38]. JHPBs are only found in arthropods but are part of a larger TULIP family of lipid binding proteins which play myriad roles in other organisms [39].

Herein, we generated anti-DYW antibodies and biochemically characterized DYW protein in adult flies and cultured *Drosophila* cells. Our findings indicate that DYW undergoes signal-peptide dependent cleavage and secretion via a mechanism that involves a key glycosylation event. Whole brain staining shows

that DYW is expressed in numerous cells in the brain, including key clock neurons. DYW protein levels are modulated by *dmpi8* splicing efficiency and daily temperature, in a manner consistent midday siesta levels.

Materials & Methods

Drosophila Maintenance

Drosophila stocks were routinely maintained at 25°C in vials or bottles containing Bloomington Standard Medium (1.6% Yeast, 0.5% Soy Flour, 7% Yellow Cornmeal, 1% Agar, 7.5% Light Corn Syrup, 0.5% Propionic acid, 0.2% Tegosept), unless otherwise noted. In general, prior to an experiment, young adult flies (3-5 day old) were first exposed to several daily 12 h light/ 12 h dark cycles [LD; where Zeitgeber 0 (ZT0) = lights-on] at the indicated temperature, prior to removal at desired times. Flies used in this study include, wildtype Canton-S (BDSC #64349), natural populations from Australia [21], *w*¹¹¹⁸, UAS-*dyw* [22], *per*-Gal4 (BDSC #7127), *Gmr*-Gal4 (BDSC #1104), *Cry16*-Gal4 (BDSC #24514), RNAi-*dyw* (BDSC #56988).

DAYWAKE Antigen and Antibody Generation

The open reading frame encoding amino acid residues 26 through 260 of *dyw* [*dyw*(Δ 1-25)] was subcloned into the pET-16b vector using restriction sites NdeI and BamHI such that the 6xHis tag was situated in frame at the N terminus. Constructs were transformed into Tuner(DE3)pLysS competent cells [*F*⁻ *ompT* *hsdS_B* (*r_B*⁻ *m_B*⁻) *gal dcm lacY1*(DE3) pLysS (Cam^R)] a kind gift from Elliot Campbell

and Steven Anderson. Expression was induced by the addition of isopropyl- β -D-thiogalactoside (IPTG) to a final concentration of 0.5mM when the media reached an $OD_{600} = 0.6$. After 2 hours of induction, cells were harvested by centrifugation at 3,000xg for 15 minutes. Subsequently, cells were resuspended in 5ml of Lysis Buffer (20mM Tris·HCl [pH 8.0], 150mM NaCl, 6M Urea), sonicated and incubated on ice for 30 minutes. Insoluble debris was removed by centrifugation at ~27,000xg for 20 minutes at 4°C, and the supernatant was used for downstream affinity purification.

His-TALON Affinity Resin was washed in cold 1xTBS (150 mM NaCl, 50 mM Tris [pH 7.6]) and equilibrated in lysis buffer for 10 minutes. Supernatant was loaded onto the resin and incubated at 4°C with end over end rotation for 30 minutes. Resin was collected via centrifugation and washed 3 times in cold 1x Wash Buffer (20mM Tris [pH 8.0], 150mM NaCl, 25mM Imidazole, 6M Urea). The bound fraction was eluted by incubating resin in 900 μ l of Elution Buffer (20mM Tris [pH 8.0], 150mM NaCl, 200mM Imidazole, 6M Urea) at room temperature for 10 minutes with occasional mixing. Eluates were analyzed by SDS-polyacrylamide gel electrophoresis (SDS-PAGE) followed by Coomassie staining to determine DYW(Δ 1-25) protein purity and yield. Briefly, protein samples were resolved by 12% SDS-polyacrylamide gel electrophoresis (PAGE; 12% resolving gel; 29.6%Acrylamide/0.4%N,N'-Methylene-bis-acrylamide, 0.4M Tris·HCl [pH 8.8], 0.1% SDS, 0.05% Ammonium Persulfate, 0.02% Temed) and then fixed in a 50% methanol, 10% glacial acetic acid solution for 1 hour at room temperature. After fixation, the gel was stained using a 0.1% Coomassie Brilliant Blue R-250, 50%

methanol, 10% glacial acetic acid solution for 20 minutes at room temperature. Gels were then de-stained in a 40% methanol, 10% glacial acetic acid solution at room temperature, replacing the de-staining solution as necessary until background staining had disappeared.

Aliquots of purified DYW(Δ 1-25) protein were sent to Cocalico Biologicals (Stevens, PA) where they injected one guinea pig and two rat hosts using Freund's Adjuvant System. In this study, only results with the guinea pig antibody (GP49) are shown, as it produced less background (see Addendum 1).

Protein Extract Preparation from Adult Flies

Flies were kept at 25°C in Bloomington Standard Medium (1.6% Yeast, 0.5% Soy Flour, 7% Yellow Cornmeal, 1% Agar, 7.5% Light Corn Syrup, 0.5% Propionic acid, 0.2% Tegosept), unless otherwise noted. In general, adult flies were first entrained in daily 12 h light/ 12 h dark cycles [LD; where Zeitgeber 0 (ZT0) = lights-on] for several days at the indicated temperature, removed at desired times, then immediately frozen on dry ice. Head extracts were prepared as previously reported [40] and body extracts were prepared in the same manner. Briefly, heads and bodies were isolated by mechanical agitation and sorted using nested sieves (Newark Wire Cloth Company, Sieve nos. 40 and 25, 425 μ m and 710 μ m, openings respectively). Heads/bodies were homogenized in modified RIPA buffer (50mM Tris·HCl [pH 7.5], 150mM NaCl, 1% Nonidet P-40, 0.25% Sodium Deoxycholate, 1x Protease inhibitor cocktail [Roche cat# 11873580001]) using a motorized pellet pestle (Kimble cat#749521-1590) (Kontes cat# 749540-0000). Homogenized

samples were then centrifuged at $\sim 17,000 \times g$ for 20 minutes at 4°C to remove lipid and insoluble protein fractions. Soluble protein in the supernatant were assayed for concentration was assessed using the Pierce Coomassie Plus Assay Kit. Samples were then stored at -80°C or used straight away.

Western Blotting of Fly Protein Samples

(Please see Addendum 1 for further details on optimization of Western blotting conditions for detecting DYW). Fly protein samples were added to 4x SDS-PAGE sample buffer (final concentration 62.5mM Tris·HCl [pH 6.8], 2.5% SDS, 0.002% Bromophenol Blue, 10% glycerol) and boiled at 95°C for 5 minutes. Equal total protein was loaded onto a 12% SDS-polyacrylamide gel (12%; 29.6%Acrylamide/0.4%N,N'-Methylene-bis-acrylamide, 0.4M Tris·HCl [pH 8.8], 0.1% SDS, 0.05% Ammonium Persulfate, 0.02% Temed). Following electrophoresis, resolved proteins were transferred onto a $0.45\mu\text{m}$ pore size nitrocellulose membrane (GE Amersham cat#10600002) using a BioRad Trans-Blot SD semidry transfer cell (BioRad cat# 1703940).

Membranes were subsequently washed in 1x Tris Buffered Saline with Tween (1xTBST: 20mM Tris [pH 7.5], 150mM NaCl, 0.05% Tween-20) for 10 minutes after transfer, and blocked in 1% Blotting-Grade Blocker (BioRad cat#1706404) diluted in 1xTBST for 30 minutes. After blocking, membranes were washed with 1xTBST and incubated with shaking for 1 hour at 4°C with anti-DYW antibody GP-49 diluted 1:4000 in 0.1% Blocker (diluted in 1xTBST). Membranes were then washed with 1xTBST and incubated for 1 hour in anti-guinea pig HRP

conjugated antibody diluted 1:10,000 in 0.1% Blocker (diluted in 1xTBST). Signal was detected using Amersham ECL Prime (GE cat# RPN2232) and imaged either on an Azure Biosystems c600 imager or exposed to radiographic film (LabScientific cat#XAR ALF 1318) and developed using an AFP Imaging Corp. mini-medical automatic developer.

Affinity Purification of DYW-3xFLAG from Adult Flies

Expression of *dyw* in clock cells using the UAS-Gal4 system, decreases midday siesta [22]. In unpublished work, Dr. Yang also generated transgenic flies carrying a UAS-*dyw* transgene that includes a 3xFLAG epitope at the C-terminus of the *dyw* open reading frame, termed UAS-*dyw*-3xFLAG (personal communication, Yong Yang). Similar to UAS-*dyw*, UAS-*dyw*-3xFLAG is functional when expressed in *Drosophila* using several different clock drivers such as *per*-Gal4 (unpublished results, Yong Yang). Herein, I used these flies to further validate the specificity of our anti-DYW antibodies. Briefly, we crossed virgin female *per*-Gal4 and male UAS-*dyw*-3xFLAG flies. Adult progeny from this cross were kept at 25°C, entrained for 3-5 days in LD and collected at the same time. Head extracts were prepared as described above using modified RIPA buffer, and DYW-3xFLAG purified via affinity purification using an anti-FLAG resin. Briefly, a 1:1 slurry containing magnetic anti-FLAG affinity resin (Millipore Sigma cat# M8823) was washed 3x in 1xTBS in 1.5 microcentrifuge tubes. Resin was collected using a magnetic particle separator (MPS) (ThermoFisher cat#A13346) and equilibrated in modified RIPA buffer for 5 minutes on ice. Subsequently, *Drosophila* protein

head extract (≥ 50 heads) was mixed with 50 μ l pre-equilibrated resin, followed by end-over-end incubation at 4°C for 1 hour. The resin was washed 2x with cold modified RIPA buffer, and bound DYW-3xFLAG eluted by incubating 95°C in modified elution buffer (150mM Tris·HCl [pH 6.8], 6mM EDTA, 3% SDS, 30% Glycerol) for 5 minutes. Eluates were separated from the resin using an MPS and stored at -80°C. The affinity purified DYW-3xFLAG was visualized by immunoblotting as described above using commercially available anti-FLAG antibody (Millipore Sigma cat#M8823-1ML)

Whole Brain Imaging

Adult flies were collected at the indicated times during entrainment in LD and fixed in 4% paraformaldehyde at room temperature (RT). After fixation, brains were isolated and washed in cold phosphate buffered saline (PBS) solution. Subsequently, brains were incubated in blocking solution (10% goat serum in PBS) for 1 h at RT. After blocking, brains were incubated in darkness overnight at 4°C with anti-DYW and anti-Pigment-Dispersing Factor (PDF) antibodies diluted 1:500 and 1:50 in blocking solution, respectively. Brains were then washed with cold PBS and incubated overnight in darkness at 4°C with goat serum at a final concentration of 10% in 1XPBS containing the secondary antibodies Alexa Fluor 488-conjugated anti-guinea pig IgG and Alexa Fluor 488-conjugated anti-mouse IgG, both at a final dilution of 1:200. After extensive washing with cold PBS, brains were mounted on slides using Vectashield (Vector Laboratories cat# H-1000).

Confocal images were obtained with a Leica SP2 confocal microscope at 40x magnification and processed with LCS Lite software.

Generation of *daywake* constructs for expression in S2 cells

dyw inserts were generated by amplifying the *dyw* coding sequence using forward primers NdeI_0.9FL_F or NdeI_0.9(26-260)_F with reverse primer BamHI_0.9R for generating constructs pMT-DYW and pMT-DYW(Δ 1-25), respectively (primers listed in Table 2.1). The resulting amplified fragments were cloned into pMT-V5/His (ThermoFisher cat#V412020) using NdeI and BamHI. Constructs were transformed into JM109 *E. coli* competent cells (*endA1*, *recA1*, *gyrA96*, *thi*, *hsdR17* (r_k^- , m_k^+), *relA1*, *supE44*, Δ (*lac-proAB*), [F' *traD36*, *proAB*, *lacI^qZ Δ M15*]) (Promega cat# L2005). After antibiotic selection on LB agar plates, plasmid DNA was isolated from 5 transformants and the correct sequences verified by Sanger sequencing using the MT_Forward primer (Table 2.1).

The DYW(N182) mutant was generated from the pMT-DYW construct using the QuikChange II XL site directed mutagenesis kit (Agilent cat#200521) using primers 09_N182A_F and 09_N182A_R (Table 2.1). Constructs were transformed into XL-10 Gold *E. coli* (Tet^r Δ (*mcrA*)183 Δ (*mcrCB-hsdSMR-mrr*)173 *endA1* *supE44* *thi-1* *recA1* *gyrA96* *relA1* *lac* Hte[F' *proAB* *lacI^qZ Δ M15* Tn10 (Tet^r) Amy Cam^r]); transformants were verified as described above.

Recombinant plasmid DNA was prepared using Nucleospin Plasmid recovery kits according to manufacturer's protocol (Macherey Nagel cat# 740588.250).

Culture and Transfection of *daywake* Constructs in *Drosophila* S2 Cells

Drosophila S2 cells (ThermoFisher cat#69007) were kept in 25cm² tissue culture flasks (Falcon cat#353014) containing 5ml Schneider's Media (ThermoFisher cat#21720001) at 18°C. Cells were split 1:10 every 7 days into fresh Schneider's media.

Constructs were transfected into cultured *Drosophila* S2 cells using the Effectene transfection system (Qiagen cat#301427). Briefly 1x10⁵ cells were seeded into 6-well tissue culture plates (Falcon cat#353046) containing 1.6ml Schneider's Media. Cells were allowed to grow for 24 hours after which 400ng of recombinant plasmid DNA was added to the media. After incubation for 3 days, cells were washed with 1xPhosphate Buffered Saline (PBS; 137mM NaCl, 2.7mM KCl, 10mM Na₂HPO₄, KH₂HPO₄). After washing, 1.6ml Schneider's media containing CuSO₄ at a concentration of 0.5mM was added to induce expression of metallothionein promoter-based constructs (pMT), and cells were cultured for another 24 hours.

Protein Extract Preparation from Cultured *Drosophila* S2 Cells and Culture Media

Cells were collected in 15ml conical tubes by centrifuging at 2000 RPM (Beckman model TJ-6). Culture media was removed and stored for further analysis at 4°C (see below). Following centrifugation, pelleted cells were resuspended in 1ml 1xPBS and transferred to 1.5 microfuge tubes, washed 3x by resuspension in 1xPBS followed by centrifugation at ~17,000xg. After washing, pellets were

homogenized in 50 μ l modified RIPA buffer (see above for composition) with a motorized pellet pestle, followed by 30 min incubation on ice. Homogenized samples were subsequently centrifuged at \sim 17,000 \times g and the supernatant containing soluble protein was assayed for concentration using the Pierce Coomassie Plus Assay Kit, as described above.

Endoglycosidase H Treatment of Protein Extracts from Cultured *Drosophila* S2 Cells

As per manufacturer's protocol (Promega cat# V4871), 20 μ g total protein from intracellular extracts (representing \sim 1 \times 10⁴ cells or \sim 3% of total cells) and 5 μ l culture media (representing \sim 0.3-0.5% of the available media) was added to ddH₂O and 1 μ l 10xDenaturing Buffer (5% SDS, 400mM DTT) to a final volume of 10 μ l. This mixture was incubated for 5 minutes at 95°C and then allowed to cool to room temperature. 2 μ l 10xEndoH Reaction buffer, 2500U EndoH and ddH₂O were then added to a final volume of 20 μ l (final concentrations; 1 μ g/ μ l protein, 0.25% SDS, 20mM DTT, 50mM sodium citrate [pH 5.5]). The reaction was allowed to continue at 37°C for 4 h whereupon equal volumes of the reaction mixtures for each condition were run on a 12% SDS-PAGE gel and probed for DYW by immunoblotting as described above (following Table 2.1, next page).

Table 2.1 List of primers

Primer Name	Sequence (5'→3')
NdeI_0.9(26-260)_F	GTGTGCATATGTCCGAAGGATTTCCATCGCCGCT GAAGCG
BamHI_0.9R	GTGTGGGATCCTCATTCTTTTCGAAGAACTCGT CGTAGGGAATGTTGGC
NdeI_0.9FL_F	GTGTGCATATGATGCAGCTAACCGGTGCCTCTAT GTTCTCG
0.9(A>D_25)F	GGAAATCCTTCGGAGTCGTCCACTCTGCAGG
0.9(A>D_25)R	CCTGCAGAGTGGACGACTCCGAAGGATTTCC
09_N182A_F	GTCTTGTAGTCGGTGATGGCGAGATAGGTGTGG CCATC
09_N182A_R	GATGGCCACACCTATCTCGCCATCACCGACTACA AGAC
MT_Forward	CATCTCAGTGCAACTAAA

Results

DAYWAKE is found in adult *Drosophila* heads and is responsive to temperature and *dmpi8* splicing efficiency

In order to biochemically characterize the DYW protein, we raised antibodies via immunization of guinea pig and rat hosts using a recombinant derived DYW immunogen. Using the ProtScale program [41] we determined that DYW residues 1-25 likely comprise a highly hydrophobic signal peptide region which may affect our ability to generate and purify sufficient antigen (Fig. 2.1A). To avoid this, DYW immunogen was generated by cloning a recombinant *dyw* ORF with a deletion of the region encoding aa1-25 into the pET-16b vector in frame with a 6xHistidine tag for expression in Tuner(DE3)pLysS *E. coli* (see materials and methods) and purified via His-TALON affinity chromatography (Fig. 2.1B and C).

Sera was initially tested against the *E. coli* expressed DYW(Δ 1-25) immunogen used for injection, in addition to fly head homogenate from *w*¹¹¹⁸ wildtype flies. Heads were used as the initial tissue to probe because *dyw* mRNA is expressed there and manipulating its expression in clock cells affects midday siesta [22]. Following immunoblotting, a signal migrating at an apparent molecular weight (MW) of ~30kDa, consistent with the theoretical 29.18 kDa molecular mass of DYW, was detected in both *E. coli* and *Drosophila* extracts (Fig. 2.1D, lanes 1 and 2). This signal was not present when using pre-immunized control serum on the same samples (Fig. 2.1D, lanes 3 and 4). We observed a closely running doublet when probing fly material, whereby the smallest electrophoretic isoform in flies co-migrated with that observed in the bacterial sample (compare lanes 1 and

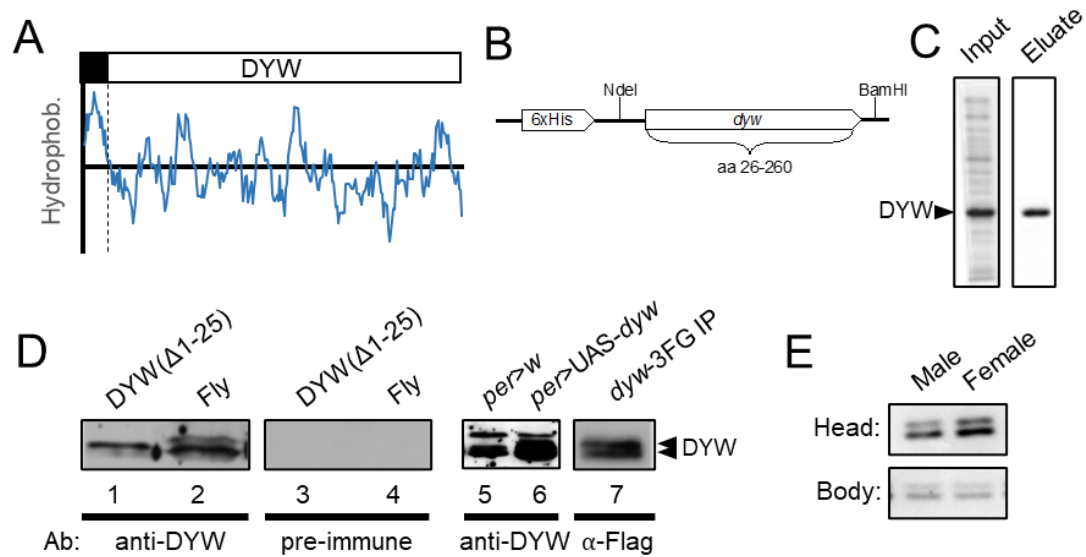


Figure 2.1. Anti-DYW antibody identifies a closely migrating DYW doublet in flies. **(A)** Residues 1-25 in the DYW protein sequence (left of dotted line) are predicted to be a signal peptide. **(B)** Schematic of construct for immunogen. **(C)** Aliquots of starting extract (input) and purified 6xHis-DYW(Δ1-25) (eluate) were resolved by SDS-PAGE and visualized by commassie staining. **(D)** Immunoblotting using anti-DYW antibodies identifies a doublet in fly head extracts. The faster migrating band in flies co-migrates with DYW(Δ1-25) produced in bacteria (compare lanes 1 and 2). Several controls: Absence of signal with pre-immune sera (lanes 3 and 4); increased DYW levels in flies with UAS-Gal4 mediated expression of *dyw* in *per*-expressing cells (*per*>UAS-*dyw*, lane 6) compared to control flies (*per*>*w*¹¹¹⁸, lane 5); and, detection of DYW-3xFlag in head extracts from *per*>UAS-*dyw*-3xFLAG transgenic flies following purification using an anti-FLAG resin (lane 7). **(E)** Equal protein amounts were loaded for both head and body extracts from wildtype flies, representing ~15-20 heads and ~5-6 bodies.

2). This suggests that at least some DYW in flies is cleaved (see below). Several test experiments showed that sera from the guinea pig host was strongest with the least background, and hence was used throughout this thesis (data not shown, see Addendum 1). To further validate our anti-DYW antibodies, we immunoblotted fly head protein extracts from transgenic *Drosophila* ectopically expressing either *dyw* [22] or *dyw-3xFlag* (to be described elsewhere). A stronger signal over background was observed when overexpressing *dyw* (Fig. 2.1D, compare lanes 5 and 6). Likewise, a similar doublet was observed after affinity purification of recombinant DYW-3xFLAG (Fig. 2.1.D, lane 7). Additionally, DYW was detected in both the heads and bodies of male and female flies suggesting that it may play roles both in neuronal as well as other physiological responses.

Prior work showed that *dyw* expression is higher at cooler temperatures, almost certainly due to more efficient *dmpi8* splicing efficiency [22] (see Fig. 2.2, A and B). As an initial attempt to evaluate the thermal responsiveness of DYW levels in fly heads, we exposed flies to either 18°C or 25°C and entrained them to several cycles of LD. We collected flies 12 h apart at ZT2 and ZT14 as *dyw* transcript levels exhibit at best a low-amplitude daily rhythm [22]. In addition, we probed males and females separately, since females exhibit lower midday siesta levels compared to males [6]. In general, the results indicate that DYW protein levels are elevated at 18°C compared to 25°C (Fig. 2.2, C and D). Several independent experiments verify that DYW levels are higher at cooler temperatures, whereas any differences due to gender or time-of-day requires further examination (data not shown).

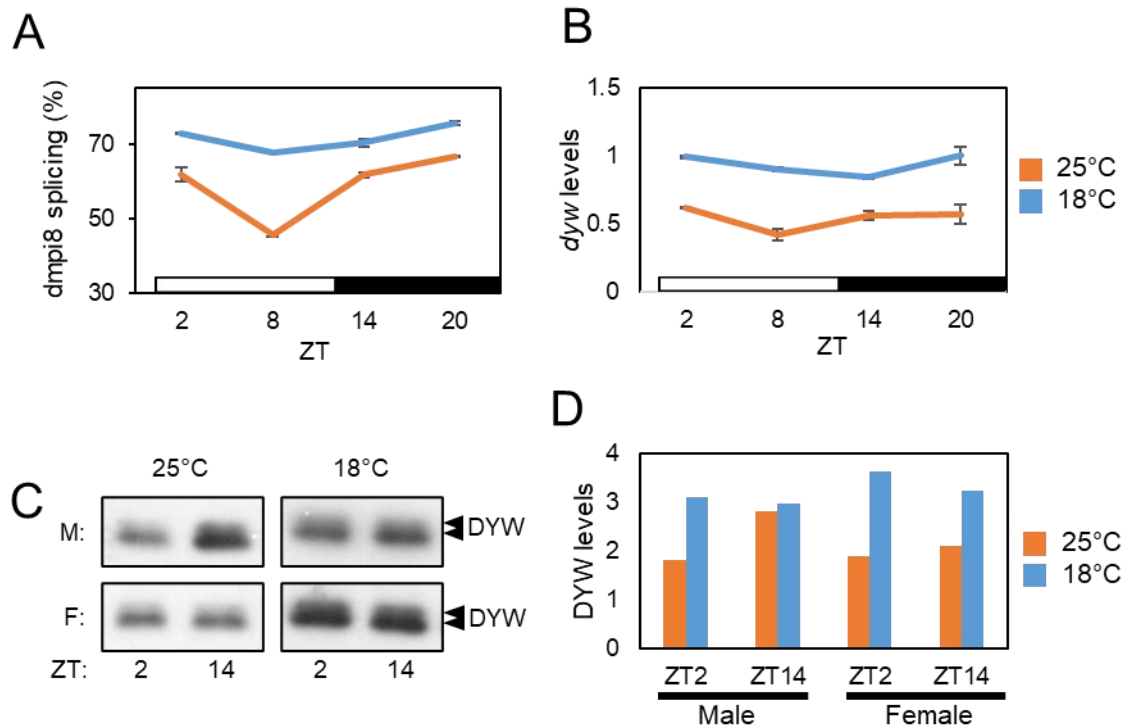


Figure 2.2. Decreasing daily temperature leads to an increase in DYW protein levels. Flies were entrained for 4 days in LD at the indicated temperature (18° or 25°C) and collected on the fifth day at the indicated time [where zeitgeber time 0 (ZT0) is defined as lights-on]. **(A, B)** Total RNA was isolated from fly head extracts and used to measure *dmpi8* splicing efficiency (A) and the relative levels of *dyw* transcript (B). Horizontal bars represent 12 h of light (white) and 12 h of dark (black). Male and Female adult flies were processed together. Data shown in panels A and B adapted from [22]. **(C, D)** Males (M) and females (F) were separated prior to entrainment in LD. DYW protein was detected by immunoblotting of fly heads (C), and quantification of the results is shown in (D).

In another set of experiments, we measured DYW levels in several different natural populations of *D. melanogaster*. The underlying rationale is that *dmpi8* splicing efficiency is strongly influenced by a single nucleotide polymorphism in the *per* 3' UTR (termed SNP3) (Fig. 2.3A). SNP3 exists exclusively as either an A or G variant; when SNP3 is a G the splicing efficiency of *dmpi8* is higher compared to A [7, 21]. Therefore, we predicted that *dyw* transcript and DYW protein levels would be elevated in SNP3G carrying populations compared to their SNP3A carrying counterparts. Indeed, both transcript and protein levels were significantly higher in SNP3G flies (Fig. 2.3, B and C). Taken together, these results indicate that not only *dyw* transcript levels but also DYW protein abundance is regulated by *dmpi8* splicing efficiency. We note that we also immunoblotted body extracts and detected DYW (data not shown). This is a potentially interesting observation that will require future studies to determine if DYW has a physiological role in adults outside of the head.

DAYWAKE is expressed in circadian clock neurons in the fly brain

Prior work using the UAS-Gal4 system in combination with RNA interference (RNAi) suggested that clock cells are key sites for DYW production in regulating midday sleep [22]. This is not surprising since *dyw* mRNA levels are modulated by splicing of the *dmpi8* intron, and hence, there should be some overlap in the spatial expression patterns of *dyw* and *per* (see Fig. 1.7). Thus, we predicted that downregulation of *dyw* in clock cells would lead to an observable reduction in DYW protein levels. Indeed, expression of RNAi-*dyw* (*dyw-i*) using drivers that widely

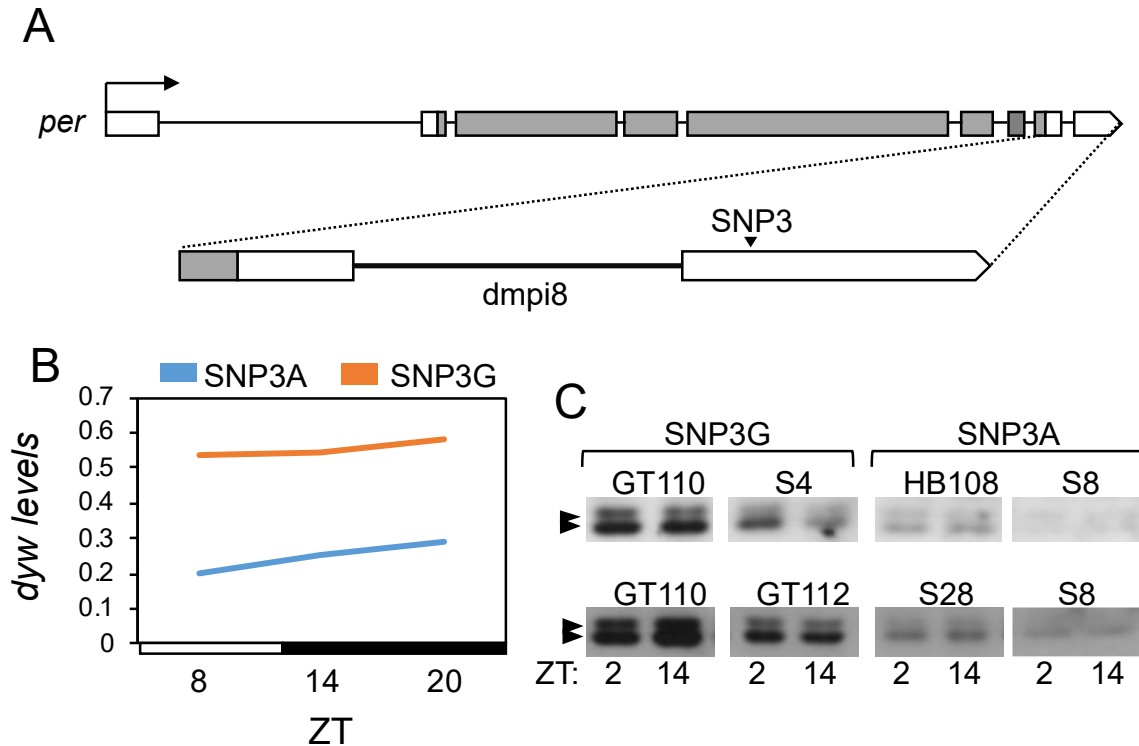


Figure 2.3. DYW protein levels are elevated in natural populations of *Drosophila* which differ in their *dmpi8* splicing efficiencies. (A) Schematic representation of the *per* transcription unit showing the location of SNP3 in the 3' UTR. Open bars, non-coding region; gray bars, coding regions; lines, introns; arrow, start of transcription. (B, C) Flies were exposed to 4 days of LD at 25°C, collected on the fifth day at the indicated times [where zeitgeber time ZT0 is defined as lights-on], and head extracts prepared to measure either *dyw* transcript (B) or protein (C) levels. Results shown in panels B and C come from different experiments. For panel B the following lines of Australian populations were used (SNP3G: GT110, S4; SNP3A: HB22, HB106, HB108, GT46, GT92, S22, S28, HB25, S3, S7 S8, S12, S34). For panel B, the lines are indicated (top of panels).

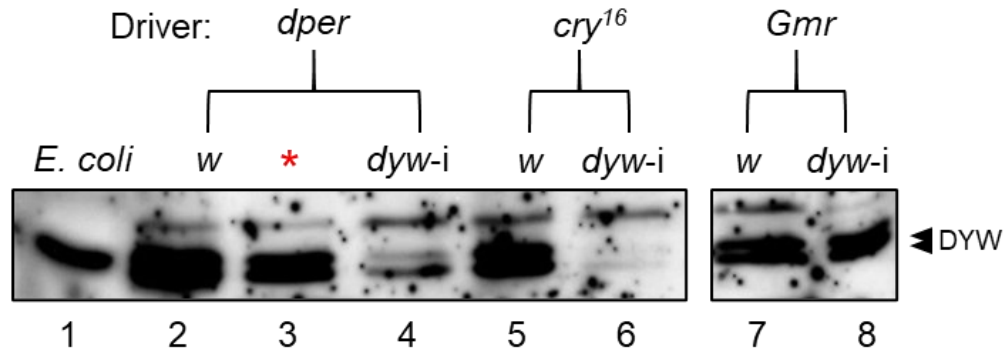


Figure 2.4. A major amount of DAYWAKE detected in the head is produced in circadian clock cells. *Drosophila* carrying the indicated Gal4-drivers (i.e., *per*, *cry16* and *Gmr*) were crossed with either *w¹¹¹⁸* flies (*w*), or transgenic flies expressing RNAi against *dyw* under the control of the UAS promoter (herein abbreviated, *dyw-i*). A second control cross included *dyw-i* and *w¹¹¹⁸* (lane 3). Progeny from the crosses were entrained for 5 days at 25°C and collected at the same time. Head extracts were prepared and DYW visualized following immunoblotting (lanes 2-8); DYW(Δ 1-25) produced in bacteria was included as a positive control (lane 1). Note that expression of *dyw-i* in *per*- or *cry*-expressing cells significantly reduces endogenous levels of the DYW doublet, whereas *dyw-i* in the eyes (*Gmr*) does not. These results are consistent with those reported by Yang and Edery (2019), whereby downregulating *dyw* expression in *per*- and *cry*-expressing cells increased midday siesta but had no significant effect when expressed in the eyes.

express in clock cells (e.g., *per* and *cry*) led to significant decreases in DYW levels compared to control crosses (Fig. 2.4, lanes 2-6). Conversely, no changes in DYW protein levels were seen when driving *dyw*-RNAi in the eyes (lanes 7, 8), aligning with prior work showing no effect on midday siesta levels under these conditions [22]. Thus, in the adult head, DYW is widely expressed in circadian clock cells.

We also stained whole brains to better identify specific cells where DYW is located. Specific staining was observed in numerous neurons and likely glia throughout the brain (data not shown). The cell-specific cataloging of DYW staining requires extensive analysis based on a number of strategies, including co-staining of known markers and tissue-specific drivers. To date, we focused on the pigment-dispersing factor (PDF)-expressing circadian clock cells that are key to circadian rhythmicity. These cells comprise the small- and large-ventrolateral pacemaker neurons (s-LNvs and l-LNvs) (Fig. 2.5D), all of which except one (5th s-LNv), produces PDF. Whole brains were probed with anti-PDF and anti-DYW antibodies and the merged images from confocal microscopy are shown in Fig 2.5 Panel C. DYW is located in both the l-LNvs and s-LNvs (note that in the focal plane shown, staining is most readily observed in the larger l-LNvs). Although the subcellular localization of DYW is not fully established, staining was observed in the cytoplasm but not nucleus in PDF-expressing cells (similar to PDF). It is important to note, however, that at least some DYW is likely to be secreted (see

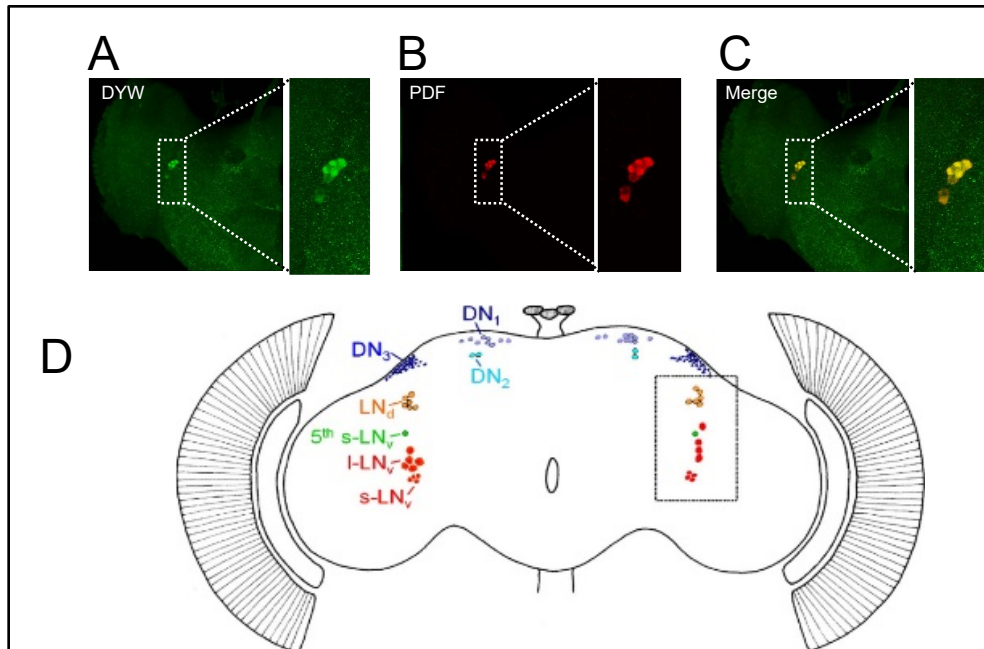


Figure 2.5. DYW is expressed in the key circadian small- and large-ventrolateral neurons (s-LNv and I-LNv) in the fly brain. (A-C) Adult w^{1118} flies were kept in LD at 25°C for four days, and on the fifth day collected at ZT22. Whole brains were isolated, incubated with anti-DYW and anti-PDF antibodies, then fluorescent secondary antibodies, and imaged using a confocal microscope (see Materials and Methods). DYW signal is shown in green (A), PDF signal in red (B), and an overlay of both (C). Although DYW staining is observed in numerous areas of the brain (not shown), shown here are representative images of DYW co-staining with the key PDF-expressing ventral-lateral clock neurons (LNvs). In the focal plane shown, co-staining can be seen in 4 of the 5 large LNvs (I-LNvs) and 1 of the 4 small-LNvs (s-LNvs) that express PDF. PDF leads to a “doughnut” cytoplasmic staining, which is similar for DYW. **(D)** Schematic of adult fly head showing the different ~150 clock cells (bilaterally distributed); PDF-expressing cells shown in red.

next section). Further studies are aimed at determining if DYW is found in the hemolymph and identify tissues in the body where DYW is present.

DAYWAKE is stabilized by glycosylation and undergoes cleavage mediated secretion in cultured *Drosophila* cells

As previously mentioned, DYW residues 1-25 form a highly hydrophobic N-terminal region in DYW (Fig. 2.1A). Short, hydrophobic, N-terminal regions are classic hallmarks of a class of ubiquitous protein secretion markers known as signal peptides (SPs) [42, 43]. In eukaryotes, SPs target nascent peptide chains and their associated ribosome to the ER membrane where synthesis continues across the membrane into the ER lumen. Signal peptides are then cleaved co-translationally by ER-membrane bound signal peptidases, allowing the clipped protein to continue along secretory pathways. As DYW is predicted to be a JHBP, which are often secreted into the hemolymph, a SP secretory marker is not altogether surprising. As a preliminary test to determine if this region could be functioning as an SP, DYW amino acid sequence was assessed using the SignalP-5.0 signal peptide prediction program [44]. Indeed, aa1-25 were very strongly predicted to comprise an SP cleaved after residue A25 (Fig. 2.6A). Two testable predictions are; 1) if DYW is secreted, we might be able to recapitulate this in a *Drosophila* cell culture assay and detect its presence in the growth media, and if so, 2) deletion of the predicted SP would reduce or abolish DYW secretory potential.

To this end, we expressed a full-length version of DYW and one missing the first 25 aa DYW(Δ 1-25) in *Drosophila* Schneider 2 (S2) cultured cells. Consistent with our hypothesis, full-length DYW was observed in cellular protein extracts and the growth media of DYW (Fig. 2.6B, lane 1, top and bottom). Remarkably, we were able to detect DYW in growth media without the need for purification or concentration, suggesting that DYW possesses high secretory activity. In sharp contrast, the large majority of DYW(Δ 1-25) was confined to the cell with relatively little presence in the media (Fig. 2.6B, lane 2, top and bottom).

Interestingly, in addition to the two major isoforms observed when immunoblotting fly head extracts, we observed a third minor isoform that ran above the other two species (herein termed 'c', see Fig. 2.6B; bands 'a' and 'b' comigrate with the two isoforms from flies; data not shown). The two higher isoforms (i.e., 'c' and 'b') are not observed when analyzing DYW(Δ 1-25) in either the cellular fraction or media (Fig. 2.6B, compare lane 2). This suggests that forms 'c' and 'b' are dependent on cleavage of the signal peptide (see below). The fact that DYW(Δ 1-25) attains relatively high levels in the cell (Fig 2.6B, lane 2) also suggests that deletion of aa1-25 does not affect DYW stability, merely its ability to exit the cell.

Due to the high secretory potential of DYW, we were curious if other posttranslational modifications were present on DYW further targeting it for secretion. Aside from signal peptides, a common signal of protein secretion is N-linked glycosylation on arginine residues [45, 46]. Analysis of DYW using the NetNGlyc-1.0 glycosylation site prediction program implicated N182 as a very likely site for glycosylation (Fig. 2.6C). We tested this possibility by treatment with

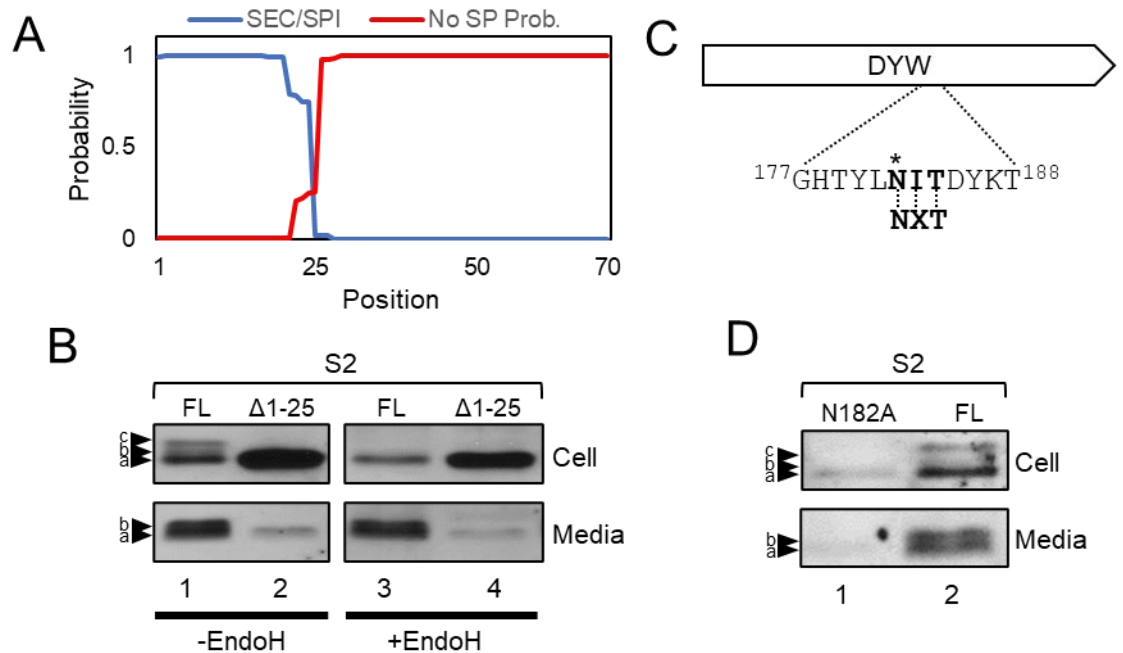


Figure 2.6. DYW produced in S2 cells is secreted in a signal-peptide dependent manner and stabilized by glycosylation at amino acid N182. (A) Residues 1-25 of DYW are predicted to be a signal peptide (SignalP-5.0 prediction program). Blue, high probability of signal peptide; red, low probability. (B, D) *Drosophila* S2 cells were transfected with plasmids containing the entire open reading frame of *dyw* (FL), *dyw*(Δ 1-25), or *dyw*(N182A), as indicated (top of panels). Cells were incubated at 18°C in 5ml of Schnieder's *Drosophila* media in 25cm² culture flasks, followed by collecting cells and media separately. Aliquots from cell extracts (top panels) and media (bottom panels) were either mock-treated (B, lanes 2 and 3), or treated with Endoglycosidase H (EndoH) (B, lanes 4 and 5), followed by immunoblotting in the presence of anti-DYW antibodies. Three closely running mobility isoforms of DYW are observed in S2 cells (denoted; a, b, c), wherein the 'a' form does not appear to be detected in flies. (C) N182 is part of a typical N-X-S/T glycosylation sequon, where "X" is any aa except Pro.

endoglycosidase-H (EndoH) to remove high mannose and/or hybrid glycans. For DYW localized in the cell, EndoH treatment of full length DYW resulted in the disappearance/reduction of the two slower migrating isoforms. The remaining DYW isoform ('a') co-migrates with DYW(Δ 1-25) (Fig. 2.6B, compare lanes 3 and 4, top), indicating that forms 'c' and 'b' are cleaved at the signal peptide but have altered mobility due to glycosylation. The mobility of DYW(Δ 1-25) was unchanged upon EndoH treatment indicating that it was unable to undergo glycosylation. Applying these findings to our fly studies suggests that the majority of detectable DYW is cleaved and is comprised of two major isoforms; i.e., one isoform that is not glycosylated, and another that is glycosylated-

Close inspection of DYW isoforms in the media revealed the presence of a closely running doublet, almost certainly the 'a' and 'b' species observed in flies. Interestingly, EndoH treatment of DYW in the media did not reduce/eliminate the slower migrating 'b' isoform as was the case with DYW localized to the cell (Fig. 2.6B, compare lanes 1 and 3). This may be due to glycan maturation in the Golgi prior to secretion, resulting in EndoH resistant complex glycan modifications [47].

Having established that DYW is indeed glycosylated and that this glycosylation is highly predicted to occur at residue N182, we tested the effects of altering residue N182 to Ala [DYW(N182A)] in cultured cells. Unexpectedly, drastic reductions in both intra- and extra-cellular levels were observed for DYW(N182A) compared to full-length DYW, suggesting that residue N182 is crucial for DYW expression and/or stability (Fig. 2.6D, compare lanes 1 and 2 top and bottom). Protein glycosylation often occurs co-translationally in the lumen of

the endoplasmic reticulum [48, 49] facilitating entry into the Calnexin-calreticulin cycle which plays a crucial role in proper glycoprotein folding in the ER [48, 50, 51]. It is possible, then, that glycosylation of N182 may serve a protective role for DYW and that abrogating the ability of this residue to be modified carries detrimental effects for DYW stability (see Discussion).

Taken together, our results based on a simplified cell-culture system demonstrates that DYW can be highly secreted in a manner reliant on the signal peptide. Further, DYW is glycosylated on residue N182 which appears to be critical for protein stability and possibly secretion.

Discussion

Herein, we performed the first biochemical analysis of the DYW protein, using both flies and cultured S2 cells. Overall, our results strongly support the notion that DYW is a functional JHBP present in the brain of adult flies (Figs. 2.1, 2.4, 2.5 and 2.6). Moreover, it confirms a role for thermal regulation of DYW protein levels in the head via *dmpi8* splicing efficiency (Figs. 2.2 and 2.3), consistent with prior results analyzing *dyw* mRNA levels [22]. The combined analysis in flies and S2 cells indicate that there is little to no uncleaved DYW that accumulates. Rather, only DYW that is cleaved of its signal peptide is detectable, and a portion of that is also glycosylated (Fig. 2.1, 2.4 and 2.5). Since DYW co-stains with PDF it implies that substantial amounts of cleaved DYW can reside in the cytoplasm of cells in which it is produced, at least for clock neurons (Fig. 2.5). Nonetheless, based on results using S2 cells, it also appears that a major portion of DYW is secreted (Fig.

2.6), as is typical of JHBPs. These considerations raise the intriguing possibility that DYW regulates midday siesta via a complex network involving local effects in the brain and more distal targets reached by secretion into the hemolymph.

Although not unexpected [22], the fact that DYW protein levels are also elevated at cooler temperatures similar to RNA levels further reinforces the idea that temperature-dependent changes in the levels of DYW protein are critical to the thermal adaptation of midday siesta in *D. melanogaster* (Fig. 2.2). Our analysis of wildtype flies also suggests that DYW levels might differ between males and females (Fig. 2.2, C and D), although more extensive work will be required to better evaluate any possible sexual dimorphism. It is well established that females exhibit less midday siesta compared to males and that the juvenile hormone signaling pathway is involved [29, 37], however there is currently no indication that *dyw* plays a role.

That DYW levels are regulated by *dmpi8* splicing efficiency is further supported by studies using natural populations of *Drosophila* (Fig. 2.3). SNP3 in the *per* 3' UTR is a major regulator of *dmpi8* splicing efficiency, with the SNP3G variant leading to higher baseline splicing efficiency compared to the SNP3A variant [7-9, 21]. Moreover, flies carrying the SNP3G variant exhibit diminished midday siesta compared to those with SNP3A irrespective of temperature [21]. This was observed in natural *D. melanogaster* populations from the United States, Africa and Australia [7, 20, 21]. Our analysis of several *D. melanogaster* populations from the eastern coast of Australia clearly demonstrates that SNP3G variants have higher levels of *dyw* mRNA and protein (Fig. 2.3). For *D.*

melanogaster populations from tropical and temperate regions along the eastern coast of Australia we previously identified several *per* 3' UTR SNP combinations that show clinal variation. None of these included SNP3 and the effects on splicing efficiency were more subtle compared to variations in SNP3. However, those spatially segregated SNPs contribute to the higher and lower midday siesta observed in tropical and temperate populations, respectively [21]. Future studies are aimed at determining if DYW levels differ between the 'tropical' and 'temperate' *per* 3' UTR variants. In any case, our results reveal that genetically based differences in DYW levels can contribute to natural variation in the midday sleep of naturally occurring *D. melanogaster*.

In the adult head, DYW appears to be predominantly located in clock cells. RNAi knockdown of *dyw* in *per*- and *cry*- expressing cells resulted in significantly less DYW compared to controls indicating that a substantial proportion of observable DYW in adult fly heads are produced in these cells (Fig. 2.4). Conversely, RNAi-*dyw* driven in the eye resulted in no observable change in DYW levels suggesting DYW is not made in appreciable amounts in these tissues. We therefore conclude that the majority of DYW staining in head extracts is due to brain expression (Fig. 2.1). It should be noted that about 50% of PER protein staining in head extracts is found in the eyes [52, 53]. Thus, the spatial distribution of DYW does not fully parallel that of PER in the head. Whole brain staining of adult fly brains established that DYW is located in PDF-expressing lateral neurons (Fig. 2.5), key circadian pacemakers. We did observe DYW staining in non-clock cells in the brain, and it is clear that not all clock cells in the brain have detectable

levels of DYW (data not shown). From this combined data, it appears that in the head, the majority of DYW accumulates in *per*-expressing clock cells but is also present in other neurons of currently unknown identity.

Clearly, the fact that *dmpi8* splicing from the *per* gene can regulate *dyw* mRNA and protein levels in-trans (see Fig. 1.7) would imply that *per* and *dyw* should be co-expressed in the same cells. Thus, it is not surprising to find strong staining of DYW in clock cells. Nonetheless, DYW modulates midday siesta in a circadian and PER protein independent manner [22]. For example, placing a premature stop codon in the *per* open reading frame did not abolish the ability of *dmpi8* to regulate *dyw* levels and midday siesta. These findings suggest that DYW function on midday sleep, although emanating from clock cells, is not gated by the clock mechanism. Indeed, we do not observe major changes in *dyw* mRNA or protein levels throughout a daily cycle ([22] and Fig. 2.3; and data not shown). Rather, all data points towards DYW functioning to lower the threshold for sensory-mediated arousal [17]. Furthermore, direct manipulation of *dyw* transcript levels independent of changes in *dmpi8* splicing still lead to changes in midday siesta [22]. It is possible that expression of *dyw* in *per*-expressing cells is central to thermal regulation of midday siesta, whereas expression of *dyw* in non-clock cells might be responsive to other cues (see Chapter 3). The presence of DYW protein in the body also implies a broad spatial distribution that is not solely defined by *per* expression.

Trying to deduce DYW function from its spatial distribution is further confounded by the fact that it belongs to the juvenile hormone binding protein

(JHBP) superfamily. JHBPs are found in arthropods and function by being secreted into the hemolymph where they bind the hydrophobic JH, protecting it against degradation and carrying it to target tissues, initiating signaling cascades that result in transcriptional changes [24-26]. There are approximately 15-20 JHBPs in the *D. melanogaster* genome. Juvenile hormone is a major player in insect development [24-26]. In addition to development, JHBPs have been shown to regulate behavior. One of the best studied JHBP in *D. melanogaster* is *takeout* (*to*), which regulates feeding behavior in adult flies [54]. Although TO shares the highest protein sequence similarity with DYW and is also expressed in the head, it does not affect midday siesta. Thus, despite binding JH and possibly entering the circulatory system, JHBPs mediate different functions.

Results from cultured *Drosophila* cells are remarkably consistent with the notion that DYW undergoes signal peptide mediated secretion via the ER and Golgi (Fig. 2.6). Secretion of DYW into the media is greatly facilitated by the N-terminal signal peptide. DYW(Δ 1-25) comigrates with the smallest observed DYW isoform (i.e., 'a') produced from the full-length open reading frame (Fig. 2.6B). The fastest migrating isoforms of DYW detected in S2 cells and flies co-migrate with DYW(Δ 1-25) made in S2 cells or bacteria (Fig. 2.1D). It is thus clear that the majority of DYW accumulating in fly heads and brains is cleaved and that very little, if any, uncleaved DYW remains for long. When we first noted the upper band in fly heads, we assumed it might be the uncleaved form of DYW. A similar closely running doublet was also observed for TO in adult fly brains, and it was assumed to be the uncleaved form. However, our findings in cultured *Drosophila* S2 cells

leads us to revise this assumption. Most notably, EndoH treatment of full-length DYW collapsed the multiple mobility isoforms to that of DYW(Δ 1-25) residing in cells (Fig. 2.6B, top, compare lanes 1-4). The simplest interpretation is that the two higher electrophoretic isoforms ('c' and 'b') represent cleaved DYW carrying different glycan modifications; possibly intermediates involved in glycan maturation.

We do note however, that an additional slower migrating isoform was detected in DYW extracted in the cellular fraction from cultured S2 cells (species 'c') compared to the doublet in flies (Figs. 2.1 and 2.6). This slower mobility isoform was not detected in the media. The physiological significance of this 'additional' species, presumably reflecting differential glycan modification, is presently not clear and might be an artifact of over-expressing in S2 cells possibly overwhelming the endogenous glycan maturation machinery. Intriguingly, the relative abundance of the glycosylated species ('b') relative to presumably non-glycosylated ('a') is much higher in the media compared to the cellular fraction. This suggests that glycosylation enhances secretion. Curiously, EndoH treatment of DYW secreted into the media did not eliminate this glycosylated isoform as it did for DYW residing in the cell (Fig. 2.6, compare lanes 1 and 3, top and bottom). A possible explanation is that glycan maturation in the ER and Golgi prior to secretion may lead to EndoH resistant glycan complexes [55-57]. It may be possible to use this differential enzymatic response as a surrogate for secreted DYW in flies.

Scanning the DYW protein sequence identified a likely site for glycan modification, aa N182 (Fig. 2.6C). Unexpectedly, cells expressing DYW(N182A)

mutants exhibited highly reduced DYW levels in the cell or media (Fig. 2.6D). We propose that DYW(N182A), while lacking the ability to be glycosylated, can still be targeted to the ER lumen by recognition of its signal peptide. However, because precursor oligosaccharide cannot be added, this prevents entry into the Calnexin-calreticulin (CC) cycle, critical for proper glycoprotein folding ER [45, 58-60]. Accumulation of misfolded protein in the ER induces ER stress, triggering retrotranslocation of the misfolded protein into the cytoplasm, ultimately leading to proteasome mediated degradation of proteins which failed successfully undergo folding [61-64]. Taken together these results suggest a model whereby DYW is targeted to the ER lumen by co-translational recognition of its signal peptide. SP cleavage and core oligosaccharide addition to N182 subsequently occur co-translationally during synthesis across the ER membrane into the lumen, generating a glyco-DYW(26-260) intermediate. The addition of the precursor glycan allows this intermediate DYW entry into the CC cycle facilitating folding into its native state. Once properly folded, glyco-DYW(26-260) is allowed to continue along the secretory pathway eventually entering the Golgi where the precursor oligosaccharide undergoes maturation producing a complex glycan which is resistant to digestion by EndoH.

Conclusion

In summary, our findings indicate that a major center for DYW protein accumulation is in brain clock cells, allowing for *in-trans* regulation by thermosensitive splicing of the *dmpi8* intron. However, DYW is also present in

non-clock cells in the brain and in the body. In addition, it appears that the majority of DYW found in flies is cleaved, and a portion of it is stably glycosylated. While this implies secretion and indeed studies in S2 cells show DYW can be secreted, staining of whole brains shows that DYW is detected inside clock cells where it is presumably produced. Thus, although it is not clear how DYW regulates midday siesta we propose that it functions within a complex network of tissues that include intracellular mechanisms in local brain centers and extracellular mechanisms via entering the hemolymph, traversing the blood-brain barrier and signaling to target tissues. This model also raises the intriguing possibility that DYW responds to other signals besides temperature in the regulation of midday siesta (see Chapter 3).

STAR★Methods

Table 2.2 Key Resources Table

REAGENT or RESOURCE	SOURCE	IDENTIFIER
Chemicals, Peptides & Recombinant Proteins		
His-TALON Metal Affinity Resin	Clontech	635501
Protease Inhibitor Cocktail	Roche	11873580001
Blotting Grade Blocker	BioRad	1706404
ECL Prime Western Blotting Detection Reagents	GE	RPN2232
NdeI	New England Biolabs	R0111S
BamHI	New England Biolabs	R0136S
T4 DNA Ligase	Promega	M180A
Ampicillin		
Chloramphenicol		

Anti-FLAG M2 Magnetic Beads	Millipore Sigma	M8823-1ML
AccuPrime <i>Taq</i> DNA Polymerase, high fidelity	Invitrogen (ThermoFisher Sci.)	12346086
SYBR Safe DNA Gel Stain	Invitrogen (ThermoFisher Sci.)	S33102
Drosophila agar (fly food)	LabScientific	FLY-8020
Drosophila yeast (fly food)	LabScientific	FLY-8040
Yellow Cornmeal (fly food)	LabScientific	FLY-8010
Light corn syrup (fly food)	LabScientific	FLY-8007
Propionic Acid (fly food)	Millipore Sigma	402907-500ML; CAS 79-09-4
Tegosept (fly food preservative)	Apex (Genesee Scientific, USA)	Cat# 20-258; CAS, 99-76-3
Bacto-Agar (behavior tubes)	VWR	Cat# 90000-760
Sucrose (behavior tubes)	Millipore Sigma	Cat# S7903-5KG
Bacto-Agar (behavior tubes)	VWR	Cat# 90000-760
Sucrose (behavior tubes)	Millipore Sigma	Cat# S7903-5KG
Isopropyl β -d-1-thiogalactopyranoside (IPTG)	Millipore Sigma	Cat# 10724815001
Vectashield	Vector Laboratories	Cat# H-1000
Schneider's Media	ThermoFisher	Cat# 21720001
Coomassie Brilliant Blue R-250	BioRad	Cat#1610400
anti-DYW antibody GP49	This paper	GP49

Critical Commercial Assays

QuikChange II XL Site Directed Mutagenesis Kit	Agilent Technologies	200521
Coomassie Plus Assay Kit	ThermoFisher	1856210
Effectene Transfection Reagent	Qiagen	301427
NucleoSpin Plasmid (DNA purification)	Macherey Nagel	Cat# 740588.250

Experimental Models: Organisms/Strains

Tuner (DE3) pLysS competent cells	Novagen	70624-3
JM109 Competent Cells	Promega	L2005
Drosophila S2 Cells	ThermoFisher	Cat# 69007

<i>Drosophila melanogaster</i> : per-Gal4	BDSC	RRID: BDSC_7127
<i>Drosophila melanogaster</i> : Cry16-Gal4	BDSC	RRID: BDSC_24514
<i>Drosophila melanogaster</i> : Gmr-Gal4	BDSC	RRID: BDSC_1104
<i>Drosophila melanogaster</i> : RNAi-0.9	BDSC	RRID: BDSC_56988
<i>Drosophila melanogaster</i> : UAS-0.9	Yang 2019	
<i>Drosophila melanogaster</i> : Canton-S	BDSC	RRID: BDSC_64349
<i>Drosophila melanogaster</i> : GT110	[21]	
<i>Drosophila melanogaster</i> : S4	[21]	
<i>Drosophila melanogaster</i> : HB22	[21]	
<i>Drosophila melanogaster</i> : HB106	[21]	
<i>Drosophila melanogaster</i> : HB108	[21]	
<i>Drosophila melanogaster</i> : GT46	[21]	
<i>Drosophila melanogaster</i> : GT92	[21]	
<i>Drosophila melanogaster</i> : S22	[21]	
<i>Drosophila melanogaster</i> : S28	[21]	
<i>Drosophila melanogaster</i> : HB25	[21]	
<i>Drosophila melanogaster</i> : S3	[21]	
<i>Drosophila melanogaster</i> : S7	[21]	
<i>Drosophila melanogaster</i> : S8	[21]	
<i>Drosophila melanogaster</i> : S12	[21]	
<i>Drosophila melanogaster</i> : S34	[21]	
<i>Drosophila melanogaster</i> : UAS-dyw-3xFLAG	unpublished	
<i>Drosophila melanogaster</i> : w[1118]	BDSC	

Recombinant DNA

plasmid: pMT-V5/His	ThermoFisher	V412020
plasmid: pET-16b		
plasmid: pMT-DYW	this paper	
plasmid: pMT-DYW(Δ 1-25)	this paper	
plasmid: pMT-DYW(N182A)	this paper	

Software and Algorithms		
MATLAB	MathWorks	MATLAB_R2019A
DAMSystem3 Data Collection Software	TriKinetics, USA	N/A
ImageJ Software	https://imagej.nih.gov/ij/	N/A
Oligonucleotides		
See Table 2.1		

Chapter 3: *Daywake* regulates sleep behavior in a temperature, sex and nutrition dependent manner

Abstract

We recently discovered a gene termed *daywake* (*dyw*) that is stimulated by cold temperatures and functions to diminish midday siesta in *D. melanogaster*, with little to no effect on nighttime sleep. Herein, to better study the contribution of *dyw* to daily wake-sleep behavior we used CRISPR technology to create *dyw* knock out (*dyw*) flies. Consistent with earlier work, *dyw*-KO flies exhibit higher levels of midday siesta compared to wildtype controls, although the magnitude of the effect varied depending on gender and temperature. As a secondary condition to modulate sleep behavior besides temperature, we also challenged flies with malnutrition. Many animals respond to starvation/hunger by suppressing sleep, presumably to increase foraging activity in the hopes of identifying better food resources. *dyw*-KO flies exhibit hunger-induced suppression of sleep but still sleep more during the day compared to wildtype flies. Surprisingly, malnutrition revealed an unexpected major role for *dyw* in regulating nighttime sleep. Whereas wildtype flies show a potent reduction in nighttime sleep, *dyw*-KO flies do not. We suggest that when flies are confronted with hunger, *dyw* enhances foraging at night where the risks from exposure to the hot sun are eliminated. Thus, *dyw* appears to calibrate day-night wake-sleep needs relative to other survival risks such as heat exposure and starvation

Introduction

Why animals sleep is not clear but numerous lines of evidence indicate it is essential for survival [65]. The balance between sleep and arousal throughout a daily cycle is regulated by several interconnecting pathways that include the circadian timing system, homeostatic control and environmental signals [1]. While the circadian timing system is mainly viewed as regulating the timing of sleep, homeostatic systems modulate sleep need. *Drosophila melanogaster* is an excellent model system to study the molecular and neurobiological aspects of daily wake-sleep behavior [66]. *Drosophila* mostly sleep during the night but also display a midday siesta that is more prominent on warm days [9, 17, 67]. Sleeping during the midday is a common behavior found in diurnal animals, including humans [68-71]. Although a midday nap has been shown to have beneficial effects in humans, excessive daytime sleepiness or “sickness” behavior is linked to poor outcomes in many disease states [30-32]. However, many studies have focused on nighttime sleep, but less is known about the pathways regulating daytime sleep.

Recently, we identified the first “anti-siesta” gene, isolated in *Drosophila melanogaster*, that we termed *daywake* (*dyw*) [22]. Using a range of transgenic models, it was shown that decreases in *dyw* levels enhance midday sleep, whereas higher *dyw* levels are accompanied by increased wake during the day. Although *dyw* modulates the midday balance between arousal and sleep, little effect was observed on nighttime sleep levels. Current evidence suggests that a major function of *dyw* is to counteract genetically based programs that drive midday sleep. The ability of *dyw* to counteract midday sleep drive is more

prominent at cooler temperatures. This serves as a thermal adaptive mechanism enabling *D. melanogaster* to remain active during the midday when the risks from heat exposure are minimized. Intriguingly, the levels of *dyw* transcripts are responsive to splicing of the thermosensitive *dmpi8* intron found in the 3' untranslated region (UTR) of the slightly overlapping and reverse oriented *period* (*per*) gene, a key component of the circadian clock. As ambient temperatures get cooler, *dmpi8* splicing efficiency increases, somehow leading to higher *dyw* expression, and hence promoting wakefulness during the midday (Fig. 1.7).

Although it is not clear how *dyw* regulates daytime sleep/wake levels, it encodes a predicted juvenile hormone binding protein (JHPB), best known for regulating development in arthropods (see Chapter 2). JHBPs bind juvenile hormone (JH) and act as a carrier in the hemolymph to deliver JH to target cells, leading to downstream signaling cascades (Fig. 1.8). To better understand the role of *dyw* in daily wake-sleep we generated *dyw*-knockout (*dyw*-KO) flies using CRISPR technology [72, 73]. As expected from prior work using transgenic models, *dyw*-KO flies exhibit increased daytime sleep compared to control flies at cooler temperatures. We also examined sleep behavior under conditions of malnutrition, which acts as a stimulus to suppress sleep and promote foraging activity [74-76]. Remarkably, inactivation of *dyw* revealed a dramatic effect on nighttime sleep when flies were challenged with malnutrition. Other effects of *dyw* on day and/or night sleep/wake behavior varies with sex and temperature. Our findings suggest that *dyw* is a key nexus in the real-time optimization of daily sleep/wake behavior to physiological state and environmental conditions.

Materials & Methods

Generation of CRISPR *dyw*-KO flies

Generation of *dyw*-knock out flies (*dyw*-KO) was performed by a commercial entity, WellsGenetics, Inc. (Tapei, Taiwan). Briefly, they used CRISPR/Cas9-mediated genome editing by homology-dependent repair to edit the genome of the standard laboratory strain *w*¹¹¹⁸. Essentially, the *dyw* codons for amino acids 21 (Cys) and 22 (Arg) were changed at two positions, resulting in a pair of consecutive stop codons (5'-TGC AGA-3' → 5'-TGA IGA-3'). This was accomplished in a two-step procedure by first introducing a 3xPBacDsRed cassette into the *dyw* opening reading frame to facilitate genetic screening. After screening and excision of the DsRed cassette by Piggy Bac transposase, mutant flies with the two stop codons were confirmed by PCR and DNA sequencing. Ultimately, five independent *dyw*-KO lines were obtained, along with the parental *w*¹¹¹⁸ host strain used in the mutagenesis scheme.

Generation of transgenic flies in a *dyw*-KO genetic background

Three previously reported plasmids were used to introduce a functional copy of *dyw* into the *dyw*-KO genetic background; i.e., VT1.1 [7], in addition to *dmpi8WT* and *dmpi8UP* [8]. In all cases the plasmids also contain a functional copy of *per* since the *dyw* gene slightly overlaps and is also regulated *in-trans* by splicing of the *per dmpi8* intron [22]. The *dmpi8UP* and *dmpi8WT* plasmids are identical except for several base pair changes resulting in more efficient splicing of *dmpi8* (*dmpi8UP*) compared to the wildtype control (*dmpi8WT*) [8]. The VT1.1 plasmid

carries a wildtype version of the *dmpi8* intron but includes a larger 5' upstream genomic region of the *per* gene compared to the *dmpi8*WT/UP constructs. Transgenic flies were generated by Rainbow Transgenic Flies, Inc, (Camarillo, CA, USA) using P-element transformation into a *w*¹¹¹⁸, *dyw*-KO background (see above). Multiple independent lines were obtained for each transgene (herein referred to as *dyw*-KO[*dmpi8*WT], *dyw*-KO[*dmpi8*UP] and *dyw*-KO[VT1.1]. Results shown are based on pooling data from multiple independent lines for each transgene.

Analysis of daily activity and sleep

Daily locomotor activity and sleep profiles of individual male or female flies (3-6 days old) were continuously monitored and recorded using the Trikinetics system (Waltham, MA, USA), essentially as previously reported [17]. Briefly, individual flies were slightly anesthetized and placed in glass tubes containing at one end different final concentrations of sucrose (1-5%) dissolved in 2% bacto-agar to generate a solid food source. The tubes were then loaded into the DAM2 Activity Monitors (Trikinetics), which were placed inside environmental incubators (Percival Scientific) and maintained at the indicated temperature (18°, 25°) for at least 5 days of 12 h light: 12 h dark cycles [LD; where zeitgeber time 0 (ZT0) is defined as lights-on]. In some cases, LD was followed by constant light (LL) or constant darkness (DD) for several days. Activity counts were collected using the DAMSystem3 Software and analyzed using MATLAB R019A (scripts available). We used the widely accepted operational definition of sleep using this

experimental platform; i.e., sleep is defined as continuous inactivity lasting five or more min [6]. For each genotype, sex and condition, data from at least 16 individual flies was pooled to generate a group average. The main difference from our prior experimental procedure is how we reared flies immediately prior to using flies for sleep analysis. For each genotype, flies were first reared in multiple vials at low density and the resulting progeny lightly anesthetized and pooled prior to loading into tubes. We found that this resulted in more reproducible results compared to taking flies from large bottles or only one vial.

Western Blotting

Head extracts from adult flies were prepared in modified RIPA buffer, resolved by 12% SDS-PAGE, and DYW probed by immunoblotting in the presence of anti-DYW antibodies as described above (see Chapter 2). Briefly, blots were incubated with 10ml of anti-DYW antibody GP49 diluted 1:4000 in 0.1% Blocking Buffer, followed by incubation with Anti-Guinea Pig Horseradish Peroxidase (HRP) conjugated antibody diluted 1:10,000 in 0.1% Blocking Buffer. Membranes were incubated with ECL Prime (GE cat#RPN2232) for ~3 min. Blots were imaged either using the Azure Biosystems c600 imager or exposed to radiographic film (LabScientific cat#XAR ALF 1318).

Results

Generation of *dyw*-KO flies

To better understand the physiological role of *dyw*, CRISPR technology was used to generate mutant flies by introducing two consecutive stop codons into the open reading frame of *dyw* (Fig. 3.1A). This was achieved by changing two nucleotides in the codons for amino acids 21 and 22. The overall strategy involved intermediate steps that also generated flies whereby the gene encoding the fluorescent protein DsRed was inserted into the *dyw* open reading frame. The host flies for the CRISPR mutagenesis scheme were the standard laboratory strain of *w*¹¹¹⁸, and the introduced mutations confirmed by PCR and DNA sequencing. We obtained five separate lines of flies with the desired two stop codons, herein referred to as *dyw*-KO flies. Immunoblotting in the presence of anti-DYW antibodies confirmed that DYW is not detectable in the *dyw*-KO flies (Fig 3.1B). Although we did not do a comprehensive analysis, *dyw* is not an essential gene and obvious defects in development or overall health were not observed for *dyw*-KO male or female flies.

The anti-siesta activity of *dyw* is readily observed at cooler temperatures in both males and females

Prior work showed that downregulating *dyw* expression using RNAi led to higher daytime sleep levels, whereas nighttime sleep levels were less affected, if at all [22]. Although we observed daytime sleep increases by inhibiting *dyw* expression in flies evaluated over a range of standard temperatures (i.e., 18°, 25°, 29°C), the

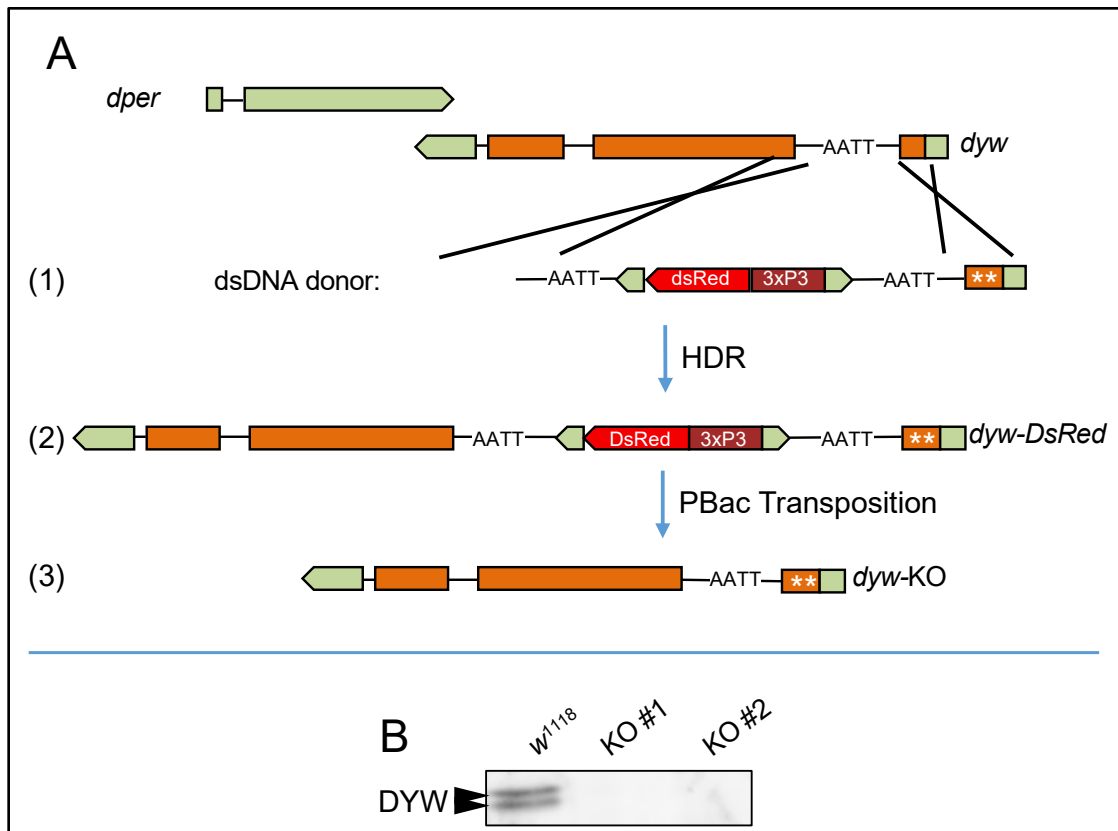


Figure 3.1. Strategy for generating *dyw*-KO flies using CRISPR. (A) Key steps are shown, as follows: 1) Donor double-stranded DNA containing two premature stop codons in place of codons 21 and 22 of the *dyw* open reading frame (asterisks) as well as the fluorescent protein DsRed was inserted into the *dyw* gene using CRISPR-Cas9 in a wildtype *w¹¹¹⁸* host. 2) Several *dyw*-DsRed lines were obtained, and also used as an intermediate to remove the fluorescent DsRed tag via PiggyBack transposition resulting in 3) *dyw*-KO flies. Using this strategy, we obtained 3 *dyw*-DsRed lines and 5 lines of *dyw*-KO. **(B)** Head extracts were prepared from the parental *w¹¹¹⁸* strain and two of the *dyw*-KO lines (herein termed, KO#1 and KO#2). Immunoblotting in the presence of anti-DYW antibodies of *dyw*-KO fly head extracts confirm no DYW protein is detectable.

magnitude of the effect was larger at the cooler temperature. This is not surprising because *dyw* levels increase as daily temperatures drop, augmenting its ability to reduce baseline midday sleep levels [22]. At higher temperatures, midday sleep promoting pathways are more potent [8, 9, 77] and *dyw* expression is reduced [22]. Therefore, the anti-siesta activity of *dyw* is more readily observed at cooler temperatures, which provides a more sensitized experimental format to detect manipulations that increase daytime sleep.

Thus, to initially characterize *dyw*-KO flies we measured their daily sleep patterns under standard 12 h light: 12 h dark cycles [LD; where Zeitgeber time 0 (ZT0) is lights-on and ZT12 is lights-off] for several days at 18°C, and compared them to the host wildtype *w¹¹¹⁸* strain. We evaluated both male and female flies due to sexual dimorphism in daytime sleep levels [78], whereby males have enhanced siesta compared to females (Fig. 3.2, Panels A and B respectively). Overall daytime sleep levels are significantly increased in all five *dyw*-KO lines compared to the wildtype case (Fig. 3.2; and data not shown). This was observed in both males and females, although there are some gender differences in the relative changes occurring during daytime sleep. Daytime sleep levels for both wildtype and *dyw*-KO female flies are lower compared to their male counterparts. Moreover, the daytime sleep differences between wildtype and *dyw*-KO flies are of smaller magnitude in females, and essentially disappear after several days in LD (Fig. 3.2B). Daytime sleep levels also show a slight reduction in males, especially for the wildtype control flies with prolonged time in LD. Although the reason(s) for this downward trend in daytime sleep levels with prolonged duration

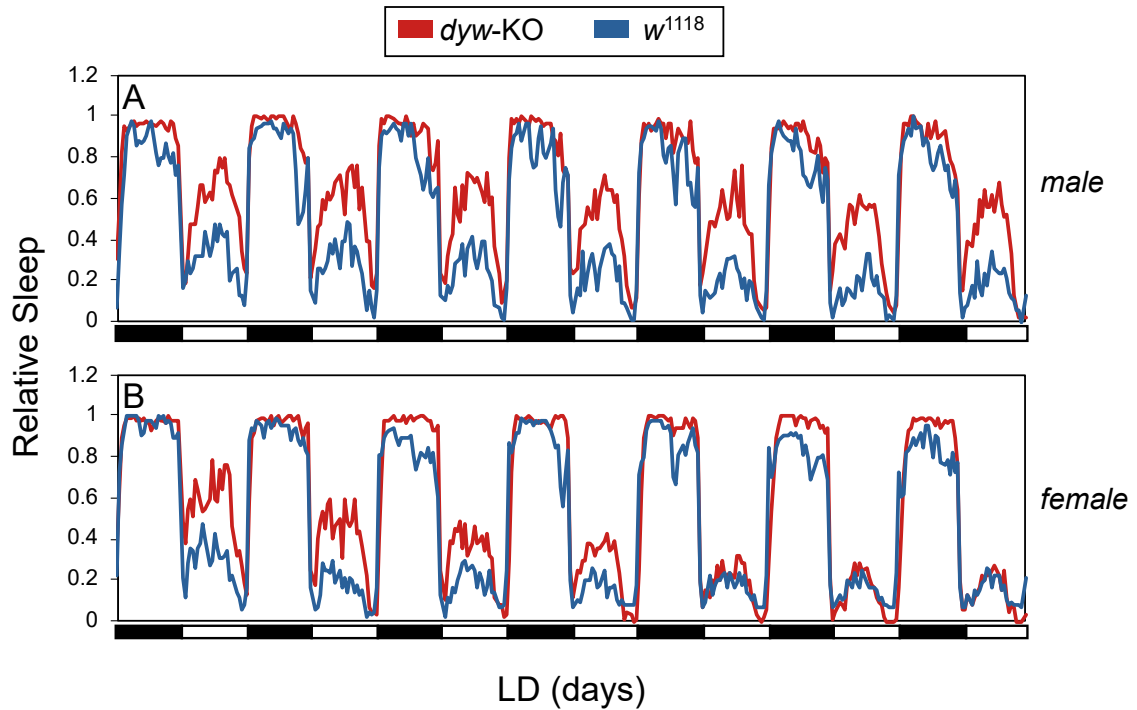


Figure 3.2. *dyw-KO* flies exhibit increased midday siesta at 18°C. (A, B) Young male and female *dyw-KO* and wildtype *w¹¹¹⁸* control flies were exposed to several days of LD at 18°C. Activity was continuously recorded and shown are group averages of the daily sleep profiles for *dyw-KO* (red) and control *w¹¹¹⁸* (blue) flies. Results for males are shown in panel A, whereas those for females are shown in panel B. For each genotype and sex, data from 16 individual flies were analyzed and pooled. Sleep values were normalized (1 = 100% sleep for the group). Black and white bars beneath panels represent lights-off and lights-on respectively.

in LD is presently not clear, a recent study showed that very young flies tend to sleep more during the day and this 'baby' sleep is lost as they age [79, 80].

Nighttime sleep levels showed minor but reproducible differences between *dyw*-KO and control flies. For *dyw*-KO females, sleep is elevated throughout the night compared to the wildtype control case (Fig. 3.2). For males, the main genotypic difference in nighttime sleep is during the late night where wildtype flies exhibit a more rapid drop in sleep levels, most likely due to the clock-controlled anticipation of "sunrise" [4, 29, 78, 81, 82]. Indeed, *dyw*-KO flies manifest higher sleep levels during lights-on, suggesting they are in a deeper sleep and harder to arouse. We find that nighttime sleep levels are higher in *dyw*-KO females compared to males at 18°C. It is possible that the sustained elevated nighttime sleep in *dyw*-KO flies leads to decreased daytime sleep need over time, hence minimizing the effects of *dyw* on daytime sleep levels in females.

An increase in midday siesta levels for *dyw*-KO mutant flies is also observed at 25°C. As previously noted, daytime sleep levels are higher at 25°C compared to 18°C [8, 9, 22]. Thus, due to the higher baseline sleep levels in wildtype flies, this likely explains the reduced magnitude of increased daytime sleep by inactivating *dyw* function at 25°C compared to 18°C (Fig 3.3, panels A and B). This is especially true for males which already have higher baseline levels in daytime sleep compared to females [78]. Any possible effects of knocking out *dyw* on nighttime sleep were less obvious at 25°C.

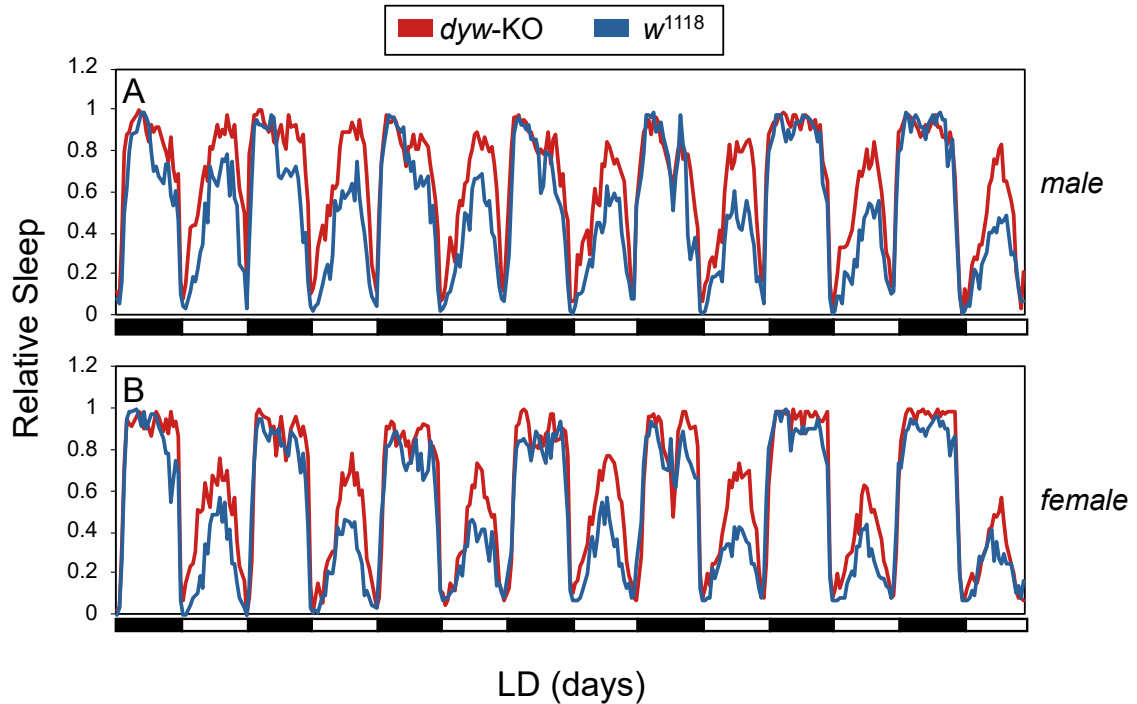


Figure 3.3. *dyw*-KO flies exhibit increased midday siesta at 25°C. (A, B) Young male and female *dyw*-KO and wildtype *w*¹¹¹⁸ control flies were exposed to several days of LD at 25°C. Activity was continuously recorded and shown are group averages of the daily sleep profiles for *dyw*-KO (red) and control *w*¹¹¹⁸ (blue) flies. Results for males are shown in panel A, whereas those for females are shown in panel B. For each genotype and sex, data from 16 individual flies were analyzed and pooled. Sleep values were normalized (1 = 100% sleep for the group). Black and white bars beneath panels represent lights-off and lights-on respectively. **Note:** The data shown here are derived from the same experiment as that shown in Fig. 3.3.

Taken together, the results strongly reinforce the “anti-siesta” role previously ascribed to *dyw* [22]. We proposed that as average daily temperatures drop, the increase in *dyw* expression more potently counterbalances against pathways that promote midday siesta, thus enabling *D. melanogaster* to remain active when the risks from heat exposure are minimized [22]. The notion that *dyw* acts against an actively engaged mechanism promoting midday sleep drive is supported by results at 18°C (Fig. 3.2). Without *dyw* function there is still a robust midday siesta even at 18°C. In addition, eliminating *dyw* function reveals a less prominent but noticeable effect on sustaining or augmenting late night sleep on cold days. At 25°C where *dyw* levels are normally decreased [22], the effects of abolishing *dyw* function are generally less pronounced for daytime sleep and any nighttime effect is at best small. Further studies will be helpful in further establishing if *dyw* plays any role on daytime sleep during hot days (e.g., 29°C).

Transgenic rescue of *dyw*-KO flies shows a role for *dmpi8* splicing efficiency in mediating the effects of *dyw* on daily sleep regulation

To further verify that the *dyw*-KO sleep behavior is due to eliminating *dyw* function, we introduced *dyw*-containing transgenes into the germline of *dyw*-KO knockouts using P-element transformation. Our initial attempts at rescuing the *dyw*-KO phenotype used the *dmpi8*UP and *dmpi8*WT constructs previously described ([8, 22]; see also Fig. 1.6). Because *per* and *dyw* slightly overlap, in addition to the trans-regulation of *dyw* via *dmpi8* splicing [22], the most physiologically relevant *dyw* constructs also include the *per* gene. Splicing of the *dmpi8* intron is higher in

dmpi8UP compared to dmpi8WT flies which carry the wildtype version of the dmpi8 intron [8, 22]. Prior work showed that even in a *dyw* containing genetic background, flies carrying the dmpi8UP transgene show reduced midday sleep compared to dmpi8WT flies [8, 22]. Multiple independent germline transformants of *dyw*-KO flies harboring either the dmpi8WT or dmpi8UP transgenes were obtained and evaluated (herein referred to as *dyw*-KO;[dmpi8WT]) and *dyw*-KO;[dmpi8UP], respectively).

Less daytime sleep was observed for both *dyw*-KO;[dmpi8WT] and *dyw*-KO;[dmpi8UP] flies compared to control *dyw*-KO flies (Fig 3.4A), indicating that supplying *dyw* function rescues the siesta phenotype in the mutant flies. Transgenics with the dmpi8UP version have the least amount of daytime sleep, supporting our original observation that increasing dmpi8 splicing efficiency leads to lower siesta levels [7, 8, 17, 22]. Moreover, we noticed that sleep levels were higher for the *dyw*-KO flies during the lights-on and lights-off transitions compared to *dyw*-KO;[dmpi8WT]) and *dyw*-KO;[dmpi8UP] transgenics (Fig. 3.4A, arrows). During the light-to-dark and dark-to-light transitions, flies normally show a “startle” response with a brief burst in activity [83]. Indeed, *dyw*-KO flies have blunted activity responses at both light/dark transitions compared to the rescue transgenics (Fig 3.4B, see arrows). These findings are consistent with prior work showing that sensory-dependent arousal thresholds are higher when *dyw* levels are reduced [17, 22]. Reversal of increased daytime sleep in *dyw*-KO flies was also observed using the more expansive VT1.1 transgene (see Fig. 1.5) that includes the natural *per* promoter (Fig. 3.5).

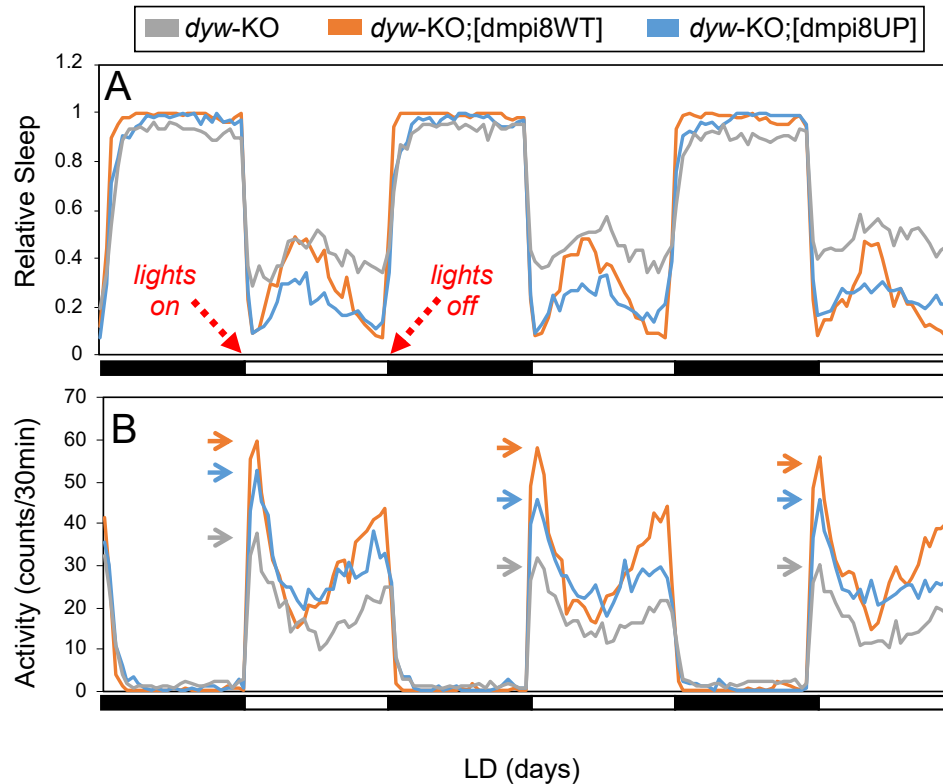


Figure 3.4. *dyw*-containing transgenes reverse the increased daytime sleep observed in *dyw*-KO mutant flies in a manner consistent with *dmpi8* splicing efficiency. (A, B) Transgenic *dyw*-KO flies bearing either the *dmpi8*WT or *dmpi8*UP transgenes (see Fig. 1.6) were maintained in LD at 25°C for several days. Shown are group averages ($n = 16$) of percent time sleep (A), and total activity (B) for male flies of the parental *dyw*-KO mutant (gray), and *dyw*-KO mutants carrying either the *dmpi8*WT (orange) or *dmpi8*UP (blue) transgene. Black and white bars beneath panels represent lights-off and lights-on respectively. Data shown in panels A and B are taken from the same experiment. Arrows (panel B) indicate height of lights-on “startle” response. As predicted, increasing *daywake* levels in the different flies ($dyw\text{-KO};[dmpi8UP] > dyw\text{-KO};[dmpi8WT] > dyw\text{-KO}$) is linked to progressively smaller midday siesta (A) and higher lights-on startle response (B).

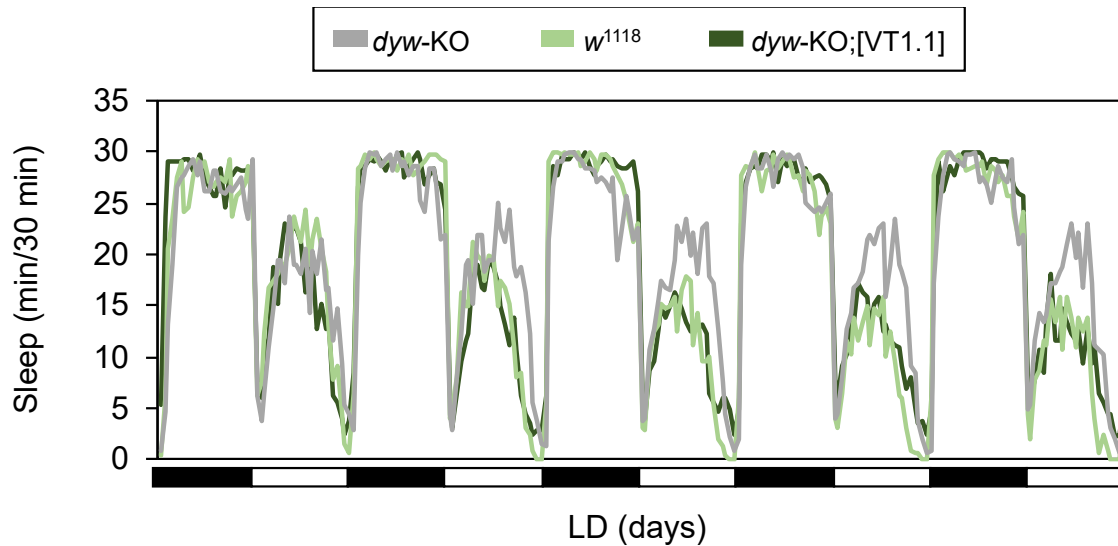


Figure 3.5. A more expansive *dyw*-containing transgene also reverses the increased daytime sleep observed in *dyw-KO* flies. Flies were maintained at 18°C in LD for several days. Shown are daily sleep profiles of *dyw-KO* (gray), *w¹¹¹⁸* parental control (light green), and *dyw-KO;[VT1.1]* transgenic flies (dark green). The VT1.1 transgene has a more expansive genomic unit that contains the entire per gene (see Fig. 1.5). Black and white bars beneath panels represent lights-off and lights-on respectively.

Malnutrition reveals an unexpected effect on nighttime sleep in *dyw*-KO flies

In addition to temperature and other environmental cues, daily wake-sleep patterns can be influenced by nutritional state [75, 84, 85]. Many animals respond to starvation or malnutrition by suppressing sleep and increasing arousal, presumably a survival response that enhances foraging activity [86-89]. A diet consisting of solely a simple nutritive sugar (e.g., sucrose) is sufficient for long-term survival of *D. melanogaster*. The sugar is dissolved in water with agar (~2%) to prevent dehydration and provide a solid matrix for food consumption. A concentration of 5-10% sugar is widely used as a normal nutritive diet in many behavioral assays for adult flies, including wake-sleep cycles [17, 21, 22, 90, 91]. Starvation leads to rapid decreases in both day and night sleep, but starved flies die within a few days [75]. Although not as intensely studied, diets with low sugar (e.g., 1%) also disrupt sleep yet allow for extended survival compared to starvation conditions [92] (unpublished observations; also, see Fig. 3.7).

To the best of our knowledge, analysis of *Drosophila* wake-sleep behavior that includes varying sex, temperature and sugar concentration has not been reported previously. As an initial attempt to determine if malnutrition differentially modulates the daily sleep profiles between *dyw*-KO and wildtype control flies, we used diets containing 1% (malnutrition; S1%) and 5% (standard; S5%) sugar.

On the S1% diet *dyw*-KO flies generally exhibit higher daily sleep levels compared to their wildtype cohorts (Fig. 3.6), consistent with findings using standard sugar diet (Figs. 3.2 and 3.3). The outlier in this relationship is females at 18°C; i.e., although *dyw*-KO might exhibit slightly higher daytime sleep at the

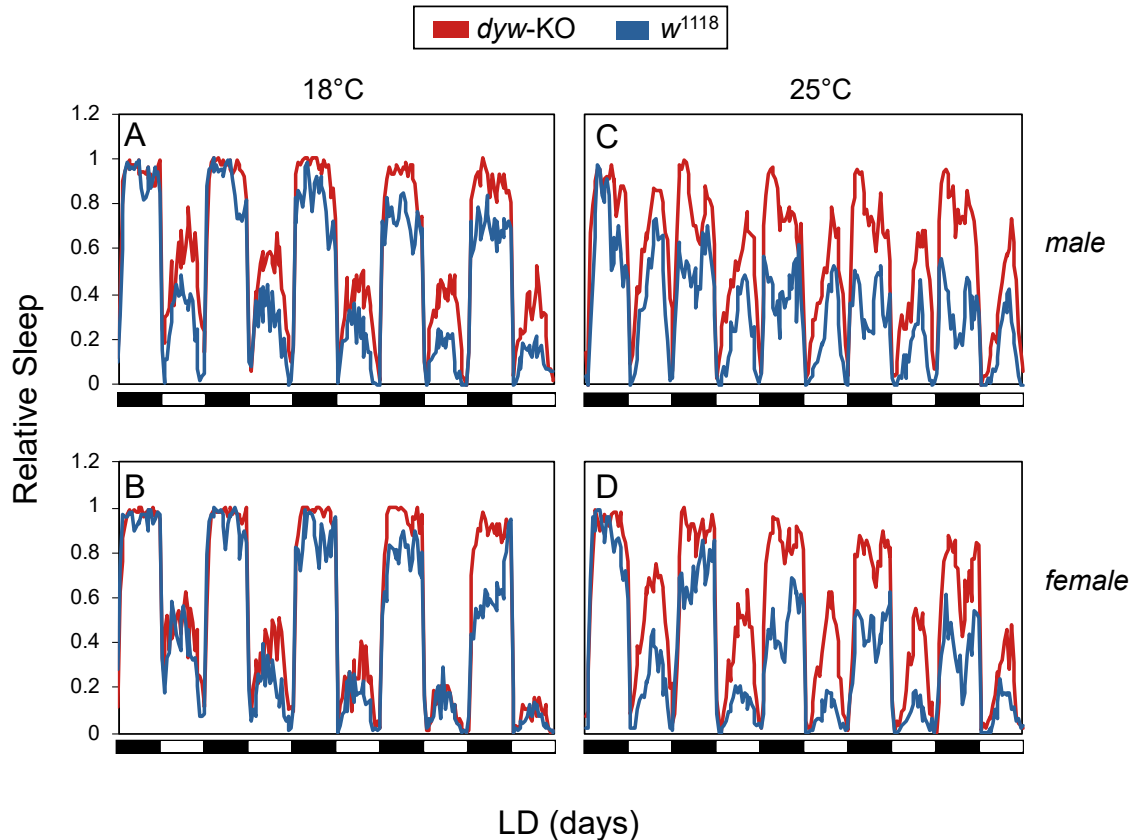


Figure 3.6. Malnutrition reveals a large effect on nighttime sleep in *dyw-KO* flies. (A – D) Young male and female *dyw-KO* and wildtype *w¹¹¹⁸* control flies were placed in activity tubes containing 1% sucrose media, exposed to several days of LD at either 18°C (left panels) or 25°C (right panels). Activity was continuously recorded and shown are group averages of the daily sleep profiles for *dyw-KO* (red) and control *w¹¹¹⁸* (blue) flies. For each genotype and sex, data from 16 individual flies were analyzed and pooled. Sleep values were normalized (1 = 100% sleep for the group). Black and white bars beneath panels represent lights-off and lights-on respectively. **Note:** The data shown here are derived from the same experiment as that shown in Fig. 3.3.

beginning of the experiment, this genotypic difference quickly disappears (Fig. 3.6, left bottom). Although not as rapid, this observation is reminiscent of what occurs at 18°C for females on standard 5% sugar (Fig. 3.2). We suggest that since females already have a low starting daytime sleep baseline, which further decreases throughout the experiment, additional wake-promoting conditions, such as low temperature and/or hunger-induced foraging activity, minimizes any 'additional' contributions from the wake-promoting activity of *dyw*.

An overlay of results for S1% and S5% shows that a change in diet not only affects the daily sleep behavior of wildtype flies as expected, but also the *dyw*-KO mutant (Fig. 3.7). In general, daytime sleep levels are consistently lower on the S1% diet for both *dyw*-KO and wildtype flies compared to the S5% diet (Fig. 3.7). Furthermore, this diet-dependent difference increased with time. A reasonable explanation is that as flies become increasingly malnourished on S1%, there is an increase in the magnitude of hunger-induced suppression of sleep increases.

We do note that beyond the generalities discussed above, altering sugar levels in the diet reveals complex interactions with genotype, temperature and gender. For example, at 25°C *dyw*-KO male and female flies manifest smaller diet-based differences in daytime sleep levels compared to wildtype control flies (Fig. 3.7, compare B and D, to F and H). This might be due to the increased midday sleep drive in *dyw*-KO flies, which in turn delays and/or attenuates the ability of hunger to act as an arousal cue. However, this trend is reversed at 18°C, whereby *dyw*-KO flies now show a greater difference in daytime sleep levels between the S1 and S5% diets compared to the relatively mild effects in wildtype flies (Fig. 3.7,

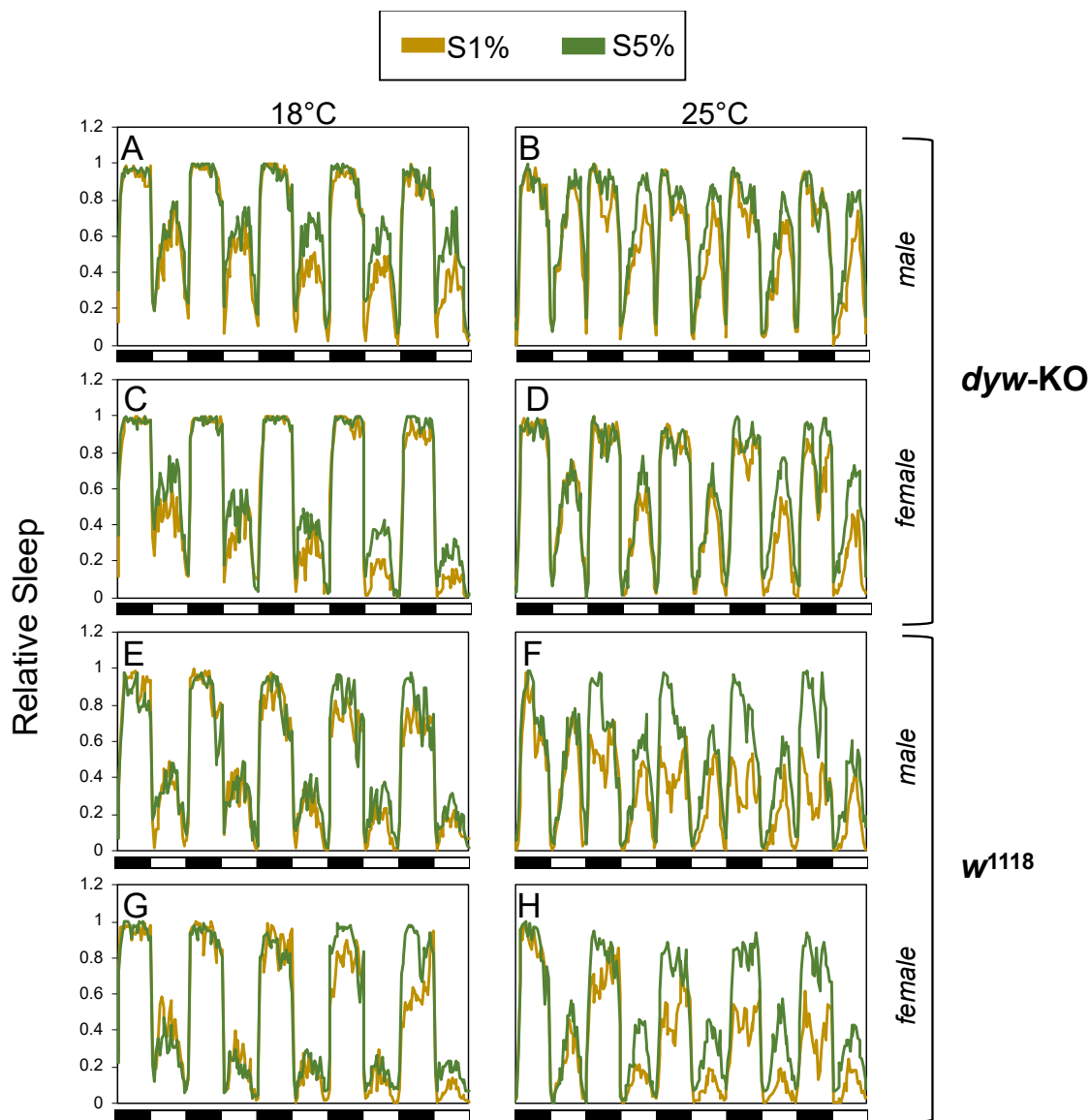


Figure 3.7. Malnutrition generally leads to reduced daytime and nighttime sleep in both *dyw-KO* and wildtype flies. (A – H) Overlay of results for S5% and S1% shown in figures 3.2, 3.3 and 3.6.

compare A and C, to E and G). Although further studies will be required to better understand these complex interactions, our results suggest the following; inactivating *dyw* does not impede hunger-induced stimulation of activity but it does alter its calibration as a function of temperature and possibly gender (see Discussion).

Surprisingly, assaying sleep behavior when flies are kept in nutrient poor conditions revealed an unexpectedly large effect of inactivating *dyw* function on nighttime sleep (Fig. 3.6). *Dyw*-KO flies sleep significantly more during the night compared to wildtype controls. This was even the case for female flies at 18°C which showed little effect of inactivating *dyw* function on daytime sleep (Fig. 3.6B). Even with prolonged malnutrition, nighttime sleep levels remained relatively high in *dyw*-KO flies. In contrast, nighttime sleep levels steadily declined for wildtype flies. We also noted that differences in nighttime sleep levels between *dyw*-KO and wildtype flies are more dramatic at 25°C (Fig. 3.6, compare panels C and D, to A and B). It appears that as flies become hungrier, *dyw* increasingly stimulates the ability of flies to forage at night. Without *dyw* function, flies apparently do not adjust their nighttime sleep behavior to accommodate this new survival risk (see Discussion).

Motivated by these results, we wondered if the VT1.1 transgene that reversed the daytime sleep increase of *dyw*-KO flies (Fig. 3.5) under standard conditions, would do the same for the nighttime effect observed when flies are placed on the more nutrient poor 1% sugar diet. Remarkably, whereas the

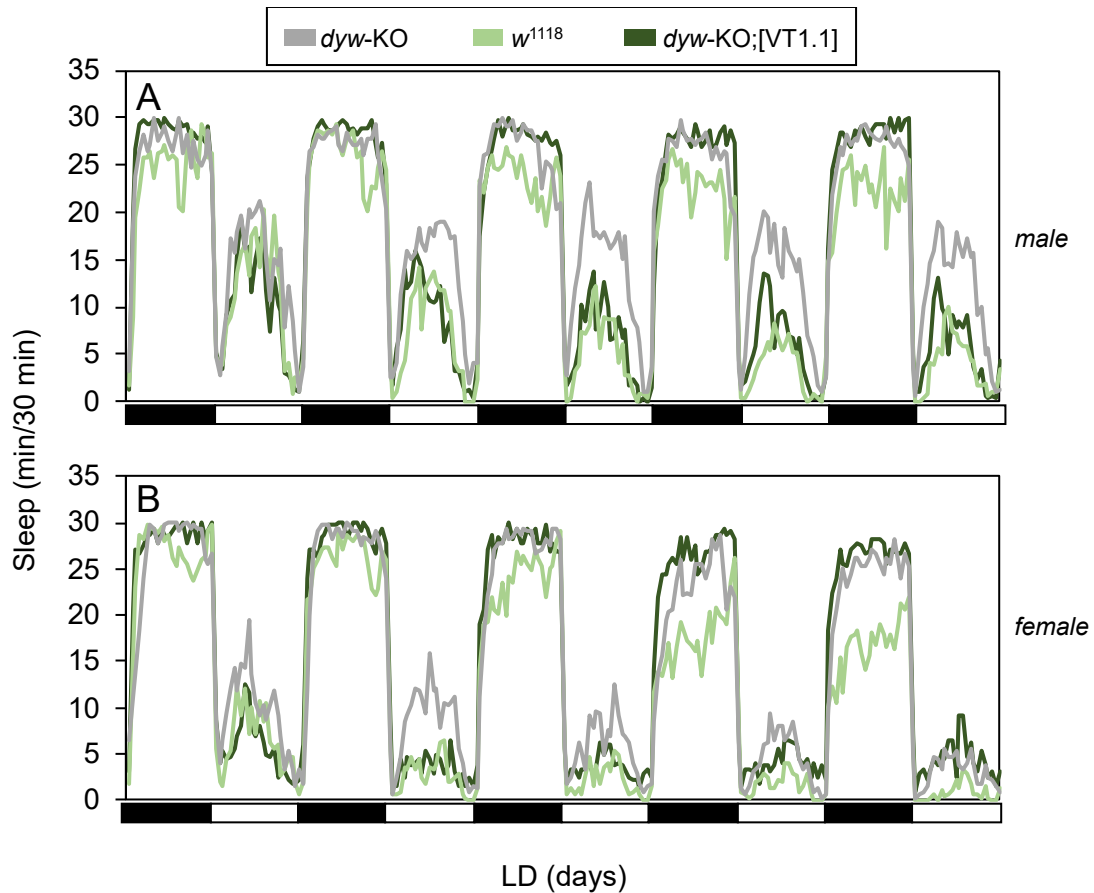


Figure 3.8. A *dyw*-containing transgene reverses the increased daytime but not nighttime sleep in *dyw*-KO flies under conditions of malnutrition. (A, B) Flies were maintained at 18°C in LD for several days on S1% diet. Shown are daily sleep profiles of male (A) and female (B) *dyw*-KO (gray), *w¹¹¹⁸* parental control (light green), and *dyw*-KO;*[VT1.1]* transgenic flies (dark green). Whereas the *dyw*-containing transgene lowers daytime sleep in a *dyw*-KO background to those similar in wildtype flies, little to no effect is observed on nighttime sleep levels. Black and white bars beneath panels represent lights-off and lights-on respectively. **Note:** this experiment was performed at the same time as that shown in figure 3.5.

increase in daytime sleep is reversed to that of the wildtype control, there is no effect on nighttime sleep levels of (Fig. 3.8).

Discussion

Prior work using transgenic flies showed that the effects of *dmpi8* splicing efficiency on midday siesta is mediated *in-trans* by regulating *dyw* expression [22]. A role for *dyw* in modulating midday siesta was further supported by genetic manipulation of *dyw* levels independent on *dmpi8* splicing. Decrease in *dyw* expression using RNAi led to higher midday siesta with little to no effect on nighttime sleep levels. Conversely, ectopic expression of *dyw* in clock cells lowered daytime sleep levels compared to parental controls. Although the magnitude of the effects on daytime sleep by down- and up-regulating *dyw* levels showed some variance depending on temperature or sex, the overall conclusion was that *dyw* mainly functions as an anti-siesta gene. To further explore the role of *dyw* on daily sleep behavior we generated flies where the endogenous *dyw* gene was inactivated by introducing premature stop codons into the *dyw* coding region (Fig. 3.1). Results with *dyw*-KO flies clearly support an anti-siesta role for *dyw* but reveal a much broader role in regulating nighttime sleep. Remarkably, the differential day-night effects of *dyw* are strongly influenced by nutritional status.

Drosophila melanogaster has been used as an animal model system to study sleep for the past 20 years [3, 4, 66]. Building on earlier work analyzing circadian rhythms, daily sleep behavior is routinely measured by recording the locomotor activity of individual flies over the course of many days [6]. Standard

conditions in the field involve exposing flies to light-dark cycles for at least several days at 25°C with a solid food source containing 5% sugar. Under these conditions, *dyw*-KO flies clearly support earlier results indicating a major role in attenuating midday siesta with little to no effect on nighttime sleep levels (Fig. 3.3). This was observed for both males and females. Likewise, for *dyw*-KO flies compared to wildtype controls when exposed to 18°C (Fig. 3.2). In our prior analysis of *dyw* function using transgenic flies we used similar conditions of LD with a 5% sugar diet at 18° and 25°C [22]. Thus, the results we obtained comparing the daily sleep of *dyw*-KO and wildtype controls at 18° and 25°C with a 5% sugar diet are highly similar to those we reported earlier using RNAi to downregulate *dyw* levels.

Nonetheless, at 18°C the *dyw*-KO flies revealed a small but noticeable effect on nighttime sleep behavior. Most notably, overall nighttime sleep levels are higher in *dyw*-KO mutants, an observation that is more prevalent in females (Fig. 3.2). It is possible that increased nighttime sleep was not observed with RNAi-mediated knock-down of *dyw* in flies tested at 18°C because sleep drive during the night is already very high and hence less sensitive to reductions in *dyw* activity. Otherwise stated, only in the complete absence of *dyw* can a further increase in nighttime sleep be observed. This might also explain why any effect of *dyw*-KO on nighttime sleep at 25°C is minimal; i.e., nighttime sleep in satiated wildtype flies is near maximal levels.

We also noticed a previously unrecognized steady decrease in overall daytime sleep levels over the course of the experiment, especially in females at

18°C (Fig. 3.2). We are not aware of any reports having made this observation. However, the majority of sleep experiments using *D. melanogaster* are carried out at 25°C for only several days and use either male or females but not both. A recent report indicated that very young flies (1-2 day old) sleep more compared to older flies [80], but it is not clear if such an explanation applies here. Intriguingly, after several days in LD daytime sleep levels in *dyw*-KO females at 18°C were similar to those observed in wildtype females, whereas nighttime sleep differences remained (Fig. 3.2). This suggests that under conditions where sleep drive is very low (e.g., daytime sleep in females at 18°C), the strong wake-promoting mechanisms in play override any sleep-promoting effects from loss of *dyw* function. At this stage it is not clear if the progressive decrease in daytime sleep levels for females at 18°C is due to duration in the experimental set-up or a physiologically relevant phenomenon related to aging. Prior work has shown that sleep becomes more fragmented in older flies [93, 94].

To summarize our observations under normal diet conditions, it is clear that abolishing *dyw* activity increases midday siesta for both sexes at multiple temperatures. However, the influence of *dyw* on different aspects of daily sleep behavior shows plasticity related to temperature and gender. For daytime sleep, the absence of *dyw* has a more limited effect on increasing midday siesta in females compared to males. Any increased sleep in *dyw*-KO females compared to their wildtype counterparts appears to progressively dissipate with time (Figs. 3.2 and 3.3). It is possible that the reduced effect of abrogating *dyw* activity on daytime sleep levels in females is related to the fact that wildtype females sleep

less during the day compared to males [78]. In addition, we also noted that midday siesta levels decline throughout the experiment for wildtype females, suggesting females naturally lose daytime sleep drive with time (at least, under the experimental set-up used) (e.g., Fig. 3.2). Since *dyw* counteracts daytime sleep promoting pathways [22], its absence may have little influence under conditions where daytime sleep drive is minimal. With regards to nighttime sleep the gender-effect is somewhat inverted; inactivating *dyw* function has a greater influence in females. As expected, the magnitude of any effect caused by eliminating *dyw* is modulated by temperature, in line with its role lowering midday siesta under cooler conditions wherein the dangers from heat exposure are minimized [22]. These findings with *dyw*-KO flies suggest a more complex role for *dyw* in regulating daily sleep behavior beyond its anti-siesta function [22].

Indeed, analysis of sleep behavior using a 1% sugar diet led to the unexpected discovery of a potent role for *dyw* in regulating nighttime sleep levels (Fig. 3.6). The original logic for evaluating the daily sleep behavior of *dyw*-KO flies on 1% sugar diet was to stimulate arousal. Presumably, hunger-induced activity is a biological response to increase foraging activity in the hopes of finding more nutritious food sources. Earlier studies did show that starvation quickly suppressed both day and night sleep, however under these condition flies die within a few days [74-76]. By testing different sugar concentrations, we found that on a diet of 1% sugar, flies exhibit hunger-induced suppression of sleep (e.g., Fig. 3.7; and data not shown), but can live at least one week (longer at 18°C). The

extended time-frame facilitates evaluating differences between the daily sleep profiles of *dyw*-KO and wildtype flies when challenged with malnutrition.

Remarkably, the rapid and sustained decrease in nighttime sleep for wildtype flies observed on the 1% sugar diet is largely absent in *dyw*-KO flies (Fig. 3.6). This occurred for males and females at both test temperatures. These data clearly show that *dyw* does not simply have an anti-siesta function as earlier work indicated [22]. Most notably, under conditions where the negative costs of prolonged hunger increase, the presence of *dyw* ensures that flies also forage for food during the night when sleep pressure is higher compared to the day.

We suggest that *dyw* is a key nexus in balancing daily wake-sleep states in relation to other survival needs. If food is plentiful it mainly operates during the day to optimize the wake-sleep balance relative to the threat from exposure to heat. As we previously stated, on cool days when the risks from heat exposure are reduced, increased *dyw* activity favors wakefulness and counteracts siesta promoting pathways [22]. Since the night phase always portends less risks of heat exposure, *dyw* has little influence on nighttime sleep, which is mainly driven by mechanisms that promote long periods of consolidated sleep. However, when challenged with nutritional needs, *dyw* promotes nighttime foraging without compromising its ability to regulate midday siesta. Clearly, foraging for food during the day can be a useful survival strategy but it still has to be balanced by risks from heat exposure. This balance will certainly be adjusted depending on the real-time relative threats from heat and starvation. Since the threat from exposure to the hot midday sun is absent at night, *dyw* can-over compensate for any necessary

midday siesta by strongly promoting nighttime arousal to increase the chances of finding needed food resources. It will be of interest to determine how diet affects *dyw* levels. Our findings identify a novel wake-sleep role for *dyw* in responding to internal physiological state, in addition to environmental cues.

A final point is that the *per-dyw* transgene reversed the daytime sleep difference between *dyw*-KO and wildtype flies but not the nighttime difference (Fig. 3.8). Several lines of evidence clearly indicate that the anti-siesta function of *dyw* is largely mediated by expression in cells that also express *per* [22]. Our findings raise the intriguing possibility that a critical regulatory element that drives *dyw* expression in cells mediating its effects on nighttime sleep is absent on the *per-dyw* transgenes used. It will be of interest to further determine the spatial aspects of *dyw* expression and function.

Acknowledgement. I am very grateful to Nicholas Pontillo, a technician in our lab, for his excellent help in the sleep analysis studies shown in this Chapter.

Star★Methods

Table 3.1: Key Resources Table

REAGENT or RESOURCE	SOURCE	IDENTIFIER
Chemicals, Peptides & Recombinant Proteins		
Drosophila agar (fly food)	LabScientific	FLY-8020
Drosophila yeast (fly food)	LabScientific	FLY-8040
Yellow Cornmeal (fly food)	LabScientific	FLY-8010
Light corn syrup (fly food)	LabScientific	FLY-8007

Propionic Acid (fly food)	Millipore Sigma	402907-500ML; CAS 79-09-4
Tegosept (fly food preservative)	Apex (Genesee Scientific, USA)	Cat# 20-258; CAS, 99-76-3
Bacto-Agar (behavior tubes)	VWR	Cat# 90000-760
Sucrose (behavior tubes)	Millipore Sigma	Cat# S7903-5KG
Bacto-Agar (behavior tubes)	VWR	Cat# 90000-760
Sucrose (behavior tubes)	Millipore Sigma	Cat# S7903-5KG

Critical Commercial Assays

<i>Drosophila</i> Activity Monitoring System	Trikinetics	
Coomassie Plus Assay Kit	ThermoFisher	1856210

Experimental Models: Organisms/Strains

<i>Drosophila melanogaster</i> : w[1118]	WellsGenetics	
<i>Drosophila melanogaster</i> : dyw-KO	This paper	5142, 5143, 5144, 5145
<i>Drosophila melanogaster</i> : dyw-KO;[dmpiUP]	This paper	1, 3, 4, 5, 6, 7, 8, 10
<i>Drosophila melanogaster</i> : dyw-KO;[VT1.1]	This paper	1, 2, 3
<i>Drosophila melanogaster</i> : dyw-KO;[dmpi8WT]	This paper	1, 2, 3, 4, 6, 7

Recombinant DNA

plasmid: pCasper-Hs-cper-88kx	[8]	
plasmid: pCasper-Hs-cper-M2M1	[8]	
plasmid: pCasper-VT1.1	[7]	

Software and Algorithms

MATLAB	MathWorks	MATLAB_R2019A
DAMSystem3 Data Collection Software	TriKinetics, USA	N/A

CHAPTER 4: Summary

Sleep is a critical biological function observed in many organisms. Chronic defects in the quality or quantity of sleep in humans are associated with poor health and linked to many diseases, such as diabetes, cancer and depression [30-32]. Most animals exhibit a particular time during a daily cycle when they exhibit a majority of their sleep. The temporal partitioning of sleep is controlled by the circadian timing system, leading to, for example, nocturnal and diurnal animals [1, 2]. In addition, sleep is under homeostatic regulation, whereby the drive for sleep increases with prolonged wake [2, 95-97]. There are also dedicated arousal circuits linked to circadian timing that contribute to the overall daily wake-sleep patterns observed. Many external and internal factors modulate daily wake-sleep behavior, including light, temperature, and metabolic needs [7-9, 75, 84, 85].

When studying sleep, much focus has been placed on investigating mechanisms driving the more robust nighttime sleep, characteristic of humans and other diurnal animals. However, a 'midday siesta' is widely observed in many animals and shown to affect human health and well-being [33, 68-71]. For example, short midday naps are linked to decreased blood pressure and improved cognition, whereas excessive daytime sleepiness or 'sickness behavior' is associated with many diseases and poor prognosis [30-32]. Recent work has shown a genetic basis for natural variation in human midday siesta that differs from factors regulating nighttime sleep [34]. For many years our lab has used the model genetic system, *D. melanogaster*, to investigate the function of midday siesta and its mechanistic underpinnings [7-9, 17, 20, 40, 77, 98-101]. In a breakthrough

study, our lab identified the first ‘anti-siesta’ gene called *daywake* [22]. A major focus of my thesis revolved around the biochemical characterization of the DYW protein (Chapter 2), and analysis of *dyw*-KO flies to better understand its role(s) in governing sleep behavior (Chapter 3).

As a key strategy to characterize endogenous DYW protein, I first set out to generate polyclonal antibodies. After several optimization steps I developed a reliable method for detecting endogenous DYW by Western blotting and also whole brain staining (Chapter 2 and Addendum 1). In this thesis I show that the DYW protein is present in fly heads and bodies, and that its levels are modulated by *dmpi8* splicing efficiency and temperature in a manner similar to that observed for *dyw* transcript levels (Figs. 2.1 – 2.4). We also observe that DYW is found in key clock neurons in the adult fly brain (Fig. 2.5). Using a *Drosophila* cell culture system, I show that DYW possesses high secretory potential, consistent with its predicted function as a juvenile hormone binding protein (Fig. 2.6). Further, we show that abolishing DYW protein production via CRISPR-mediated knockout (*dyw*-KO) leads to increased midday siesta (Figs. 3.2 – 3.5), supporting earlier results obtained using RNAi mediated knock-down in clock-expressing cells. While some of these results are predictable, analysis of *dyw*-KO flies revealed a highly unexpected role for *dyw* function on nighttime sleep regulation, especially under conditions of malnutrition (Figs. 3.6 and 3.7). Taken together, these results make significant contributions to our understanding of the molecular mechanisms governing the balance between wake and sleep during the day, and lay the groundwork for future studies examining its biochemical and cellular bases.

It has long been established that the splicing efficiency of the *dmpi8* intron varies with temperature and affects daily activity rhythms [9, 77]. However, the mechanism underlying this phenomenon remained elusive until *dyw* was identified by our group [22]. The abundance of *dyw* mRNA levels are higher when *dmpi8* is spliced more efficiently, for example at cooler ambient temperature. My work further indicates that the total levels of DYW in fly heads are generally higher at 18°C compared to 25°C (Fig. 2.2). As a secondary approach to determine if DYW protein levels are responsive to *dmpi8* splicing efficiency, we analyzed natural populations of *D. melanogaster* from the eastern coast of Australia. Earlier work analyzing natural populations of *D. melanogaster* from the United States, Africa and Australia identified several single nucleotide polymorphisms (SNPs) in the 3' UTR of *per* that can influence the splicing efficiency of *dmpi8* and midday siesta levels [8, 20, 21]. In all these populations, the most influential variant is SNP3, which exists in either A or G variants [21]. Flies containing the SNP3G variant splice *dmpi8* more efficiently compared to their SNP3A counterparts and exhibit less midday sleep [7]. Indeed, SNP3G flies produce significantly more DYW compared to SNP3A containing lines (Fig. 2.3). Taken together, these results establish that *trans*-regulation of *dyw* mRNA levels by *dmpi8* splicing efficiency also lead to similar changes in the abundance of DYW accumulating in the head.

Since *dmpi8* splicing efficiency regulates *dyw* mRNA levels in a manner that is also reflected in the abundance of DYW protein, we predicted that downregulation of *dyw* expression in *per*-expressing cells should lead to a significant drop in the amount of DYW protein. Indeed, RNAi of *dyw* using *per*

specific drivers showed a marked decrease in the detectable levels of DYW protein (Fig. 2.4, lanes 2-4)). In contrast, expressing RNAi-*dyw* in the eyes does not alter DYW protein levels, suggesting that in the head DYW protein mainly accumulates in the brain (Fig. 2.4, lanes 7 and 8). Interestingly, knockdown of *dyw* using a *cryptochrome* (*cry*) driver led to perhaps even a larger decrease in total DYW protein abundance (Fig. 2.4, lanes 5 and 6). CRY is the key circadian-relevant photoreceptor in the *Drosophila* circadian timing system responsible for keeping fly rhythms in-sync with the daily light-dark cycle [102, 103]. There are approximately 150 *per*-expressing clock neurons in the brain that comprise the clock network governing the daily activity rhythm [104]. These are organized into three major spatially distinct bi-lateral clusters that also exhibit different functional properties. The clock groups include the small and large ventro-lateral neurons (s-LNvs and l-LNvs), dorsal neurons (DN1, DN2, DN3) and lateral dorsal neurons (LNds) [105-107]. While *per* and *cry* show extensive overlap in expression in the adult brain, there are *per*-expressing but not *cry*-expressing clock cells [108, 109]. This suggests that *dyw* might be preferentially expressed in the *cry*-expressing subset of clock cells. Interestingly, CRY also functions as an arousal agent [108, 109]. Since the influence of *dyw* on midday siesta is dependent on the presence of light [22], it will be of interest to determine if there is a functional connection between DYW and CRY.

To further examine spatial aspects of endogenous DYW, we used our anti-DYW antibodies to stain whole brains from adult flies (Fig. 2.5). Although preliminary, our initial attempts clearly indicate that DYW accumulates in what

appear to be clock and non-clock cells (unpublished observations). In this thesis I mainly concentrated on asking if DYW co-localizes in the PDF-expressing clock cells as co-staining with anti-PDF antibodies clearly identifies these cells. The PDF positive small and large ventro-lateral neurons (LNvs) are key cells in the fly nervous system regulating circadian rhythmicity [105-107]. Whole brain imaging using confocal microscopy in the presence of anti-PDF and anti-DYW antibodies reveal that DYW strongly co-locates with PDF, indicating that DYW accumulates in circadian neurons in the *Drosophila* brain. Previous studies have shown that *dyw* is capable of exerting its effects on daytime sleep in a clock-independent and PER protein independent manner [22]. Thus, although DYW is produced in clock cells, it might have a purely non-clock role in regulating sleep behavior. In addition, DYW also stains non-clock cells and is observed in the body, further suggesting a role for DYW outside of the clock (Fig. 2.1 and data not shown). Finally, DYW is predicted to be a secreted JHBP and as such its site of production (e.g., LNvs) might not be its sole or primary site of action. Nonetheless, the observation that DYW accumulates in clock neurons and other neurons of the brain suggests that DYW might also have a local neurological function.

To determine if DYW acts as a typical JHPB and can be secreted (presumably to the hemolymph in flies) we turned to the well-established *Drosophila* S2 cell system where we are able to more quickly evaluate biochemical properties of DYW and mutant variants. Computational analysis of the DYW coding sequence predicts that the first 25 residues are highly hydrophobic and comprise a common protein secretion marker known as a signal peptide (Fig. 2.6).

When expressed in cultured cells, wildtype DYW is detectable both intracellularly and in high amounts in the culture media without the need for purification demonstrating that DYW exhibits high secretory activity. As predicted, deletion of residues 1-25 (DYW Δ 1-25) resulted in dramatic reduction of DYW secretion into the culture media. Interestingly, an increase in intracellular DYW levels was also observed in DYW Δ 1-25 expressing cells, suggesting that the removal of aa 1-25 does not affect the translational activity or stability of DYW, and instead exclusively impacts its secretory potential.

Having established that DYW is a secreted protein, we checked for the possibility of glycosylation, another classic secretion hallmark. We treated intracellular extracts and culture media with Endoglycosidase H (EndoH) which cleaves the chitobiose core of high-mannose and some hybrid oligosaccharides. Intracellularly, we observe drastic changes in the pattern of DYW staining via western blotting (Fig. 2.6B), suggesting that higher molecular weight variants are due exclusively to glycosylation. Unexpectedly, no change in DYW banding pattern was observed in the culture media, though this is likely due to oligosaccharide maturation in the Golgi prior to secretion resulting in more complex glycans resistant to EndoH digestion [55-57].

Analysis of the DYW sequence revealed that residue Asn 182 is highly likely to be glycosylated and so we generated and expressed DYW(N182A) in cultured cells (Fig. 26, B – D). Remarkably, we observed the almost complete elimination of detectable DYW levels, suggesting that glycosylation of N182 is critical for DYW maturation and/or stability. Glycosylation often plays a critical role in proper folding

of ER-targeted secretory proteins [45, 58-60]. Proteins which undergo multiple failed folding attempts in the ER are transported from the ER into the cytoplasm via ER retro-translocation, after which they are targeted for proteasome mediated degradation [61-64]. It is possible that glycosylation of N182 is a crucial step in the proper folding of DYW in the ER and removing this key marker results in rapid degradation of DYW.

Combining our analysis of DYW in flies with results obtained in cultured cells, provide significant insights into the characteristics and behavior of the DYW protein. Most notably, DYW accumulates in clock neurons in the brain. It is also likely to be secreted protein via cleavage of a 25 residue signal peptide at its N-terminus and a glycosylation event at position N182 for proper processing and trafficking. In light of these results, we propose that DYW is strongly produced in clock cells in the fly and responds to temperature/SNP3-haplotype via changes in *dyw* transcript levels responding to *dmpi8* splicing efficiency. In these cells, the signal peptide targets the nascent DYW peptide along with its associated ribosome to the ER where translation continues across the ER membrane. The signal peptide comprising the first 25 residues is then cleaved co-translationally and, as protein synthesis continues, N182 is glycosylated granting access to the calnexin-calreticulin cycle ensuring proper folding. The core-oligosaccharide on N182 is then matured, likely in the Golgi. A portion of DYW is then subsequently secreted into the hemolymph, whereupon it binds juvenile hormone, possibly crossing the blood-brain barrier, and delivering it to target tissues. Action at these target tissues triggers downstream signaling cascades resulting in physiological responses

ultimately manifesting in sleep regulation. Further studies probing the presence of DYW in *Drosophila* hemolymph are necessary to confirm aspects of this proposed model.

In related studies, to further explore the role of *dyw* on sleep behavior we generated *dyw*-KO flies using CRISPR technology by introducing premature stop codons in the *dyw* coding sequence (Fig. 3.1). Daily sleep behavior of *dyw*-KO mutants compared to their genetic wildtype controls is consistent with previous results showing *dyw* to have anti-siesta activity [22]. However, we discovered an additional role for *dyw* in modulating nighttime sleep which is heavily dependent on nutritional status.

Initial experiments examining the sleep behavior of *dyw*-KO flies used standard conditions widely used in the field; i.e., exposing flies to light-dark cycles over several days at 25 (or other temperatures) with a solid food source containing 5% sucrose [17, 21, 22, 90, 91]. Analysis of *dyw*-KO flies compared to wildtype genetic controls clearly support earlier reports that *dyw* plays a critical role in modulating daytime sleep, with little to no effects on nighttime sleep [22]. We did note slight differences in nighttime sleep levels, especially for female flies at 18°C, wherein overall nighttime sleep levels are elevated in *dyw*-KO mutant (Fig. 3.2). This is in contrast to previous reports using RNAi against *dyw* which showed no effect on nighttime sleep [22]. It is possible that this modest effect of increasing nighttime sleep is only observable in the complete absence of functional *dyw*. Females might provide a more sensitive background to observe conditions that lead to increased sleep as they generally sleep less compared to males [78].

Additionally, we also observed a consistent decrease in overall daytime sleep levels over the course of our behavior experiments. We are not aware of any reports which have shown this, though this is likely because standard *Drosophila* sleep/activity experiments take place over the course of several days, while ours continued for significantly longer [17, 21, 22, 90, 91]. It is not clear if this downward trend is a result of aging, as it has been established that sleep in older adult *Drosophila* is more fragmented [93, 94].

We also observed that P-element insertion of the *dyw* gene into *dyw*-KO lines was sufficient to rescue the siesta phenotype in mutant flies (Figs. 3.4 and 3.5). As predicted *dyw*-KO;*[dmpi8UP]* flies showed significant reductions in daytime sleep compared to their *dyw*-KO;*[dmpi8WT]* counterparts and both slept less than *dyw*-KO control flies (Fig. 3.4). Interestingly, we found that sleep levels were higher in *dyw*-KO flies during the transition from lights-on to lights-off (and vice versa) (Fig. 3.4) suggesting that *dyw* deficient flies exhibit increased arousal thresholds, consistent with prior evidence [17, 22]. Rescue of *dyw*-KO flies using the VT1.1 *per-dyw* transgene, which is more representative of the natural *per-dyw* genomic region showed similar reduction in daytime sleep compared to *dyw*-KO flies further confirming the role for *dyw* in daytime sleep regulation (Fig. 3.5).

Though standard conditions for behavioral assays in *Drosophila* typically use a ~2% agar, 5% carbohydrate mixture as a food source, hunger in flies results in reduced sleep, presumably as the flies are more active foraging for food [74-76]. Thus, to stimulate arousal we evaluated *dyw*-KO flies kept on a 1% sugar diet, predicting that the sleep-promoting effect of the lack of *dyw* might render *dyw*-KO

flies more resistant to hunger induced sleep suppression. Surprisingly, in both males and females and at both 18° and 25°C, we observed a sustained increase in nighttime sleep in *dyw*-KO flies compared to wildtype controls. We suggest a novel role for *dyw*, ensuring that when the risk of starvation outweighs the negative effects of sleep deprivation, flies are able to forgo sleep during the night to forage for food. In the absence of *dyw*, flies appear less sensitive to risks from malnutrition and prevent arousal during the night.

In conclusion, the work presented in this thesis lays out the basis for the functional characterization of *dyw* both biochemically and behaviorally. We have shown that DYW is a secreted protein that accumulates in key circadian neurons in the brain. Additionally, in contrast to prior work, we have demonstrated a novel role for *dyw* in sleep regulation, serving as a link between wake-sleep needs and other survival risks. These results shed new light onto the regulation of sleep and may provide a basis to better understand the still poorly understood dynamic balance between wake and sleep states when challenged with survival threats that benefit from either enhanced quiescence or vigilance; e.g., sleep to avoid dangers associated with exposure to the hot sun, but increase wake to forage for food when hungry.

Addendum 1: Optimization of anti-DYW antibody

Brief Overview

Herein I describe some of the procedures I did to optimize our anti-DYW antibodies in the hopes that the results are of value to others. Three antibodies were raised against DYW(26-260) and the sera from immunized animals (Guinea Pig, GP49; and Rat, R17, R18) was used for Western Blotting (WB) applications (see Chapter 2). Initially, we used our standard protocol for WB. Briefly, protein samples were added to 1x SDS sample buffer (50mM TrisHCL [pH=6.8], 2% SDS, 10% glycerol, 1% β -mercaptoethanol, 12.5mM EDTA, 0.02% bromophenol blue) and loaded onto 12% polyacrylamide gels. Following transfer onto a 0.45 μ m pore size nitrocellulose membrane (GE Amersham cat#10600002), 5% blotting grade blocker was used as both the blocking agent and antibody diluent. For my work, it was imperative that any anti-DYW antibodies generated could visualize endogenous DYW in fly extracts. Representative immunoblotting results using the three anti-DYW antibodies are shown in Fig. A1.1. Antibody R17 yielded the weakest signal and so further optimization steps focused on antibodies GP49 and R18. Signals from these antibodies revealed a doublet of ~26kDa, in agreement with the predicted molecular mass of DYW. However, the signal was weak and there was prominent background staining and “speckling” patterns. Thus, while we were successful in generating antibodies which could detect DYW in fly extracts, additional optimization was required to yield reliable and reproducible results.

Figure A1. Initial results testing the anti-DYW antibodies using our standard

Western Blotting conditions. Heads from adult flies expressing DYW-3xFLAG were prepared in modified RIPA buffer and detected via Western Blotting using either GP49, R17, R18 using our standard Western Blotting protocol. Lanes 1, 3 and 5; fly head extracts from flies overexpressing DYW using the *e/av*-GAL4 promoter. Lanes 2, 5 and 6; fly head extracts from *dmpi8UP* flies. Typical example of early results is shown.

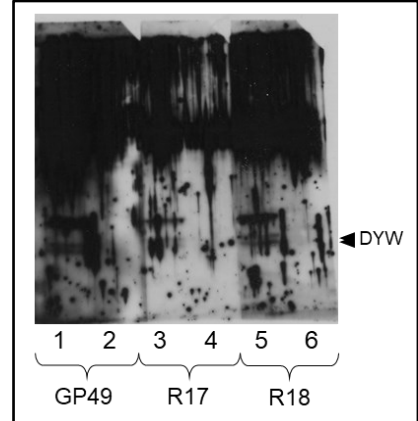
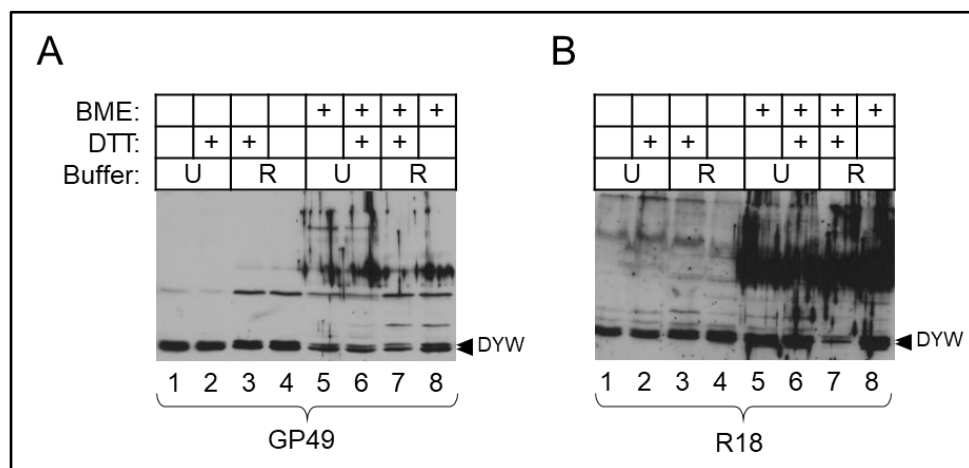


Figure A1.2. Optimization of anti-DYW antibodies for immunoblotting. (A, B)

Canton S fly heads were prepared in either modified RIPA (R) or urea (U) buffers, followed by incubating in 1x sample buffer with (+) or without (-) β -mercaptoethanol (BME) and/or dithiothreitol (DTT). Panels B and C were blotted using anti-DYW antibodies GP49 and R18, respectively. Note that much of the background staining can be reduced by eliminating BME from the sample buffer.



Optimization steps

To address this issue, we undertook a multi-fold troubleshooting procedure; with main points highlighted below (note, we relied on collating many optimization protocols for Western blotting from commercial entities and open forums, such as Researchgate.net):

(1) High Background and Speckling.

To address the high background the blocker concentration was reduced from 5% to 1%. In addition, in order to reduce “speckling” the blocking buffer was incubated at 4°C overnight with end-over-end rotation to ensure the buffer was completely dissolved.

(2) Extraction buffer stringency.

Typically, fly heads are homogenized in modified RIPA buffer (R) using a motorized pellet pestle (see Chapter 2 materials and methods). To see if a more stringent buffer would yield more reliable results, we also homogenized heads in 6M urea buffer (U) (6M Urea, 150mM NaCl, 20mM Tris·HCl [pH=8.0]), another commonly used extraction buffer.

(3) Streaking indicative of keratin cross-reactivity.

A prominent streaking pattern could be observed at ~60 kDa (Fig A1.1), suggesting that all of our antibody species may be keratin sensitive and that our samples were routinely contaminated by keratin (typically due to the presence of reducing agents in the sample which strip keratin from nearby sources such as unsterile gloves or non-sterile tubes/pipettes) [110, 111]. Our standard sample loading buffer (see above) contained the reducing agent β -mercaptoethanol thus we tested what

effects the removal of BME or its replacement with the alternative reducing agent dithiothreitol (DTT) would have on blot quality.

Summary of results

A summary of the main variables we tried and the results of are shown in Fig. A1.2. Changes to the blocker concentration, as well as allowing it to fully dissolve overnight, dramatically improved background as well as completely eliminated “speckling” for both antibodies GP49 and R18 (Fig. A1.1A and B all lanes). In contrast, the changes we made to extraction buffer composition made little to no difference in overall quality (Fig A1.1, A and B, compare “U” and “R” lanes). However, removal of β -mercaptoethanol from the loading buffer completely abrogated the streaking consistent with keratin cross-sensitivity, while DTT had little no effect. The overall quality and sensitivity of antibody GP49 compared to R18 led us to use GP49 as our standard anti-DYW antibody moving forward. In addition, based on the low background and high sensitivity using modified RIPA buffer for extraction and no reducing agent in the loading buffer, these conditions were followed throughout this thesis (Chapters 2 and 3). Taken together, these optimizations enabled us to reliably biochemically characterize the DYW protein in *Drosophila*.

Addendum 2: Proteomic approach to characterize relationship between PER phosphorylation and structure

Brief Overview

Circadian rhythms (~24 h) have been documented in organisms ranging from cyanobacteria to humans and the molecular workings of these rhythms have been extensively studied in several model systems. The PER proteins are key clock components in animals and their daily life-cycles are regulated by time-of-day specific phosphorylation events [1]. In *Drosophila*, the PER protein undergoes a progressive phosphorylation cascade throughout the day, which is critical for progression of the circadian cycle [98, 99, 101, 112, 113], and is the main “state-variable” in maintaining the pace of the clock [114-116]. Our lab identified approximately 30 phosphorylation sites on *Drosophila* PER [99, 101, 117-120]. Among the phospho-sites, phosphorylation of Ser47 is critical as it promotes binding of the F-box protein SLIMB, targeting PER for rapid degradation by the proteasome during the early day, leading to another round of CLOCK-CYCLE-mediated transcription (see Fig. 1.1) [99]. Phosphorylation of Ser47 is first observed in the late-night, after PER already attains a hyper-phosphorylated state and just prior to its rapid degradation [99]. Based on differential sensitivity to partial proteolysis [98], we proposed that the time-dependent increases in PER phosphorylation eventually leads to a more open conformation in the Ser47 region, stimulating its phosphorylation and hence SLIMB binding [98] (Fig A2.1A). Intriguingly, after this model was proposed, a similar observation was made for the key phospho-clock

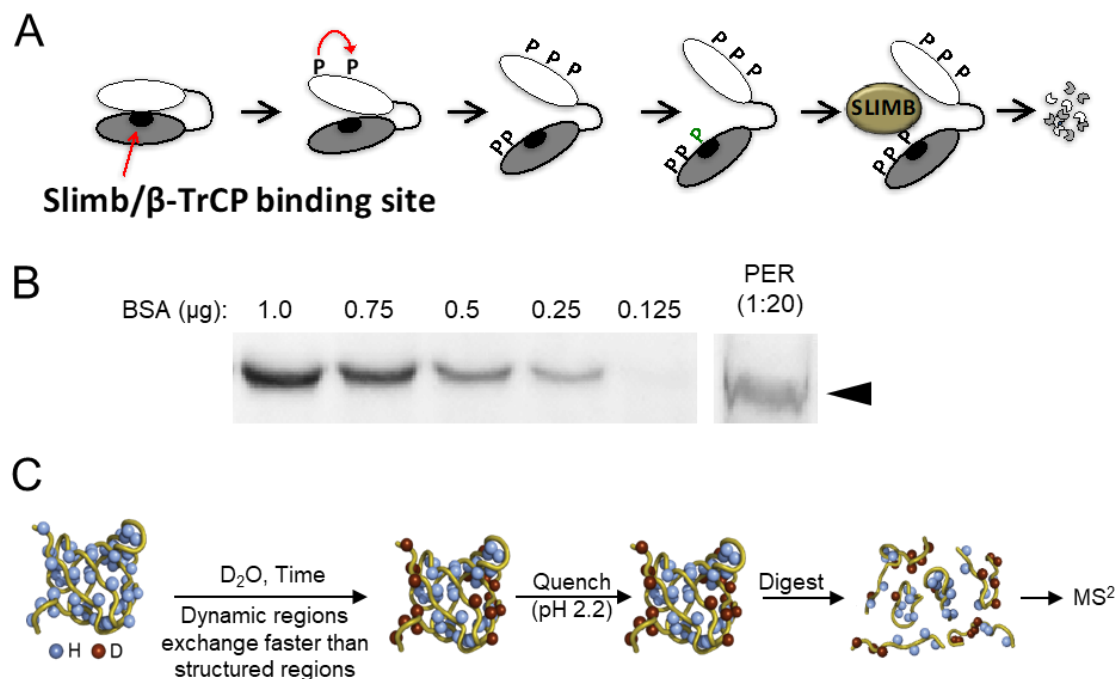


Figure A2.1. Use of Hydrogen-Deuterium Exchange Mass Spectroscopy to investigate if hyper-phosphorylated PER has a more open conformation compared to its non-phosphorylated state. (A) Schematic representation of the proposed mechanism by which progressive phosphorylation opens up the conformation of PER, facilitating proteasome mediated degradation via the binding of the F-Box protein SLIMB. **(B)** PER protein expressed in *Drosophila* S2 cells was isolated using anti-FLAG affinity purification and compared to known concentrations of Bovine Serum Albumin (BSA) to determine concentration for further processing. **(C)** Schematic representation of the principals behind hydrogen-deuterium exchange followed by mass spectrometry (HDX-MS).

protein in *Neurospora* termed FREQUENCY (FRQ) [121-124]. Mutations leading to altered phosphorylation of PER proteins leads to familial sleep disorders in humans [125, 126], which may play roles in other disease outcomes such as Seasonal Affective Disorder, non-24, alcoholism and a range of metabolic syndromes, cancers [127-131]. Thus, understanding the relationship between PER phosphorylation and its conformation could lead to the development of better “designer” drugs to combat diseases linked to clock malfunctions.

Rationale for experimental approach

We faced several limitations when designing an experimental strategy to investigate the structure of PER in relation to its phosphorylated state. Although expression in *E. coli* of recombinant *per* could yield amounts of protein necessary for crystallization, this host is not capable of phosphorylating PER in a physiologically relevant manner. Expression in cultured S2 cells, while able to recapitulate PER phosphorylation [98-100], is not be able to yield mgs of purified protein sufficient for X-ray crystallography. Additionally, crystallization requires a structurally homogenous protein population and as PER contains >30 phosphorylation sites, obtaining a homogenous population for crystallization was simply not possible.

Other methods to study PER conformation were also explored such as nuclear magnetic resonance (NMR) and cryo-electron microscopy (cryo-EM). However, PER fell outside of the detection region for both, being too large for NMR [132] while also not ideal for the larger structures normally amenable to cryo-EM

studies [133]. Based on size and production limits for physiologically relevant PER [99, 101], we decided to focus on using Hydrogen-deuterium exchange coupled with mass spectrometry (HDX-MS), the theory of which is summarized in [134] and Fig. A2.1C Briefly, protein in its native state is introduced to a deuterated environment (H_2O is replaced with D_2O) whereupon amide hydrogens in the peptide backbone are replaced with deuterium (H^3 or simply “D”). Highly structured or buried regions exchange amide hydrogens at a slower rate than exposed surface regions and the shift in weight from H^2 to H^3 can be detected using MS^2 allowing us to infer the accessibility of different regions within PER.

In order to study the effects of phosphorylation on the dynamic conformation of PER we set out to compare the deuterium exchange efficiencies of hyper- and hypo-phosphorylated PER isoforms. Typically, generating hyperphosphorylated PER is accomplished in tissue culture by co-expressing the primary kinase responsible for PER phosphorylation, DOUBLETIME (DBT), with mutant PER(S44-48A) which lacks critical Serine residues responsible for phosphorylation dependent degradation resulting in highly stable hyperphosphorylated PER protein [99]. However, overexpressed DBT binds strongly to PER in a 1:1 stoichiometric ratio [135], which adds an additional complication as the stable interaction of DBT would also affect deuterium exchange reactions on PER. Instead, we used a second approach that also leads to the progressive phosphorylation of PER in S2 cells. Namely, addition of the phosphatase inhibitor Calyculin A (calA) is sufficient to enable the limited amount of endogenous DBT to generate hyperphosphorylated PER(S44-48A) [99, 136].

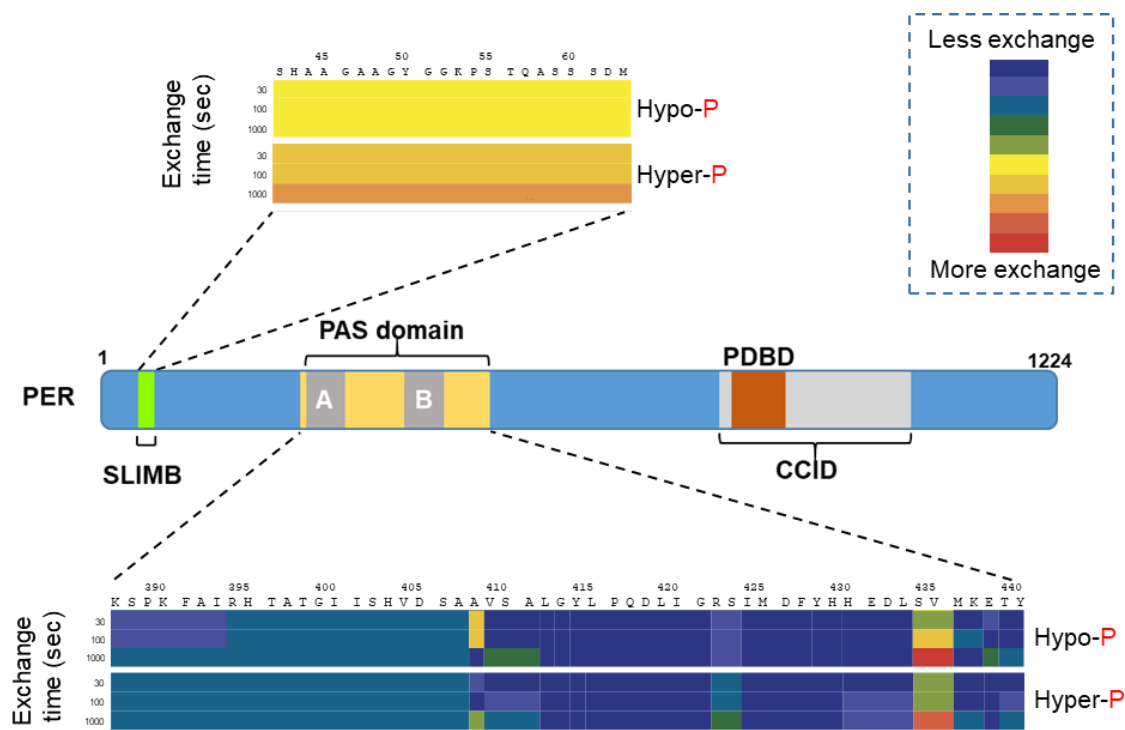


Figure A2.2. HDX-MS suggests that hyperphosphorylation of PER leads to a more open conformation of the SLIMB binding region but no effect on the PAS region. Cultures of S2 cells expressing a recombinant version of *per* were split, whereby one half was treated with CalA. Purified PER protein that was either hypo-phosphorylated (Hypo-P) or hyper-phosphorylated (Hyper-P) were divided into three aliquots, subjected to HDX, and quenched after 30, 100 and 1000 sec (left of panels). Shown are heat maps (scale; top right) representing results for the SLIMB-binding region (top) and the PAS dimerization domain (bottom). A schematic of the PER open reading frame with several different domains is shown (middle; PDBD; PER DBT Binding Domain; CCID, CLOCK-CYCLE Inhibitory Domain). Note that there is clearly more exchange for the SLIMB region of the Hyper-P sample compared to the Hypo-P sample, whereas the PAS region is basically inaccessible irrespective of phosphorylation status.

Cultured S2 cells transfected with pMT-3xFLAG-*per*(S44-48A) were induced using copper sulfate as previously described (see Chapter 2, Materials and Methods) in either the presence or absence of calA. We were able to purify ~15 μ g of PER protein per 1L of S2 cell culture using a magnetic FLAG resin (Millipore Sigma cat#M8823-1ML) (Fig A2.1B, see Ch. 2, Materials and Methods for detailed protocol). Deuterium exchange was performed by incubating resin bound protein in deuterated modified RIPA buffer for 30, 100 and 1000 seconds. The pH of the buffer was then lowered to 2.2 using 12N HCl, quenching the exchange reaction (locking in deuteration) while also denaturing the FLAG resin thus releasing hyper- and hypo-PER(44-48A) from the column ready for digestion and MS² analysis.

MS² analysis of PER(44-48A) fragments after pepsin digestion was unable to provide coverage of the entire protein sequence, however we were able to study two crucial regions of PER, the SLIMB binding domain and the PAS dimerization domain. We were glad to observe that, the critical SLIMB binding domain adopts a more open configuration when PER(44-48A) is hyperphosphorylated (Fig. A2.2A). This further supports our earlier proposal that suggested the overall structure of PER was more open when hyperphosphorylated [99], but offers a more detailed analysis of the key region driving phosphorylation-mediated degradation. Conversely, the PAS region appears to be quite buried in PER and largely inaccessible to solvent irrespective of phosphorylation status. Indeed, prior X-ray crystallography of the PER PAS region expressed in bacteria revealed that this region is highly hydrophobic and largely involved in PER-PER inter- and intra-molecular interactions [137, 138]. In addition, the PAS region is also critical in

forming stable PER:TIM dimer complexes [139, 140]. The fact that hyperphosphorylation increased solvent accessibility to the SLIMB binding region but not the more rigid PAS domain, suggest that our experimental design is reporting physiologically relevant changes in conformation.

While our results are limited in scope, we have demonstrated that the overall strategy employed, from using the PER(44-48A) mutant to carrying the exchange while PER is still bound in its native form to affinity column, is able to distinguish between structured and dynamic regions. It is hoped that with further, higher resolution data with greater sequence coverage will be obtained to better elucidate the dynamic relationship between PER phosphorylation state and conformation.

Addendum 3: Transgenic *Drosophila* models generated that were not used in this thesis

Transgenic *Drosophila* models listed in table A3.1 were generated in a *dyw*-KO background but were not utilized in this thesis due to time constraints. However, they will serve as tools for further studies into the function of *dyw* on sleep. Below I give a brief summary of what these novel transgenic flies will/can be used for.

Table A3.1. List of lines generated in *dyw*-KO backgrounds.

Transgene	Construct	Backbone
<i>dyw</i> -KO; <i>[per⁰/dmpi8WT]</i>	Per0-88kx	pCaSpeR 3
<i>dyw</i> -KO; <i>[dmpi8WT,dyw-3xFG]</i>	pCasper-88-0.9FL	pCaSpeR 3
<i>dyw</i> -KO; <i>[UAS-dyw-3xFG]</i>	pUAST-0.9-3FL	pUAST
<i>dyw</i> -KO; <i>[dmpi8WT, dyw-stop]</i>	88kx-0.9stop	pCaSpeR 3
<i>dyw</i> -KO <i>[DsRed]</i>		

- 1) *dyw*-KO;*[dmpi8WT,dyw-3xFG]* flies were generated to aid in investigating spatial/temporal aspects of *dyw* function. Because the transgene has been introduced into the *dyw*-KO background, the only source of DYW is FLAG-tagged, enabling the visualization of DYW in physiologically relevant places. These flies will serve as an additional strategy to using our anti-DYW antibodies described in Chapter 2. Similarly, *dyw*-KO;*[UAS-dyw-3xFG]* will allow us to visualize the expression patterns of DYW resulting from the use of different

- Gal4 driver lines. It is also possible that because DYW is tagged with 3xFLAG epitope this could facilitate its purification. For example, this might be useful when trying to determine if DYW is present in the hemolymph of adult flies, or to isolate partners using mass spectrometry.
- 2) The *dyw*-KO[DsRed] are very useful as they report where *dyw* is expressed at the transcript level. This construct has a DsRed fluorescent tag inserted into the *dyw* gene, abolishing *dyw* expression and replacing it with *dsRed*. Thus, using fluorescent microscopy we will be able to reliably and easily determine sites of *dyw* expression either in cells or whole flies. Indeed, initial results are very encouraging with these flies and we can easily detect specific DsRed staining in the head and body of adult flies.
 - 3) Finally, although of less import, *dyw*-KO;*[per⁰/dmpi8WT]* express a *per* null mutant carrying the wildtype *dmpi8* splice site and *dyw* coding region. This *per*-null containing transgene was generated to serve as a further control for the transgenic flies reported above in Chapter 3 (see Fig. 3.4). Essentially, we expect that inactivating *per* function in the transgene will not affect the ability of this transgene to rescue the sleep phenotype in *dyw*-KO flies since functional *dyw* is still provided. On the flip side, *dyw*-KO;*[dmpi8WT, dyw-stop]* should not rescue the sleep changes observed in *dyw*-KO flies.

-These tools, while not utilized in this thesis, will serve as the basis for future studies, as well as expanding the results presented in Chapters 2 and 3.

References

1. Edery, I., *Circadian rhythms in a nutshell*. *Physiological Genomics*, 2000. **3**(2): p. 59-74.
2. Dubowy, C. and A. Sehgal, *Circadian Rhythms and Sleep in Drosophila melanogaster*. *Genetics*, 2017. **205**(4): p. 1373-1397.
3. Hendricks, J.C., et al., *Rest in Drosophila Is a Sleep-like State*. *Neuron*, 2000. **25**: p. 129-138.
4. Shaw, P.J., et al., *Correlates of Sleep and Waking in Drosophila melanogaster*. *Science*, 2000. **287**(5459): p. 1834-1837.
5. Bushey, D. and C. Cirelli, *From genetics to structure to function: exploring sleep in Drosophila*. *International Review of Neurobiology*, 2011. **99**: p. 213-244.
6. Cirelli, C., *Searching for sleep mutants of Drosophila melanogaster*. *Bioassays*, 2003. **25**: p. 940-949.
7. Low, K.H., et al., *Natural variation in the Drosophila melanogaster clock gene period modulates splicing of its 3'-terminal intron and mid-day siesta*. *PLoS One*, 2012. **7**(11): p. e49536.
8. Low, K.H., et al., *Natural Variation in the Splice Site Strength of a Clock Gene and Species-Specific Thermal Adaptation*. *Neuron*, 2008. **60**(6): p. 1054-1067.
9. Majercak, J., et al., *How a Circadian Clock Adapts to Seasonal Decreases in Temperature and Day Length*. *Neuron*, 1999. **24**(1): p. 219-230.
10. Cheng, Y., B. Gvakharia, and P.E. Hardin, *Two Alternatively Spliced Transcripts from the Drosophila period Gene Rescue Rhythms Having Different Molecular and Behavioral Characteristics*. *Molecular and Cellular Biology*, 1998. **18**(11): p. 6505-6514.
11. Colot, H.V., J.J. Loros, and J.C. Dunlap, *Temperature-modulated Alternative Splicing and Promoter Use in the Circadian Clock Gene frequency*. *Molecular Biology of the Cell*, 2005. **16**(12): p. 5563-5571.
12. Diernfellner, A.C.R., et al., *Molecular mechanism of temperature sensing by the circadian clock of Neurospora crassa*. *Genes & Development*, 2005. **19**(17): p. 1968-1973.
13. Reese, M.G., et al., *Improved splice site detection in Genie*. *Journal of Computational Biology*, 1998. **4**: p. 311-323.
14. Ainsworth, J.R., L.M. Rossi, and E.C. Murphy, Jr., *The Moloney murine sarcoma virus ts110 5' splice site signal contributes to the regulation of splicing efficiency and thermosensitivity*. *Journal of Virology*, 1996. **70**: p. 6474-6478.
15. Wouchman, J.W., et al., *Branchpoint and polypyrimidine tract mutations mediating the loss and partial recovery of the Moloney murine sarcoma virus MuSVts110 thermosensitive splicing phenotype*. *Journal of Virology*, 1995. **69**: p. 7724-7733.

16. Ishimoto, H., A. Lark, and T. Kitamoto, *Factors that differentially affect daytime and nighttime sleep in Drosophila melanogaster*. *Frontiers in Neurology*, 2012. **3**: p. 24.
17. Cao, W. and I. Edery, *A Novel Pathway for Sensory-Mediated Arousal Involves Splicing of an Intron in the period Clock Gene*. *Sleep*, 2015. **38**(1): p. 41-51.
18. Demerec, M., *Biology of Drosophila*. 1950, New York, NY: John Wiley & Sons, Inc.
19. J.R., D. and C. P., *Genetic variation of Drosophila melanogaster natural populations*. *Trends in Genetics*, 1988. **4**(4): p. 106-111.
20. Cao, W. and I. Edery, *Mid-day siesta in natural populations of D. melanogaster from Africa exhibits an altitudinal cline and is regulated by splicing of a thermosensitive intron in the period clock gene*. *BMC evolutionary biology*, 2017. **17**(1): p. 32.
21. Yang, Y. and I. Edery, *Parallel clinal variation in the mid-day siesta of Drosophila melanogaster implicates continent-specific targets of natural selection*. *PLoS genetics*, 2018. **14**(9): p. e1007612.
22. Yang, Y. and I. Edery, *Daywake, an Anti-siesta Gene Linked to a Splicing-Based Thermostat from an Adjoining Clock Gene*. *Current Biology*, 2019. **29**(10): p. 1728-1734.e4.
23. Chen, W.F., et al., *Thermosensitive Splicing of a Clock Gene and Seasonal Adaptation*. *Cold Spring Harbor symposia on quantitative biology*, 2007. **72**(1): p. 599-606.
24. Prestwich, G.D., et al., *Biochemistry of Proteins That Bind and Metabolize Juvenile Hormones*. *Archives of Insect Biochemistry and Physiology*, 1996. **32**(3-4): p. 407-419.
25. Gilbert, L.I., N.A. Granger, and R.M. Roe, *The juvenile hormones: historical facts and speculations on future research directions*. *Insect Biochemistry and Molecular Biology*, 2000. **30**: p. 617-644.
26. Li, K., Q.Q. Jia, and S. Li, *Juvenile hormone signaling - a mini review*. *Insect Sci*, 2019. **26**(4): p. 600-606.
27. Gruntenko, N.E., et al., *Decrease in juvenile hormone level as a result of genetic ablation of the corpus allatum cells affects the synthesis and metabolism of stress related hormones in Drosophila*. *J Insect Physiol*, 2012. **58**(1): p. 49-55.
28. Suzuki, R., et al., *Structural mechanism of JH delivery in hemolymph by JHBP of silkworm, Bombyx mori*. *Sci Rep*, 2011. **1**: p. 133.
29. Wu, B., et al., *Sexual dimorphism of sleep regulated by juvenile hormone signaling in Drosophila*. *PLoS Genet*, 2018. **14**(4): p. e1007318.
30. Larcher, S., et al., *Sleep habits and diabetes*. *Diabetes Metab*, 2015. **41**(4): p. 263-71.
31. Soucise, A., et al., *Sleep quality, duration, and breast cancer aggressiveness*. *Breast Cancer Res Treat*, 2017. **164**(1): p. 169-178.
32. Scullin, M.K. and D.L. Bliwise, *Sleep, cognition, and normal aging: integrating a half century of multidisciplinary research*. *Perspect Psychol Sci*, 2015. **10**(1): p. 97-137.

33. Rosato, E. and C.P. Kyriacou, *Analysis of locomotor activity rhythms in Drosophila*. Nat Protoc, 2006. **1**(2): p. 559-68.
34. Lopez-Minguez, J., et al., *Heritability of siesta and night-time sleep as continuously assessed by a circadian-related integrated measure*. Sci Rep, 2017. **7**(1): p. 12340.
35. Shi, L., et al., *Sleep disturbances increase the risk of dementia: A systematic review and meta-analysis*. Sleep Med Rev, 2018. **40**: p. 4-16.
36. Poggiogalle, E., H. Jamshed, and C.M. Peterson, *Circadian regulation of glucose, lipid, and energy metabolism in humans*. Metabolism, 2018. **84**: p. 11-27.
37. Meunier, N., Y.H. Belgacem, and J.R. Martin, *Regulation of feeding behaviour and locomotor activity by takeout in Drosophila*. J Exp Biol, 2007. **210**(Pt 8): p. 1424-34.
38. Dauwalder, B., et al., *The Drosophila takeout gene is regulated by the somatic sex-determination pathway and affects male courtship behavior*. Genes Dev, 2002. **16**(22): p. 2879-92.
39. Wong, L.H. and T.P. Leving, *Tubular lipid binding proteins (TULIPs) growing everywhere*. Biochimica et biophysica acta. Molecular cell research, 2017. **1864**(9): p. 1439-1449.
40. Kim, E.Y., et al., *A DOUBLETIME kinase binding domain on the Drosophila PERIOD protein is essential for its hyperphosphorylation, transcriptional repression, and circadian clock function*. Mol Cell Biol, 2007. **27**(13): p. 5014-28.
41. E., G., et al., *Protein Identification and Analysis Tools on the ExPASy Server*. 2005: Humana Press.
42. Freudl, R., *Signal peptides for recombinant protein secretion in bacterial expression systems*. Microb Cell Fact, 2018. **17**(1): p. 52.
43. Owji, H., et al., *A comprehensive review of signal peptides: Structure, roles, and applications*. Eur J Cell Biol, 2018. **97**(6): p. 422-441.
44. Almagro Armenteros, J.J., et al., *SignalP 5.0 improves signal peptide predictions using deep neural networks*. Nat Biotechnol, 2019. **37**(4): p. 420-423.
45. Braakman, I. and D.N. Hebert, *Protein folding in the endoplasmic reticulum*. Cold Spring Harb Perspect Biol, 2013. **5**(5): p. a013201.
46. Sagt, C.M.J., et al., *Introduction of an N-Glycosylation Site Increases Secretion of Heterologous Proteins in Yeasts*. Applied and Environmental Microbiology, 2000. **66**(11): p. 4940-4944.
47. Maley, F., et al., *Characterization of glycoproteins and their associated oligosaccharides through the use of endoglycosidases*. Analytical Biochemistry, 1989. **180**(2): p. 195-204.
48. Shental-Bechor, D. and Y. Levy, *Effect of glycosylation on protein folding: a close look at thermodynamic stabilization*. Proc Natl Acad Sci U S A, 2008. **105**(24): p. 8256-61.
49. Helenius, A. and M. Aebi, *Roles of N-linked glycans in the endoplasmic reticulum*. Annu Rev Biochem, 2004. **73**: p. 1019-49.

50. Zhou, Q. and H. Qiu, *The Mechanistic Impact of N-Glycosylation on Stability, Pharmacokinetics, and Immunogenicity of Therapeutic Proteins*. J Pharm Sci, 2019. **108**(4): p. 1366-1377.
51. Sola, R.J., J.A. Rodriguez-Martinez, and K. Griebenow, *Modulation of protein biophysical properties by chemical glycosylation: biochemical insights and biomedical implications*. Cell Mol Life Sci, 2007. **64**(16): p. 2133-52.
52. Hall, J.C., *Molecular Neurogenetics of Biological Rhythms*. Journal of Neurogenetics, 1998. **12**(3): p. 115-181.
53. Rachidi, M., et al., *Analysis of Period Circadian Expression in the Drosophila Head by in Situ Hybridization*. Journal of Neurogenetics, 1997. **11**(3-4): p. 255-263.
54. Sarov-Blat, L., et al., *The *Drosophila takeout* Gene Is a Novel Molecular Link between Circadian Rhythms and Feeding Behavior*. Cell, 2000. **101**(6): p. 647-656.
55. Zhang, X. and Y. Wang, *Glycosylation Quality Control by the Golgi Structure*. Journal of molecular biology, 2016. **428**(16): p. 3183-3193.
56. Pfeffer, S.R., *A prize for membrane magic*. Cell, 2013. **155**(6): p. 1203-1206.
57. Goldfischer, S., *The internal reticular apparatus of Camillo Golgi: a complex, heterogeneous organelle, enriched in acid, neutral, and alkaline phosphatases, and involved in glycosylation, secretion, membrane flow, lysosome formation, and intracellular digestion*. Journal of Histochemistry & Cytochemistry, 1982. **30**(7): p. 717-733.
58. Tannous, A., et al., *N-linked sugar-regulated protein folding and quality control in the ER*. Seminars in Cell & Developmental Biology, 2015. **41**: p. 79-89.
59. Araki, K. and K. Nagata, *Protein folding and quality control in the ER*. Cold Spring Harb Perspect Biol, 2011. **3**(11): p. a007526.
60. Xu, C., et al., *Futile Protein Folding Cycles in the ER Are Terminated by the Unfolded Protein O-Mannosylation Pathway*. 2013. **340**(6135): p. 978-981.
61. Schroder, M. and R.J. Kaufman, *ER stress and the unfolded protein response*. Mutat Res, 2005. **569**(1-2): p. 29-63.
62. Cnop, M., F. Foufelle, and L.A. Velloso, *Endoplasmic reticulum stress, obesity and diabetes*. Trends Mol Med, 2012. **18**(1): p. 59-68.
63. Wek, R.C. and D.R. Cavener, *Translational control and the unfolded protein response*. Antioxid Redox Signal, 2007. **9**(12): p. 2357-71.
64. Walter, P. and D. Ron, *The Unfolded Protein Response: From Stress Pathway to Homeostatic Regulation*. 2011. **334**(6059): p. 1081-1086.
65. Miyazaki, S., C.Y. Liu, and Y. Hayashi, *Sleep in vertebrate and invertebrate animals, and insights into the function and evolution of sleep*. Neurosci Res, 2017. **118**: p. 3-12.
66. Ho, K.S. and A. Sehgal, *Drosophila melanogaster: an insect model for fundamental studies of sleep*. Methods Enzymol, 2005. **393**: p. 772-93.

67. Parisky, Katherine M., et al., *Reorganization of Sleep by Temperature in Drosophila Requires Light, the Homeostat, and the Circadian Clock*. *Current Biology*, 2016. **26**(7): p. 882-892.
68. Mantua, J. and R.M.C. Spencer, *Exploring the nap paradox: are mid-day sleep bouts a friend or foe?* *Sleep Med*, 2017. **37**: p. 88-97.
69. Cross, N., et al., *Napping in older people 'at risk' of dementia: relationships with depression, cognition, medical burden and sleep quality*. *J Sleep Res*, 2015. **24**(5): p. 494-502.
70. Buysse, D.J., et al., *Napping and 24-hour sleep/wake patterns in healthy elderly and young adults*. *J Am Geriatr Soc*, 1992. **40**(8): p. 779-86.
71. Bhat, R.Y., et al., *Effect of prone and supine position on sleep, apneas, and arousal in preterm infants*. *Pediatrics*, 2006. **118**(1): p. 101-7.
72. Gratz, S.J., et al., *Genome engineering of Drosophila with the CRISPR RNA-guided Cas9 nuclease*. *Genetics*, 2013. **194**(4): p. 1029-35.
73. Bassett, A.R. and J.L. Liu, *CRISPR/Cas9 and genome editing in Drosophila*. *J Genet Genomics*, 2014. **41**(1): p. 7-19.
74. Donlea, J., et al., *Foraging alters resilience/vulnerability to sleep disruption and starvation in Drosophila*. *Proc Natl Acad Sci U S A*, 2012. **109**(7): p. 2613-8.
75. Keene, A.C., et al., *Clock and cycle limit starvation-induced sleep loss in Drosophila*. *Curr Biol*, 2010. **20**(13): p. 1209-15.
76. McDonald, D.M. and A.C. Keene, *The sleep-feeding conflict: Understanding behavioral integration through genetic analysis in Drosophila*. *Aging (Albany NY)*, 2010. **2**(8): p. 519-22.
77. Majercak, J., W.F. Chen, and I. Edery, *Splicing of the period Gene 3'-Terminal Intron Is Regulated by Light, Circadian Clock Factors, and Phospholipase C*. *Molecular and Cellular Biology*, 2004. **24**(8): p. 3359-3372.
78. Isaac, R.E., et al., *Drosophila male sex peptide inhibits siesta sleep and promotes locomotor activity in the post-mated female*. *Proc Biol Sci*, 2010. **277**(1678): p. 65-70.
79. Dilley, L.C., et al., *Behavioral and genetic features of sleep ontogeny in Drosophila*. *Sleep*, 2018. **41**(7).
80. Chakravarti Dilley, L., et al., *Identification of a molecular basis for the juvenile sleep state*. *Elife*, 2020. **9**.
81. Cirelli, C. and D. Bushey, *Sleep and wakefulness in Drosophila melanogaster*. *Ann N Y Acad Sci*, 2008. **1129**: p. 323-9.
82. Huber, R., et al., *Sleep homeostasis in Drosophila melanogaster*. *Sleep*, 2004. **27**(4): p. 628-39.
83. Wheeler, D.A., et al., *Behavior in light-dark cycles of Drosophila mutants that are arrhythmic, blind, or both*. *J Biol Rhythms*, 1993. **8**(1): p. 67-94.
84. Lee, G. and J.H. Park, *Hemolymph sugar homeostasis and starvation-induced hyperactivity affected by genetic manipulations of the adipokinetic hormone-encoding gene in Drosophila melanogaster*. *Genetics*, 2004. **167**(1): p. 311-23.

85. Murphy, K.R., et al., *Postprandial sleep mechanics in Drosophila*. Elife, 2016. **5**.
86. Yu, Y., et al., *Regulation of starvation-induced hyperactivity by insulin and glucagon signaling in adult Drosophila*. Elife, 2016. **5**.
87. Yang, Z., et al., *Octopamine mediates starvation-induced hyperactivity in adult Drosophila*. Proc Natl Acad Sci U S A, 2015. **112**(16): p. 5219-24.
88. Hua, R., et al., *Calretinin Neurons in the Midline Thalamus Modulate Starvation-Induced Arousal*. Curr Biol, 2018. **28**(24): p. 3948-3959.e4.
89. Skora, S., F. Mende, and M. Zimmer, *Energy Scarcity Promotes a Brain-wide Sleep State Modulated by Insulin Signaling in C. elegans*. Cell Rep, 2018. **22**(4): p. 953-966.
90. Lamaze, A., et al., *A Wake-Promoting Circadian Output Circuit in *Drosophila**. Current Biology, 2018. **28**(19): p. 3098-3105.e3.
91. Ni, J.D., et al., *Differential regulation of the Drosophila sleep homeostat by circadian and arousal inputs*. Elife, 2019. **8**.
92. Hasegawa, T., et al., *Sweetness induces sleep through gustatory signalling independent of nutritional value in a starved fruit fly*. Sci Rep, 2017. **7**(1): p. 14355.
93. Koh, K., et al., *A Drosophila model for age-associated changes in sleep:wake cycles*. Proc Natl Acad Sci U S A, 2006. **103**(37): p. 13843-7.
94. Vienne, J., et al., *Age-Related Reduction of Recovery Sleep and Arousal Threshold in Drosophila*. Sleep, 2016. **39**(8): p. 1613-24.
95. Borbély, A.A., *A two process model of sleep regulation*. Hum Neurobiol, 1982. **1**(3): p. 195-204.
96. Borbély, A.A. and P. Achermann, *Sleep homeostasis and models of sleep regulation*. J Biol Rhythms, 1999. **14**(6): p. 557-68.
97. Borbély, A.A., et al., *The two-process model of sleep regulation: a reappraisal*. J Sleep Res, 2016. **25**(2): p. 131-43.
98. Chiu, J.C., H.W. Ko, and I. Edery, *NEMO/NLK phosphorylates PERIOD to initiate a time-delay phosphorylation circuit that sets circadian clock speed*. Cell, 2011. **145**(3): p. 357-70.
99. Chiu, J.C., et al., *The phospho-occupancy of an atypical SLIMB-binding site on PERIOD that is phosphorylated by DOUBLETIME controls the pace of the clock*. Genes Dev, 2008. **22**(13): p. 1758-72.
100. Ko, H.W., J. Jiang, and I. Edery, *Role for Slimb in the degradation of Drosophila Period protein phosphorylated by Doubletime*. Nature, 2002. **420**(6916): p. 673-8.
101. Ko, H.W., et al., *A hierarchical phosphorylation cascade that regulates the timing of PERIOD nuclear entry reveals novel roles for proline-directed kinases and GSK-3beta/SGG in circadian clocks*. J Neurosci, 2010. **30**(38): p. 12664-75.
102. Stanewsky, R., et al., *The cryb mutation identifies cryptochrome as a circadian photoreceptor in Drosophila*. Cell, 1998. **95**(5): p. 681-92.
103. Emery, P., et al., *CRY, a Drosophila clock and light-regulated cryptochrome, is a major contributor to circadian rhythm resetting and photosensitivity*. Cell, 1998. **95**(5): p. 669-79.

104. Dissel, S., et al., *The logic of circadian organization in Drosophila*. *Curr Biol*, 2014. **24**(19): p. 2257-66.
105. Kozlov, A. and E. Nagoshi, *Decoding Drosophila circadian pacemaker circuit*. *Current Opinion in Insect Science*, 2019. **36**: p. 33-38.
106. Helfrich-Förster, C., *Development of pigment-dispersing hormone-immunoreactive neurons in the nervous system of Drosophila melanogaster*. *Journal of Comparative Neurology*, 1997. **380**(3): p. 335-354.
107. Schubert, F.K., et al., *Neuroanatomical details of the lateral neurons of Drosophila melanogaster support their functional role in the circadian system*. *Journal of Comparative Neurology*, 2018. **526**(7): p. 1209-1231.
108. Kumar, S., D. Chen, and A. Sehgal, *Dopamine acts through Cryptochrome to promote acute arousal in Drosophila*. *Genes Dev*, 2012. **26**(11): p. 1224-34.
109. Fogle, K.J., et al., *CRYPTOCHROME is a blue-light sensor that regulates neuronal firing rate*. *Science*, 2011. **331**(6023): p. 1409-13.
110. Lee, T.F. and T.W. McNellis, *Elimination of keratin artifact bands from western blots by using low concentrations of reducing agents*. *Anal Biochem*, 2008. **382**(2): p. 141-3.
111. Riches, P.G., B. Polce, and R. Hong, *Contaminant bands on SDS-polyacrylamide gel electrophoresis are recognized by antibodies in normal human serum and saliva*. *Journal of Immunological Methods*, 1988. **110**(1): p. 117-121.
112. Edery, I., et al., *Temporal phosphorylation of the Drosophila period protein*. *Proc Natl Acad Sci U S A*, 1994. **91**(6): p. 2260-4.
113. Hardin, P.E., *Molecular genetic analysis of circadian timekeeping in Drosophila*. *Adv Genet*, 2011. **74**: p. 141-73.
114. Markson, J.S. and E.K. O'Shea, *The Molecular Clockwork of a Protein-based Circadian Oscillator*. *FEBS Lett.*, 2009. **583**(24): p. 3938-3947.
115. Mehra, A., et al., *Post-translational modifications in circadian rhythms*. *Trends Biochem Sci*, 2009. **34**(10): p. 483-90.
116. Gallego, M. and D.M. Virshup, *Post-translational modifications regulate the ticking of the circadian clock*. *Nat Rev Mol Cell Biol*, 2007. **8**(2): p. 139-48.
117. Vanselow, K., et al., *Differential effects of PER2 phosphorylation: molecular basis for the human familial advanced sleep phase syndrome (FASPS)*. *Genes Dev*, 2006. **20**(19): p. 2660-72.
118. Yildirim, E., J.C. Chiu, and I. Edery, *Identification of Light-Sensitive Phosphorylation Sites on PERIOD That Regulate the Pace of Circadian Rhythms in Drosophila*. *Mol Cell Biol*, 2015. **36**(6): p. 855-70.
119. Bae, K. and I. Edery, *Regulating a circadian clock's period, phase and amplitude by phosphorylation: insights from Drosophila*. *J Biochem*, 2006. **140**(5): p. 609-17.
120. Lee, C., K. Bae, and I. Edery, *The Drosophila CLOCK protein undergoes daily rhythms in abundance, phosphorylation, and interactions with the PER-TIM complex*. *Neuron*, 1998. **21**(4): p. 857-67.

121. Yang, Y., et al., *Phosphorylation of FREQUENCY protein by casein kinase II is necessary for the function of the Neurospora circadian clock*. Mol Cell Biol, 2003. **23**(17): p. 6221-8.
122. Liu, Y., J. Loros, and J.C. Dunlap, *Phosphorylation of the Neurospora clock protein FREQUENCY determines its degradation rate and strongly influences the period length of the circadian clock*. Proc Natl Acad Sci U S A, 2000. **97**(1): p. 234-9.
123. Diernfellner, A.C. and T. Schafmeier, *Phosphorylations: Making the Neurospora crassa circadian clock tick*. FEBS Lett, 2011. **585**(10): p. 1461-6.
124. Querfurth, C., et al., *Circadian conformational change of the Neurospora clock protein FREQUENCY triggered by clustered hyperphosphorylation of a basic domain*. Mol Cell, 2011. **43**(5): p. 713-22.
125. Toh, K.L., et al., *An hPer2 Phosphorylation Site Mutation in Familial Advanced Sleep Phase Syndrome*. Science, 2001. **291**(1): p. 1040-1043.
126. Xu, Y., et al., *Functional consequences of a CK1 δ mutation causing familial advanced sleep phase syndrome*. Nature, 2005. **434**: p. 640-644.
127. Fu, L. and C.C. Lee, *The circadian clock: pacemaker and tumour suppressor*. Nat Rev Cancer, 2003. **3**(5): p. 350-61.
128. Bandin, C., et al., *Meal timing affects glucose tolerance, substrate oxidation and circadian-related variables: A randomized, crossover trial*. Int J Obes (Lond), 2015. **39**(5): p. 828-33.
129. Koren, D., K.L. O'Sullivan, and B. Mokhlesi, *Metabolic and glycemic sequelae of sleep disturbances in children and adults*. Curr Diab Rep, 2015. **15**(1): p. 562.
130. Eckel-Mahan, K. and P. Sassone-Corsi, *Metabolism control by the circadian clock and vice versa*. Nat Struct Mol Biol, 2009. **16**(5): p. 462-7.
131. Bunney, W.E. and B.G. Bunney, *Molecular Clock Genes in Man and Lower Animals: Possible Implications for Circadian Abnormalities in Depression*. Neuropsychopharmacology, 2000. **22**(4): p. 335-345.
132. Lundström, P., A. Ahlner, and A.T. Blissing, *Isotope labeling methods for large systems*. Adv Exp Med Biol, 2012. **992**: p. 3-15.
133. Yeates, T.O., M.P. Agdanowski, and Y. Liu, *Development of imaging scaffolds for cryo-electron microscopy*. Curr Opin Struct Biol, 2020. **60**: p. 142-149.
134. Liu, X.R., M.M. Zhang, and M.L. Gross, *Mass Spectrometry-Based Protein Footprinting for Higher-Order Structure Analysis: Fundamentals and Applications*. Chem Rev, 2020. **120**(10): p. 4355-4454.
135. Kloss, B., et al., *Phosphorylation of period is influenced by cycling physical associations of double-time, period, and timeless in the Drosophila clock*. Neuron, 2001. **30**(3): p. 699-706.
136. Sathyanarayanan, S., et al., *Posttranslational regulation of Drosophila PERIOD protein by protein phosphatase 2A*. Cell, 2004. **116**(4): p. 603-15.
137. King, H.A., et al., *Structure of an enclosed dimer formed by the Drosophila period protein*. J Mol Biol, 2011. **413**(3): p. 561-72.

138. Yildiz, O., et al., *Crystal structure and interactions of the PAS repeat region of the Drosophila clock protein PERIOD*. Mol Cell, 2005. **17**(1): p. 69-82.
139. Gekakis, N., et al., *Isolation of timeless by PER protein interaction: defective interaction between timeless protein and long-period mutant PERL*. Science, 1995. **270**(5237): p. 811-5.
140. Landskron, J., et al., *A role for the PERIOD:PERIOD homodimer in the Drosophila circadian clock*. PLoS Biol, 2009. **7**(4): p. e3.